New Laser Cooling Mechanisms.

C. COHEN-TANNOUDJI

Collège de France and
Departement de Physique de l'Ecole Normale Supérieure - Paris, France

1. – Introduction.

This lecture is devoted to an analysis of the new laser cooling mechanisms which, during the last three years, have allowed the performances of laser cooling to be improved by orders of magnitude.

A very important feature of these new cooling mechanisms is that they require the existence of several sublevels in the lower atomic state g. The reason is that new internal times appear in these conditions, which are the optical-pumping times τ_P between ground-state sublevels. At very low laser intensity I_L, the pumping times τ_P become very long, much longer than the radiative lifetime τ_R of the excited state e, which is the only relevant internal time for a two-level atom. Multilevel atoms can thus have very long internal times, which explains why internal variables cannot follow adiabatically the variations of the laser field «seen» by the moving atom. The important time lag which appears then between internal and translational degrees of freedom is at the origin of a large friction force.

We have thus found it useful to start this lecture by recalling in sect. 2 a few basic results concerning the effect of a weak-intensity light irradiation on an atom having several ground-state sublevels. Two types of effects are briefly reviewed: reactive effects, such as energy shifts of the ground-state sublevels (light shifts), on the one hand, dissipative effects, corresponding to irreversible transitions between ground-state sublevels (optical pumping), on the other hand. We also show that the total mean force experienced by the atom can be split into two components, one reactive and one dissipative.

We then present in sect. 3 and 4 two simple one-dimensional cooling schemes using optical pumping, light shifts and laser polarization gradients, and leading to very low temperatures. The first one is the so-called «Sisyphus cooling» mechanism (sect. 3), where strong correlations between spatially modulated light shifts and spatially modulated optical-pumping rates lead to a situation

where the moving atom is running up optical-potential hills more than down (a: did Sisyphus in the Greek mythology). The second scheme, which uses a σ^+-σ^- laser configuration, is also based on optical pumping, light shifts and polariza tion gradients (sect. 4). The physical processes responsible for the cooling are however, quite different from the Sisyphus effect. They involve a very sensi tive motion-induced imbalance between the radiation pressures exerted by the two counterpropagating laser waves. We also introduce in sect. 4 the idea of co herent population trapping for a Λ-type atomic transition. We then show in sect. 5 how the possibility of making such a coherent population trapping veloc ity selective allows one to cool atoms below the recoil limit, corresponding tc the recoil energy of an atom emitting or absorbing a single photon.

Actually, this lecture follows very closely the second part of a lecture given at Les Houches summer school in July 1990 [1]. The first part of ref. [1] deals with two-level atoms. We will refer to this first part when results concerning two-level atoms are needed.

2. – Optical pumping, light shifts and mean radiative forces.

2·1. *Introduction.* – This lecture is devoted to atoms having several sub levels in the ground state. More precisely, we consider an atomic transition con necting two levels g and e with angular momenta respectively equal to J_g and J_e, and we suppose $J_g \neq 0$. As mentioned in sect. 1, such a situation gives rise to very efficient new cooling mechanisms which we now want to analyse.

Two physical effects, which have been known for a long time, play a basic role in the new cooling mechanisms. The first one is optical pumping which con sists of a transfer of atoms from one sublevel g_μ of g to another one $g_{\mu'}$ by absorp tion-spontaneous emission cycles. The second one is an energy shift of the ground-state sublevels, which in general varies from one sublevel to the other and which is proportional to the light intensity. Such shifts are called light shifts or a.c.-Stark shifts. Up to now, these effects have been considered only in connection with the dynamics of the atomic internal degrees of freedom. Very recently, it has been realized that these effects also play a very important role in the dynamics of the atomic translational degrees of freedom. So we have thought it would be useful to recall in this sect. 2 a few properties of optical pumping and light shifts which are needed for understanding the new cooling mechanisms discussed in the following sections.

We begin in subsect. 2·2 by generalizing to multilevel atoms the equations of motion of the atomic density matrix σ and the expression of the mean force which are well known for 2-level atoms (see, for example, in Chapt. 2 of ref. [1]). We then show in subsect. 2·3 that these equations can be considerably simplified in the low-saturation and low-velocity limit, which is precisely the limit where the new cooling mechanisms are the most efficient. The existence of

two different time scales, the radiative lifetime τ_R of e and the optical-pumping time τ_P in g, with $\tau_P \gg \tau_R$, allows one to adiabatically eliminate all fast variables and to get equations of motion involving only the ground-state density matrix. Such equations of motion contain two types of terms, terms corresponding to a Hamiltonian evolution and describing the light shifts in g, and terms describing a relaxation in g associated with optical pumping. The physical content of these two types of terms is analysed, respectively, in subsect. 2·4 and 2·5. Finally, we discuss in subsect. 2·6 the new expression of the mean force in the low-saturation and the low-velocity limit, and we identify two types of terms related, respectively, to the light shifts of the ground-state sublevels and to the absorption rate from these sublevels.

2·2. *Basic equations for multilevel atoms.*

2·2.1. Approximations. We use a semi-classical description where the position operator $\boldsymbol{R}$ of the centre of mass is replaced by the c-number $\boldsymbol{r} = \boldsymbol{r}_0 + \boldsymbol{v}_0 t$.

Let P_g (respectively, P_e) be the projector onto the subspace subtended by the various Zeeman sublevels of g (respectively, e)

$$\text{(2.1)} \qquad \begin{cases} P_g = \sum_{\mu=-J_g}^{+J_g} |J_g \mu\rangle\langle J_g \mu| , \\ P_e = \sum_{m=-J_e}^{+J_e} |J_e m\rangle\langle J_e m| . \end{cases}$$

The atomic-density operator σ can be written

$$\text{(2.2)} \qquad \sigma = \sigma_{gg} + \sigma_{ge} + \sigma_{eg} + \sigma_{ee},$$

where

$$\text{(2.3)} \qquad \sigma_{ab} = P_a \sigma P_b$$

with $a, b =$ e or g. Note that σ_{ab} is now an operator and not a c-number. The two operators σ_{gg} and σ_{ee} are represented by square matrices. Their diagonal elements give the populations of the various Zeeman sublevels of g and e, whereas the off-diagonal elements describe «Zeeman coherences» which exist between them in e or g. Finally, σ_{ge} and $\sigma_{eg} = \sigma_{ge}^{\dagger}$ are represented by rectangular matrices consisting of off-diagonal elements between one sublevel of e and one sublevel of g, which are called «optical coherences».

The new expression of the atom-laser interaction Hamiltonian V_{AL}, which generalizes (2.10) of ref. [1], is given by

$$\text{(2.4)} \qquad V_{AL} = -\boldsymbol{d}^{+} \cdot \boldsymbol{E}_L^{+}(\boldsymbol{r}) \exp[-i\omega_L t] - \boldsymbol{d}^{-} \cdot \boldsymbol{E}_L^{-}(\boldsymbol{r}) \exp[+i\omega_L t],$$

where

$$\boldsymbol{d}^{+} = P_e \mathbf{d} P_g, \qquad \boldsymbol{d}^{-} = P_g \mathbf{d} P_e \tag{2.5}$$

and where $\boldsymbol{E}_L^{+}(\boldsymbol{r})$ (respectively, $\boldsymbol{E}_L^{-}(\boldsymbol{r})$) are the positive (respectively, negative) frequency components of the laser electric field:

$$\boldsymbol{E}_L(\boldsymbol{r}, t) = \boldsymbol{E}_L^{+}(\boldsymbol{r}) \exp[-i\omega_L t] + \boldsymbol{E}_L^{-}(\boldsymbol{r}) \exp[+i\omega_L t]. \tag{2.6}$$

As in (2.10) of ref. [1], the rotating-wave approximation has been used.

It will be useful for the following to introduce the internal atomic operators $G^{\pm}(\boldsymbol{r})$ defined by

$$\hbar G^{\pm}(\boldsymbol{r}) = \boldsymbol{d}^{\pm} \cdot \boldsymbol{E}_L^{\pm}(\boldsymbol{r}) \tag{2.7}$$

and to define dimensionless dipole operators $\hat{\boldsymbol{d}}^{\pm}$ in the following way. Let

$$\boldsymbol{\varepsilon}_{\pm} = \mp \frac{1}{\sqrt{2}} (\boldsymbol{\varepsilon}_x \pm i\boldsymbol{\varepsilon}_y), \qquad \boldsymbol{\varepsilon}_0 = \boldsymbol{\varepsilon}_z, \tag{2.8}$$

be a spherical basis of polarization vectors, corresponding, respectively, to the $\sigma^{\pm}$ and π polarizations. The Wigner-Eckart theorem (ref. [2], Chapt. XIII) applied to the vectorial operator $\boldsymbol{d}^{+}$ gives

$$\langle J_e m | \boldsymbol{\varepsilon}_q \cdot \boldsymbol{d}^{+} | J_g \mu \rangle = \mathscr{D} \langle J_e m | J_g 1 \mu q \rangle, \tag{2.9}$$

where $\langle J_e m | J_g 1 \mu q \rangle$ is a Clebsch-Gordan coefficient and where $\mathscr{D}$ is a reduced matrix element which can always be taken real with an appropriate choice of the relative phases of e and g, and which is independent of the magnetic quantum numbers, m, μ and q. We will put

$$\boldsymbol{d}^{+} = \mathscr{D} \hat{\boldsymbol{d}}^{+} = (\boldsymbol{d}^{-})^{\dagger}, \tag{2.10}$$

so that the matrix elements of $\boldsymbol{\varepsilon}_q \cdot \hat{\boldsymbol{d}}^{+}$ are just Clebsch-Gordan coefficients. We also introduce the polarization vector $\boldsymbol{\varepsilon}(\boldsymbol{r})$ in $\boldsymbol{r}$ by

$$\boldsymbol{E}_L^{+}(\boldsymbol{r}) = \frac{1}{2} \boldsymbol{\varepsilon}(\boldsymbol{r}) \mathscr{E}_L(\boldsymbol{r}), \tag{2.11}$$

the amplitude $\mathscr{E}_L(\boldsymbol{r})$ being real. The (generally complex) polarization vector $\boldsymbol{\varepsilon}(\boldsymbol{r})$ is normalized

$$\boldsymbol{\varepsilon}^{*}(\boldsymbol{r}) \cdot \boldsymbol{\varepsilon}(\boldsymbol{r}) = 1. \tag{2.12}$$

From $\mathscr{D}$ and $\mathscr{E}_L(\boldsymbol{r})$, we finally define the Rabi frequency in $\boldsymbol{r}$

$$\hbar \Omega_1(\boldsymbol{r}) = -\mathscr{D} \mathscr{E}_L(\boldsymbol{r}), \tag{2.13}$$

which corresponds to the Rabi frequency of a transition with Clebsch-Gordan coefficient equal to 1, excited by a laser field with amplitude $\mathscr{E}_L(\boldsymbol{r})$.

2·2.2. Operator form of optical Bloch equations. The basic equations of motion, which generalize (2.42) of ref. [1], can be now written in operator form

$$\dot{\sigma}_{ab} = -\frac{i}{\hbar} P_a [H_A^{int} + V_{AL}, \sigma] P_b + \left(\frac{d}{dt}\sigma_{ab}\right)_{sp}, \tag{2.14}$$

where V_{AL} is given in (2.4) and where

$$H_A^{int} = \hbar\omega_A P_e, \tag{2.15}$$

$\hbar\omega_A$ being the energy of e above g (we assume that all sublevels of e are degenerate as well as all sublevels of g and we take $E_g = 0$). The last term of (2.14) describes the damping due to spontaneous emission. For the excited-state density matrix σ_{ee} and for the optical coherences σ_{eg} and σ_{ge}, it has the same form as in eqs. (2.43*a*), (2.43*c*) and (2.43*d*) of ref. [1]:

$$\left(\frac{d}{dt}\sigma_{ee}\right)_{sp} = -\Gamma\sigma_{ee}, \tag{2.16a}$$

$$\left(\frac{d}{dt}\sigma_{eg}\right)_{sp} = -\frac{\Gamma}{2}\sigma_{eg}, \tag{2.16b}$$

$$\left(\frac{d}{dt}\sigma_{ge}\right)_{sp} = -\frac{\Gamma}{2}\sigma_{ge}, \tag{2.16c}$$

where Γ is the natural width of e, *i.e.* also the spontaneous-emission rate. Only eq. (2.43*b*) of ref. [1] describing the feeding of σ_{gg} from σ_{ee} by spontaneous emission has to be modified. One can show (see ref. [3], subsect. 4.3.4) that, for an atom having a degenerate ground state, the transfer to g by spontaneous emission with a rate Γ takes the form

$$\left(\frac{d}{dt}\sigma_{gg}\right)_{sp} = \Gamma \sum_{q=-1,0,+1} (\boldsymbol{\varepsilon}_q^* \cdot \hat{\boldsymbol{d}}^-)\,\sigma_{ee}\,(\boldsymbol{\varepsilon}_q \cdot \hat{\boldsymbol{d}}^+), \tag{2.16d}$$

where the dimensionless operators $\hat{\boldsymbol{d}}^{\pm}$ and the basic polarization vectors $\boldsymbol{\varepsilon}_q$ have been defined above in (2.10) and (2.8). Note that the transfer by spontaneous emission satisfies the following selection rule:

$$\langle J_e m|\sigma|J_e m'\rangle \to \langle J_g \mu|\sigma|J_g \mu'\rangle \qquad \text{with } \mu - \mu' = m - m', \tag{2.17}$$

which is actually a consequence of the rotational invariance of the atom-vacuum field interaction Hamiltonian V_{AV}. According to (2.16), the transfer rate associated with (2.17) is just the product of Γ by the two Clebsch-Gordan coefficients connecting m to μ and m' to μ'.

Calculating the commutator of (2.14), and using (2.15), (2.4) and (2.16), we finally get

$$\dot{\sigma}_{ee} = -\Gamma\sigma_{ee} + i[G^{+}(\boldsymbol{r})\tilde{\sigma}_{ge} - \tilde{\sigma}_{eg}G^{-}(\boldsymbol{r})], \tag{2.18a}$$

$$\dot{\tilde{\sigma}}_{eg} = -\left(\frac{\Gamma}{2} - i\delta\right)\tilde{\sigma}_{eg} + i[G^{+}(\boldsymbol{r})\sigma_{gg} - \sigma_{ee}G^{+}(\boldsymbol{r})], \tag{2.18b}$$

$$\dot{\sigma}_{gg} = \left(\frac{\mathrm{d}}{\mathrm{d}t}\sigma_{gg}\right)_{sp} + i[G^{-}(\boldsymbol{r})\tilde{\sigma}_{eg} - \tilde{\sigma}_{ge}G^{+}(\boldsymbol{r})], \tag{2.18c}$$

where we have used

$$\tilde{\sigma}_{eg} = \sigma_{eg}\exp[i\omega_L t] \tag{2.19a}$$

instead of σ_{eg} in order to eliminate any explicit time dependence in the coefficients of the equations and where

$$\delta = \omega_L - \omega_A \tag{2.19b}$$

is the detuning between the laser frequency ω_L and the atomic frequency ω_A. Note that, if the atom is moving, there is an implicit time dependence through $\boldsymbol{r} = \boldsymbol{r}_0 + \boldsymbol{v}_0 t$.

2·2.3. Expression of the mean force. According to (2.30) in ref. [1] and eq. (2.4) above, the mean force can be written

$$\mathscr{F}(\boldsymbol{r}, t) = -\langle \nabla V_{AL}(\boldsymbol{r}, t)\rangle = +\sum_{i=x,y,z}\langle d_i^{+}\rangle \nabla E_{Li}^{+}(\boldsymbol{r})\exp[-i\omega_L t] + \text{h.c.} \tag{2.20}$$

Using (2.5) and (2.19), the mean value of d_i^{+} which appears in (2.20) can be re-expressed as

$$\langle d_i^{+}\rangle = \mathrm{Tr}\{P_e d_i P_g \sigma\} = \mathrm{Tr}\{d_i \sigma_{ge}\} = \mathrm{Tr}\{d_i \tilde{\sigma}_{ge}\}\exp[i\omega_L t], \tag{2.21}$$

which, inserted into (2.20), yields

$$\mathscr{F}(\boldsymbol{r}, t) = \sum_{i=x,y,z}\mathrm{Tr}\{d_i \tilde{\sigma}_{ge}\}\nabla E_{Li}^{+}(\boldsymbol{r}) + \text{c.c.} \tag{2.22}$$

Equation (2.22) clearly shows that the mean radiative force only depends on the optical coherences $\tilde{\sigma}_{eg}$ and $\tilde{\sigma}_{ge}$.

2·3. *Limit of low saturation and low velocity.*

2·3.1. New possible approximations. Except for the semi-classical and rotating-wave approximations, eqs. (2.18) are exact. We now consider the low-saturation limit ($s \ll 1$), which is the relevant limit for the new cooling mechanisms. In such a limit, the characteristic times for the evolution of the ground state become much longer than those of the excited state. It follows that σ_{gg} is a slow variable compared to $\tilde{\sigma}_{eg}$ and σ_{ee}. After a short transient regime, lasting for

a time on the order of $\tau_R = \Gamma^{-1}$, σ_{gg} «slaves» the other variables by imposing its slow rate of variation on $\tilde{\sigma}_{eg}$, $\tilde{\sigma}_{ge}$ and σ_{ee}, so that one can write

$$|\dot{\sigma}_{ee}| \ll \Gamma\sigma_{ee}, \qquad |\dot{\tilde{\sigma}}_{eg}| \ll \Gamma|\tilde{\sigma}_{eg}|. \tag{2.23}$$

It is then possible to use the inequalities (2.23) to neglect the left-hand side of eqs. (2.18*a*) and (2.18*b*) in comparison with the damping terms $-\Gamma\sigma_{ee}$ and $-(\Gamma/2)\tilde{\sigma}_{eg}$ which appear in the right-hand side. This yields algebraic equations allowing σ_{ee} and $\tilde{\sigma}_{eg}$ to be re-expressed in terms of σ_{gg}. Such a procedure is called «adiabatic elimination of the fast variables» and leads for these fast variables to expressions describing how they adjust themselves at each time to the value taken at this time by the slowly varying variable.

Such an argument is in fact valid only for an atom at rest, the rate of variation of σ being only due to the absorption and emission processes. For a moving atom, one must not forget that the time derivatives $\dot{\sigma}_{ab}$ appearing in the left-hand side of (2.18) are actually total time derivatives $\mathrm{d}/\mathrm{d}t = \partial/\partial t + \boldsymbol{v}_0 \cdot \nabla$, so that one must also consider the order of magnitude of the terms $\boldsymbol{v}_0 \cdot \nabla\sigma_{ab} \simeq k_L v_0 \sigma_{ab}$. Actually, with the new cooling mechanisms, the typical r.m.s. steady-state velocities reach very low values, for which

$$\eta = \frac{k_L v_0}{\Gamma} \ll 1. \tag{2.24}$$

This is why we will restrict ourselves in the remaining part of this lecture to calculations done at the zeroth order in η. Such an approximation, which allows us to neglect $\dot{\sigma}_{ee}$ and $\dot{\tilde{\sigma}}_{eg}$ in (2.18), even for a moving atom, eliminates any possibility of taking into account Doppler cooling which appears to the first order in η, but we are interested now in new cooling mechanisms which are much more efficient than Doppler cooling, and the equations so obtained will be much simpler. Note finally that we do not neglect in (2.18*c*) $\partial\sigma_{gg}/\partial t$ and $\boldsymbol{v}_0 \cdot \nabla\sigma_{gg}$, because σ_{gg} is a slow variable and the Doppler shift $k_L v_0$ can no longer be neglected in comparison with the characteristic evolution frequencies of σ_{gg}.

2·3.2. Adiabatic elimination of the excited state. First we eliminate optical coherences. Neglecting $\dot{\tilde{\sigma}}_{eg}$ in (2.18*b*) leads to

$$\tilde{\sigma}_{eg} = -\frac{1}{\delta + i\dfrac{\Gamma}{2}} G^+(\boldsymbol{r})\,\sigma_{gg}, \tag{2.25a}$$

$$\tilde{\sigma}_{ge} = -\frac{1}{\delta - i\dfrac{\Gamma}{2}} \sigma_{gg} G^-(\boldsymbol{r}). \tag{2.25b}$$

We have actually neglected the contribution of σ_{ee} to (2.25). The reason is that σ_{ee} is at least of order 2 in the Rabi frequency Ω_1 (see eq. (2.28) below). Since σ_{ee} is multiplied in (2.18*a*) by G^+, which is of order 1 in Ω_1, the contribution of σ_{ee} to

(2.25) is at least of order 3. We restrict ourselves here to calculations up to order 2 in Ω_1. This is why σ_{ee} does not appear in (2.25).

Having re-expressed $\tilde{\sigma}_{eg}$ and $\tilde{\sigma}_{ge}$ in terms of σ_{gg}, we can now obtain a new expression for the mean force $\mathscr{F}$. Inserting (2.25) into (2.22) yields

$$\mathscr{F}(\boldsymbol{r}) = \frac{-1}{\delta - i\frac{\Gamma}{2}} \sum_{i=x,y,z} \mathrm{Tr}\{G^-(\boldsymbol{r})\, d_i^+\, \sigma_{gg}\}\, \nabla E_{Li}^+(\boldsymbol{r}) + \text{c.c.} = \tag{2.26}$$

$$= \frac{-\hbar}{\delta - i\frac{\Gamma}{2}} \langle G^-(\boldsymbol{r})\, (\nabla G^+(\boldsymbol{r}))\rangle + \text{c.c.}$$

We have used (2.7) and the simpler notation

$$\langle X\rangle = \mathrm{Tr}\{X\sigma_{gg}\}. \tag{2.27}$$

We turn now to eq. (2.18a) giving $\dot{\sigma}_{ee}$. Neglecting $\dot{\sigma}_{ee}$ and using (2.25) for eliminating $\tilde{\sigma}_{eg}$ and $\tilde{\sigma}_{ge}$, we get

$$\sigma_{ee} = -\frac{i}{\Gamma} \frac{1}{\delta - i\frac{\Gamma}{2}} G^+(\boldsymbol{r})\, \sigma_{gg}\, G^-(\boldsymbol{r}) + \text{h.c.} = \tag{2.28}$$

$$= \frac{1}{\delta^2 + \frac{\Gamma^2}{4}} G^+(\boldsymbol{r})\, \sigma_{gg}\, G^-(\boldsymbol{r}) = \frac{\frac{\Omega_1^2}{4}}{\delta^2 + \frac{\Gamma^2}{4}} (\boldsymbol{\varepsilon}(\boldsymbol{r})\cdot\hat{\boldsymbol{d}}^+)\, \sigma_{gg}\, (\boldsymbol{\varepsilon}^*(\boldsymbol{r})\cdot\hat{\boldsymbol{d}}^-).$$

2·3.3. Equation of motion of the ground-state density matrix. It remains to transform the last equation (2.18c) describing the evolution of σ_{gg}. Using (2.16), (2.25) and (2.28), we get

$$\dot{\sigma}_{gg} = \frac{-i}{\delta + i\frac{\Gamma}{2}} G^-(\boldsymbol{r})\, G^+(\boldsymbol{r})\, \sigma_{gg} + \frac{i}{\delta - i\frac{\Gamma}{2}} \sigma_{gg}\, G^-(\boldsymbol{r})\, G^+(\boldsymbol{r}) + \tag{2.29}$$

$$+ \frac{\Gamma}{\delta^2 + \frac{\Gamma^2}{4}} \sum_{q=-1,0,+1} \boldsymbol{\varepsilon}_q^* \cdot \hat{\boldsymbol{d}}^-\, G^+(\boldsymbol{r})\, \sigma_{gg}\, G^-(\boldsymbol{r})\, \boldsymbol{\varepsilon}_q \cdot \hat{\boldsymbol{d}}^+,$$

which is a closed equation of motion for σ_{gg}, since it relates $\dot{\sigma}_{gg}$ only to σ_{gg}. The first line of (2.29) describes the effect of the laser excitation, whereas the second line describes the effect of spontaneous emission.

We now separate the real and the imaginary parts of $1/(\delta \pm i\Gamma/2)$. This allows one to transform the first line of (2.29), which will be noted $(\dot{\sigma}_{gg})_{las}$, as a

sum of two terms, the first one involving a commutator and the second one an anticommutator

$$(\dot{\sigma}_{gg})_{las} = -i\frac{\delta}{\delta^2 + \frac{\Gamma^2}{4}}[G^-(\boldsymbol{r})G^+(\boldsymbol{r}), \sigma_{gg}] - \frac{\frac{\Gamma}{2}}{\delta^2 + \frac{\Gamma^2}{4}}\{G^-(\boldsymbol{r})G^+(\boldsymbol{r}), \sigma_{gg}\}_+ . \tag{2.30}$$

In (2.30), $\{X, Y\}_+$ means $XY + YX$. Note that the operator $G^-(\boldsymbol{r})G^+(\boldsymbol{r})$ is Hermitian and semi-positive since $G^- = (G^+)^\dagger$,

$$(G^-(\boldsymbol{r})G^+(\boldsymbol{r}))^\dagger = G^-(\boldsymbol{r})G^+(\boldsymbol{r}), \tag{2.31}$$

so that its eigenvalues are real and non negative. Equations having the same structure as (2.30) and (2.29) have been derived for the first time in ref. [4] and [5] dealing with the quantum theory of the optical-pumping cycle. The pumping light was not monochromatic, as is the case here, but a broad-band incoherent light, so that eqs. (2.29) and (2.30) had to be averaged over the spectral distribution $I(\omega_L)$ of the incoming light.

Equations (2.29) and (2.30) can still be transformed, using (2.7), (2.10), (2.11) and (2.13). Introducing in G^-G^+ the Hermitian, semi-positive and dimensionless operator

$$\Lambda(\boldsymbol{r}) = (\boldsymbol{\varepsilon}^*(\boldsymbol{r})\cdot\hat{\boldsymbol{d}}^-)(\boldsymbol{\varepsilon}(\boldsymbol{r})\cdot\hat{\boldsymbol{d}}^+) = \Lambda^\dagger(\boldsymbol{r}) \tag{2.32}$$

and the parameters Γ' and δ' analogous to those defined in (6.15) in ref. [1]

$$\Gamma'(\boldsymbol{r}) = \Gamma\frac{\frac{\Omega_1^2(\boldsymbol{r})}{4}}{\delta^2 + \frac{\Gamma^2}{4}} = \Gamma\frac{s(\boldsymbol{r})}{2}, \tag{2.33a}$$

$$\delta'(\boldsymbol{r}) = \delta\frac{\frac{\Omega_1^2(\boldsymbol{r})}{4}}{\delta^2 + \frac{\Gamma^2}{4}} = \delta\frac{s(\boldsymbol{r})}{2}, \tag{2.33b}$$

where the saturation parameter $s(\boldsymbol{r})$ is given by

$$s(\boldsymbol{r}) = \frac{\frac{\Omega_1^2(\boldsymbol{r})}{2}}{\delta^2 + \frac{\Gamma^2}{4}}, \tag{2.34}$$

we get for σ_{gg} the following equation of motion:

$$\dot{\sigma}_{gg} = -i\delta'(\boldsymbol{r})[\Lambda(\boldsymbol{r}), \sigma_{gg}] - \frac{\Gamma'(\boldsymbol{r})}{2}\{\Lambda(\boldsymbol{r}), \sigma_{gg}\}_+ + \Gamma'(\boldsymbol{r}) \sum_{q=-1,0,+1} (\boldsymbol{\varepsilon}_q^* \cdot \hat{\boldsymbol{d}}^-)(\boldsymbol{\varepsilon}(\boldsymbol{r}) \cdot \hat{\boldsymbol{d}}^+) \sigma_{gg} (\boldsymbol{\varepsilon}^*(\boldsymbol{r}) \cdot \hat{\boldsymbol{d}}^-)(\boldsymbol{\varepsilon}_q \cdot \hat{\boldsymbol{d}}^+). \tag{2.35}$$

2·4. *Light shifts of the ground-state sublevels.*

2·4.1. Hamiltonian part of the equations of motion. The terms involving a commutator in (2.30) and (2.35) can be written as $[H_{\text{eff}}(\boldsymbol{r}), \sigma_{gg}]/i\hbar$, where

$$H_{\text{eff}} = \frac{\hbar\delta}{\delta^2 + \dfrac{\Gamma^2}{4}} G^-(\boldsymbol{r}) G^+(\boldsymbol{r}) = \hbar\delta'(\boldsymbol{r})\Lambda(\boldsymbol{r}). \tag{2.36}$$

The corresponding rate of variation is the same as the one which would be induced by the effective Hamiltonian $H_{\text{eff}}(\boldsymbol{r})$.

We will call $|g_\alpha(\boldsymbol{r})\rangle$ the eigenstates of $\Lambda(\boldsymbol{r})$ and $\lambda_\alpha(\boldsymbol{r})$ the corresponding eigenvalues, which are real and non negative since $\Lambda(\boldsymbol{r})$ is Hermitian and semi-positive:

$$\Lambda(\boldsymbol{r})|g_\alpha(\boldsymbol{r})\rangle = \lambda_\alpha(\boldsymbol{r})|g_\alpha(\boldsymbol{r})\rangle, \qquad \lambda_\alpha(\boldsymbol{r}) \text{ real and } \geqslant 0. \tag{2.37}$$

If the term associated with (2.36) were alone in the equation of motion of σ_{gg}, one would find that the Zeeman degeneracy in g is removed (if the λ_α are all different) and that the states $|g_\alpha(\boldsymbol{r})\rangle$ get a well-defined energy shift δE_α, called light shift and equal to

$$\delta E_\alpha = \hbar\delta'\lambda_\alpha. \tag{2.38}$$

2·4.2. Properties of light shifts. The light shifts δE_α are, as δ', proportional to Ω_1^2, *i.e.* to the laser intensity I_L. Since the λ_α are positive (see (2.37)), all the δE_α have the same sign, which is the sign of δ, according to (2.33*b*).

The variations with the detuning δ of the light shifts δE_α are those of a Lorentz dispersion curve, corresponding to a reactive effect. Using the analysis of sect. 6.2 in ref. [1], and in particular the diagram *b* of fig. 9, one can also consider that the light shifts are associated with a virtual absorption and re-emission of the incident photon (contamination of $|g, \boldsymbol{p}; \boldsymbol{k}_L \boldsymbol{\varepsilon}_L\rangle$ by $|e, \boldsymbol{p} + \hbar\boldsymbol{k}_L; 0\rangle$). Light shifts can be considered as the equivalent, for the absorption process, of the Lamb shift (which is associated with the virtual emission and reabsorption of a spontaneous photon). Another equivalent picture for light shifts is to consider them as the polarization

energy of the induced atomic-dipole moment in the driving laser field, which explains the denomination «a.c.-Stark shifts» which is sometimes used.

The first observations of light shifts [5-7] predate the use of lasers in atomic physics. They were induced by the light coming from an ordinary discharge lamp (this is why they were called «Lamp shifts» by A. KASTLER, in a word play indicating their origin and their analogy with the Lamb shift). The fact that the light shifts depend on the polarization of the light beam and vary from one ground-state sublevel to the other was essential for their observation. Because of the length of relaxation times in atomic ground states, magnetic-resonance curves in atomic ground states are very narrow, and even if the light shifts of two ground-state sublevels differ only by a few Hz, such an effect can be easily detected as a shift of the magnetic-resonance curve [6].

To conclude this subsection, we point out a few symmetry properties of the effective Hamiltonian (2.36). The two operators $\hat{\boldsymbol{d}}^{\pm}$ appearing in the expression (2.32) of Λ are vectorial operators. It follows that the expansion of H_{eff} in irreducible tensor operators $T_q^{(k)}$ of rank k can contain only terms with $k = 0, 1, 2$. The corresponding terms of H_{eff} describe, respectively, a global shift of the ground state ($k = 0$) and a removal of degeneracy equivalent to the one which would be produced by a fictitious magnetic ($k = 1$) or electric ($k = 2$) static field, the direction of these fictitious fields being determined by the polarization vector $\boldsymbol{\varepsilon}(\boldsymbol{r})$. The interested reader may find more details in ref. [8, 9].

2·5. *Relaxation associated with optical pumping.*

2·5.1. Departure rates. The second term of (2.35) describes how the atomic ground state is emptied by the absorption process. The contribution of this term to the rate of variation of the diagonal element of σ in the eigenstate $|g_\alpha\rangle$ of Λ can be written

$$(\langle g_\alpha | \dot{\sigma} | g_\alpha \rangle)_{\text{abs}} = -\Gamma'_\alpha \langle g_\alpha | \sigma | g_\alpha \rangle , \tag{2.39}$$

where

$$\Gamma'_\alpha = \Gamma' \lambda_\alpha \tag{2.40}$$

can be interpreted as a rate of departure from the state $|g_\alpha\rangle$. Note that Γ'_α is nonnegative as λ_α (see eq. (2.37)), is proportional to the laser intensity $I_L \sim \Omega_1^2$ (as Γ'), and varies with the detuning δ as a Lorentz absorption curve (dissipative effect).

The fact that the λ_α's are not all equal means that the departure rates vary from one sublevel to the other. If one λ_α vanishes, there is no possibility for an atom in the corresponding sublevel $|g_\alpha\rangle$ to leave such a state by photon absorption. The sublevel $|g_\alpha\rangle$ then appears as a trap state.

2·5.2. Feeding of the ground state by spontaneous emission. The atoms which have left the ground state by photon absorption fall back in the ground state by spontaneous emission. Such an effect is described by the last term of (2.35) which is, as the second one, proportional to Γ' (dissipative effect).

One can easily check that the trace of the second term of (2.35) is opposite to the trace of the third one (*). This means that there are as many atoms leaving g per unit time as atoms falling back in g.

As a consequence of these absorption-spontaneous emission cycles, population differences can build up between the various Zeeman sublevels. This is the well-known principle of optical pumping [10]. Such a process can be actually considered as a transfer of angular momentum from the incident polarized photons to the atoms. For example, if the incident light beam is propagating along $0z$ and has a right circular polarization σ^+ corresponding to photons having an angular momentum $+\hbar$ along $0z$, one can easily show that optical pumping concentrates the atomic population in the Zeeman sublevel with the highest value of the magnetic quantum number along $0z$. An example of such a situation will be given in sect. 3.

Optical pumping appears thus as a relaxation process, described by the last two terms of (2.35), and leading the internal atomic state to a new equilibrium state, which generally is quite different from the thermodynamic equilibrium. The characteristic time constants of optical pumping are on the order of

$$\tau_P = \frac{1}{\Gamma'} . \tag{2.41}$$

The pumping time τ_P is inversely proportional to the laser intensity I_L and can become very long if $I_L \to 0$.

2·5.3. Zeeman coherence effects. It may happen that atoms are submitted to two perturbations with different symmetries. For example, a σ^+ polarized beam propagating along the $0x$ axis tends to create in the ground state a magnetization along $0x$. If one applies a static magnetic field $\boldsymbol{B}$ along the $0z$ axis, this magnetization starts to precess around $0z$ with a Larmor frequency Ω_B proportional to B. Such a precession will wash out the anisotropy along $0x$ introduced by the pumping beam if, during the characteristic damping time τ_g of the ground state (pumping time τ_P, or more generally relaxation time including the effect of collisions, the finite duration of the interaction...), the rotation angle $\Omega_B \tau_g$ is not small compared to 1. It follows that, when B is scanned around zero, the anisotropy introduced by the pumping beam in the ground state un-

(*) The trace of the first term of (2.35), which is a commutator, vanishes. This means that light shifts (which are a reactive effect) cannot change the total population of the ground state.

dergoes resonant variations which can be detected by changes in the light absorbed or emitted by the atoms. This is the well-known Hanle effect which has been first observed in atomic excited states [11]. The interest of Hanle resonances in atomic ground states is that they are very narrow, since τ_g can be very long. These resonances may thus be used to detect very small magnetic fields, smaller than 10^{-9} G [12, 13]. Note that, since Hanle resonances correspond to resonant variations of the photon absorption rate when B is scanned, the momentum transferred to the atomic trajectories varies also in a resonant way. Hanle resonances have been recently detected in this way, by monitoring the deflection of an atomic beam [14].

In eq. (2.35), the Hanle resonances appear as resonant variations of the Zeeman coherences (off-diagonal elements of σ in the basis of eigenstates of J_z). They represent an example, among others, of situations where optical pumping cannot be described only in terms of populations (see, for example, ref. [5]).

2·5.4. Case of a moving atom. All previous considerations suppose implicitly that the atom is at rest, so that it «sees» a pumping light with a constant intensity and a constant polarization. If the atom is moving, and if the laser configuration is such that the local polarization varies in space, the moving atom will «see», in its rest frame, a time-varying polarization. Since it reacts to these variations of optical pumping with a characteristic time on the order of τ_P, its internal state in $\boldsymbol{r}$ will lag behind the steady state of an atom which would be at rest at the same point. We will discuss later on the role played by such a time lag in the new cooling mechanisms.

2·6. *General properties of the mean force.* – We come back now to the approximate expression (2.26) of the mean force, deduced from the general expression (2.22) after adiabatic elimination of the optical coherences. In this last subsection, we discuss the physical content of eq. (2.26), and we point out the connection which exists, in the low-saturation and low-velocity limit, between the mean force and the light shifts and absorption rates discussed in subsect. 2·4 and 2·5. Other similar treatments can be found in ref. [15] and [16].

2·6.1. Reactive component and dissipative component. In (2.26), we split $1/(\delta - i\Gamma/2)$ into its real and imaginary parts. We will call reactive and dissipative the components of the mean force respectively proportional to these real and imaginary parts:

$$(2.42a) \qquad \mathscr{F}_{\text{react}}(\boldsymbol{r}) = -\hbar \frac{\delta}{\delta^2 + \frac{\Gamma^2}{4}} [\langle G^-(\boldsymbol{r})(\nabla G^+(\boldsymbol{r}))\rangle + \langle (\nabla G^-(\boldsymbol{r}))\, G^+(\boldsymbol{r})\rangle],$$

$$\mathscr{F}_{\text{dissip}}(\boldsymbol{r}) = i\hbar \frac{\frac{\Gamma}{2}}{\delta^2 + \frac{\Gamma^2}{4}} [\langle (\nabla G^-(\boldsymbol{r}))\, G^+(\boldsymbol{r})\rangle - \langle G^-(\boldsymbol{r})\,(\nabla G^+(\boldsymbol{r}))\rangle]. \tag{2.42b}$$

The denomination reactive and dissipative comes from the δ-dependence of the real and imaginary parts of $1/(\delta - i\Gamma/2)$. Note, however, that the δ-dependence of $\mathscr{F}_{\text{react}}$ and $\mathscr{F}_{\text{dissip}}$ is not entirely determined by the two terms which multiply the brackets of (2.42*a*) and (2.42*b*). The average values which appear inside the brackets depend on the ground-state density matrix σ_{gg} which is obtained by solving eq. (2.29). Such a solution is itself a function of δ and Γ, so that the final expressions of $\mathscr{F}_{\text{react}}$ and $\mathscr{F}_{\text{dissip}}$ will have a more complicated dependence on δ and Γ. Note also that, even if $|\delta| \gg \Gamma$, we must not conclude that $\mathscr{F}_{\text{react}}$ is much larger than $\mathscr{F}_{\text{dissip}}$, since the bracket of (2.42*b*) can be much larger than the bracket of (2.42*a*).

One can still give a useful equivalent expression of $\mathscr{F}_{\text{react}}$ and $\mathscr{F}_{\text{dissip}}$ by using an expansion of the laser electric field $\boldsymbol{E}_{\text{L}}$ in plane waves. If we use for the positive-frequency component $\boldsymbol{E}_{\text{L}}^+$ the expansion

$$\boldsymbol{E}_{\text{L}}^+(\boldsymbol{r}) = \sum_\mu \boldsymbol{E}_\mu^+(\boldsymbol{r}), \tag{2.43}$$

where the $\boldsymbol{r}$-dependence of $\boldsymbol{E}_\mu^+$ is given by

$$\boldsymbol{E}_\mu^+(\boldsymbol{r}) \sim \exp[i\boldsymbol{k}_\mu \cdot \boldsymbol{r}], \tag{2.44}$$

then we can write

$$\nabla G^\pm = \pm i \sum_\mu \boldsymbol{k}_\mu G_\mu^\pm, \tag{2.45}$$

where, according to (2.7) and (2.43),

$$\hbar G_\mu^\pm = \boldsymbol{d}^\pm \cdot \boldsymbol{E}_\mu^\pm(\boldsymbol{r}). \tag{2.46}$$

Inserting (2.45) into (2.42) finally gives

$$\mathscr{F}_{\text{react}} = -i \frac{\delta}{\delta^2 + \frac{\Gamma^2}{4}} \sum_\mu \sum_\nu \hbar \boldsymbol{k}_\mu [\langle G_\nu^- G_\mu^+\rangle - \langle G_\mu^- G_\nu^+\rangle], \tag{2.47a}$$

$$\mathscr{F}_{\text{dissip}} = +\frac{\frac{\Gamma}{2}}{\delta^2 + \frac{\Gamma^2}{4}} \sum_\mu \sum_\nu \hbar \boldsymbol{k}_\mu [\langle G_\nu^- G_\mu^+\rangle + \langle G_\mu^- G_\nu^+\rangle]. \tag{2.47b}$$

2·6.2. Interpretation of the reactive component. Comparing the expression (2.42*a*) of $\mathscr{F}_{\text{react}}$ and the expression (2.36) of the effective Hamiltonian H_{eff} describing the light shifts of the ground-state sublevels shows that $\mathscr{F}_{\text{react}}$

can be written

$$\mathscr{F}_{\text{react}} = -\langle \nabla H_{\text{eff}} \rangle , \tag{2.48}$$

which clearly demonstrates the close connection which exists between the reactive component of the mean force and light shifts.

An equivalent expression of H_{eff} in terms of its eigenvalues E_α and eigenstates $|g_\alpha\rangle$ is

$$H_{\text{eff}} = \sum_\alpha E_\alpha(\boldsymbol{r}) |g_\alpha(\boldsymbol{r})\rangle\langle g_\alpha(\boldsymbol{r})| . \tag{2.49}$$

Taking the gradient of (2.49) (and omitting $\boldsymbol{r}$ to simplify the notation) gives

$$\nabla H_{\text{eff}} = \sum_\alpha (\nabla E_\alpha) |g_\alpha\rangle\langle g_\alpha| + \sum_\alpha E_\alpha [(\nabla |g_\alpha\rangle)\langle g_\alpha| + |g_\alpha\rangle(\nabla\langle g_\alpha|)] , \tag{2.50}$$

which, inserted into (2.48), leads to

$$\begin{aligned} \mathscr{F}_{\text{react}} = & -\sum_\alpha (\nabla E_\alpha) \Pi_\alpha - \\ & - \sum_\alpha E_\alpha [\langle g_\alpha | \sigma (\nabla |g_\alpha\rangle) + (\nabla\langle g_\alpha|)\sigma |g_\alpha\rangle] , \end{aligned} \tag{2.51}$$

where

$$\Pi_\alpha = \langle g_\alpha | \sigma | g_\alpha \rangle \tag{2.52}$$

is the population of the ground-state sublevels $|g_\alpha\rangle$.

The first term of (2.51) has a straightforward interpretation, analogous to the dressed-atom interpretation of the mean dipole force given in sect. 7.3 of ref. [1] for a 2-level atom (see eq. (7.10)). This term is just the average value of the forces $-\nabla E_\alpha$ associated with the spatial gradients of the light-shifted ground-state sublevels, weighted by the probabilities of occupation Π_α of these sublevels.

In order to interpret the second line of (2.51), we suppose that the atom is displaced from $\boldsymbol{r}$ to $\boldsymbol{r} + \mathrm{d}\boldsymbol{r}$, and we calculate the work done against the reactive force

$$\begin{aligned} -\mathscr{F}_{\text{react}} \cdot \mathrm{d}\boldsymbol{r} = & \sum_\alpha \Pi_\alpha \cdot \mathrm{d}E_\alpha + \\ & + \sum_\alpha E_\alpha [\langle g_\alpha | \sigma | \mathrm{d}g_\alpha\rangle + \langle \mathrm{d}g_\alpha | \sigma | g_\alpha\rangle] , \end{aligned} \tag{2.53}$$

where $\mathrm{d}E_\alpha$ and $|\mathrm{d}g_\alpha\rangle$, given by

$$\mathrm{d}E_\alpha = \mathrm{d}\boldsymbol{r} \cdot \nabla E_\alpha , \tag{2.54a}$$

$$|\mathrm{d}g_\alpha\rangle = \mathrm{d}\boldsymbol{r} \cdot \nabla |g_\alpha\rangle , \tag{2.54b}$$

represent the variations of E_α and $|g_\alpha\rangle$ between $\boldsymbol{r}$ and $\boldsymbol{r} + \mathrm{d}\boldsymbol{r}$. The second line of (2.53), which originates from the second line of (2.51), is associated with the

spatial variations of the wave functions of the sublevels $|g_\alpha\rangle$. It can be written, to first order in $d\boldsymbol{r}$,

$$\sum_\alpha E_\alpha \, d\Pi_\alpha^{\text{nonad}}, \tag{2.55}$$

where

$$d\Pi_\alpha^{\text{nonad}} = \langle g_\alpha(\boldsymbol{r} + d\boldsymbol{r})|\sigma|g_\alpha(\boldsymbol{r} + d\boldsymbol{r})\rangle - \langle g_\alpha(\boldsymbol{r})|\sigma|g_\alpha(\boldsymbol{r})\rangle \tag{2.56}$$

is the nonadiabatic variation of the population of the state $|g_\alpha\rangle$ due to the spatial variations of the wave functions. It follows that the second line of (2.51) represents the contribution of nonadiabatic transitions between the various ground-state sublevels, induced by atomic motion and due to the spatial variations of the wave functions of the light-shifted ground-state sublevels.

Finally, we discuss the physical content of eq. (2.47*a*), deduced from the plane-wave expansion of the laser field. Since the force exerted by the laser beam comes from a disappearance of photons $\boldsymbol{k}_\mu$ from the various plane waves μ forming the laser wave, each of these photons carrying a momentum $\hbar\boldsymbol{k}_\mu$, one can interpret the coefficient of $\hbar\boldsymbol{k}_\mu$ in (2.47*a*) as the mean number of photons absorbed per unit time in the plane wave μ. The fact that this coefficient depends on ν means that the field $\boldsymbol{E}_\mu$ of the plane wave μ interacts with the atomic dipole induced by the wave ν. It follows that

$$\frac{dN_{\mu\nu}^{\text{react}}}{dt} = -i\frac{\delta}{\delta^2 + \dfrac{\Gamma^2}{4}}[\langle G_\nu^- G_\mu^+\rangle - \langle G_\mu^- G_\nu^+\rangle] \tag{2.57}$$

can be interpreted as the mean number of photons μ absorbed per unit time out of the wave μ interacting with the reactive component of the dipole moment induced by the wave ν. We take here the reactive component of the dipole moment because of the δ-dependence of (2.57). From (2.57), it follows that

$$\frac{dN_{\mu\mu}^{\text{react}}}{dt} = 0, \tag{2.58a}$$

$$\frac{dN_{\mu\nu}^{\text{react}}}{dt} = -\frac{dN_{\nu\mu}^{\text{react}}}{dt}. \tag{2.58b}$$

Such a result is easy to understand. Reactive effects involving a single wave cannot lead to photon absorption. This is the meaning of (2.58*a*). But, according to (2.58*b*), photons can disappear from one wave, μ for example, and reappear in the other wave ν of the pair $\mu\nu$. This is a redistribution process. During such a process, the total energy of the field does not change, because the waves μ, ν have the same frequency. But, since $\boldsymbol{k}_\mu \neq \boldsymbol{k}_\nu$, there is a change of momentum of the field. The corresponding change of the atomic momentum is at the origin of

$\mathscr{F}_{\text{react}}$, which can be written according to (2.57)

$$\mathscr{F}_{\text{react}} = \sum_{\text{pairs } \mu\nu} \hbar(\boldsymbol{k}_\mu - \boldsymbol{k}_\nu) \frac{\mathrm{d}N_{\mu\nu}^{\text{react}}}{\mathrm{d}t}. \tag{2.59}$$

2·6.3. Interpretation of the dissipative component. Using the same type of argument as in the previous subsection, one shows from (2.47*b*) that

$$\frac{\mathrm{d}N_{\mu\nu}^{\text{dissip}}}{\mathrm{d}t} = \frac{\frac{\Gamma}{2}}{\delta^2 + \frac{\Gamma^2}{4}} [\langle G_\nu^- G_\mu^+ \rangle + \langle G_\mu^- G_\nu^+ \rangle] \tag{2.60}$$

is the number of photons absorbed per unit time out of the wave μ interacting with the dissipative component of the dipole moment induced by the wave ν.

The equations corresponding to (2.58) are now

$$\frac{\mathrm{d}N_{\mu\mu}^{\text{dissip}}}{\mathrm{d}t} = \frac{\Gamma}{\delta^2 + \frac{\Gamma^2}{4}} \langle G_\mu^- G_\mu^+ \rangle \neq 0, \tag{2.61a}$$

$$\frac{\mathrm{d}N_{\mu\nu}^{\text{dissip}}}{\mathrm{d}t} = + \frac{\mathrm{d}N_{\nu\mu}^{\text{dissip}}}{\mathrm{d}t}. \tag{2.61b}$$

The contribution of the wave μ alone to $\mathscr{F}_{\text{dissip}}$ is different from zero and equal to

$$\frac{\Gamma}{\delta^2 + \frac{\Gamma^2}{4}} \hbar \boldsymbol{k}_\mu \langle G_\mu^- G_\mu^+ \rangle. \tag{2.62}$$

Such a term represents the radiation pressure exerted by the wave μ independently of the other waves. Note, however, that (2.62) depends implicitly on the other waves ν since the average values appearing in (2.62) are taken in σ_{gg}, which itself is determined by the total laser field $\boldsymbol{E}_L$, *i.e.* by the whole set of plane waves forming $\boldsymbol{E}_L$.

There are also crossed terms $\mu \neq \nu$ in the expression (2.47*b*) of $\mathscr{F}_{\text{dissip}}$, the contribution of the pair (μ, ν) being equal to

$$\frac{\frac{\Gamma}{2}}{\delta^2 + \frac{\Gamma^2}{4}} \hbar(\boldsymbol{k}_\mu + \boldsymbol{k}_\nu) [\langle G_\nu^- G_\mu^+ \rangle + \langle G_\mu^- G_\nu^+ \rangle]. \tag{2.63}$$

Such terms describe interference effects between the waves μ and ν. The radiation pressure exerted by the wave μ is modified by the presence of the wave ν

and *vice versa*. Equation (2.61*b*) means that, if the absorption of the wave μ is modified by the presence of the wave ν, the absorption of the wave ν is modified by the same amount by the presence of the wave μ. We have not here a redistribution process as in the previous subsection, but a similar increase (or decrease) of the absorption of both waves due to interference effects.

2·6.4. Particular case of one-dimensional molasses. Suppose that the laser configuration is formed by two counterpropagating plane waves 1 and 2, with

$$\boldsymbol{k}_1 = \boldsymbol{k}\,, \qquad \boldsymbol{k}_2 = -\boldsymbol{k}\,. \tag{2.64}$$

As shown in subsect. 2·6.2, $\mathscr{F}_{\text{react}}$ is a pure redistribution force, which does not contain single-wave terms. Equation (2.59) becomes now, taking (2.64) into account,

$$\mathscr{F}_{\text{react}} = \frac{\delta}{\delta^2 + \dfrac{\Gamma^2}{4}} 2\hbar\boldsymbol{k}i[\langle G_1^- G_2^+ \rangle - \langle G_2^- G_1^+ \rangle]\,. \tag{2.65}$$

Since $\boldsymbol{k}_1 + \boldsymbol{k}_2 = \boldsymbol{0}$, the crossed term (2.63) of $\mathscr{F}_{\text{dissip}}$ vanishes. The radiation pressure of each wave is increased by the presence of the other wave, but these extra forces have the same modulus but opposite directions, so that they cancel out. We are left with a sum of single-wave terms which can be written

$$\mathscr{F}_{\text{dissip}} = \frac{\Gamma}{\delta^2 + \dfrac{\Gamma^2}{4}} \hbar\boldsymbol{k}[\langle G_1^- G_1^+ \rangle - \langle G_2^- G_2^+ \rangle]\,. \tag{2.66}$$

It follows that, for one-dimensional molasses, $\mathscr{F}_{\text{dissip}}$ is just equal to the difference between the radiation pressures exerted separately by the two waves.

We will conclude with a remark concerning the polarizations $\boldsymbol{\varepsilon}_1$ and $\boldsymbol{\varepsilon}_2$ of the two counterpropagating waves. If we take $\boldsymbol{k}_1 = -\boldsymbol{k}_2$ along $0z$, these polarization vectors are perpendicular to $0z$, because of the transversality of the field, and can, therefore, be considered as linear superpositions of the right and left circular polarizations σ^+ and σ^-. It follows that all the matrix elements of $G_\mu^- G_\nu^+$, with $\mu, \nu = 1$ or 2, in the ground-state manifold, satisfy the selection rule $\Delta m = 0, \pm 2$, where m is the magnetic quantum number along $0z$ (G_μ^- and G_ν^+ change m by $+1$ or -1). Consequently, if the angular momentum J_g of the ground state is equal to $J_g = 1/2$, one concludes that all the $G_\mu^- G_\nu^+$ are diagonal in the basis of eigenstates of J_z, and also $G^- G^+$. In such a case, the eigenstates of the effective Hamiltonian H_{eff}, which, according to (2.36), is proportional to $G^- G^+$, are independent of z.

3. – Low-intensity Sisyphus cooling.

3·1. *Introduction.* – During the last few years, spectacular developments have allowed the performances of laser cooling to be improved by orders of magnitude. The starting point of these developments was the demonstration, by the N.I.S.T. group at Gaithersburg, that the Doppler limit could be overcome [17]. For a discussion of this experiment and of the subsequent ones from various groups, we refer the reader to Phillips's lecture in this volume. The purpose of this section and the following one is to present a few new cooling mechanisms which, we think, are responsible for the very low temperatures which have been measured.

This section 3 is devoted to the analysis of a low-intensity version of the Sisyphus cooling mechanism presented in sect. 7 of ref. [1] for a 2-level atom moving in an intense laser standing wave (see also ref. [18]). As in that section, we have an atom moving in a bipotential, and jumping preferentially from the tops of the hills of one potential curve to the bottoms of the valleys of the other potential curve, so that, on the average, the atom is running up the hills more than down, as did Sisyphus in the Greek mythology. But, now, the bipotential is no longer associated with the two dressed states originating from the excited state e and the ground state g (more precisely from $|e, N\rangle$ and $|g, N+1\rangle$, where N denotes the number of laser photons). It is associated with two ground-state Zeeman sublevels which undergo spatially modulated light shifts and between which optical-pumping transitions occur with a rate which is also spatially modulated. We show that in this case a very efficient Sisyphus cooling can appear at very low intensity, when the saturation parameter s is very small.

We begin in subsect. 3·2 by introducing a one-dimensional model consisting of a laser configuration exhibiting strong polarization gradients and of a simple atomic transition leading to a mean radiative force which is only due to the spatial gradients of light shifts. Using the results of sect. 2, we determine in subsect. 3·3 the light shifts of the atomic ground-state sublevels as well as the optical-pumping transition rates between these sublevels. We then consider in subsect. 3·4 a moving atom and we show how the spatial modulation of light shifts and optical-pumping rates in the laser polarization gradient can conspire to produce a Sisyphus cooling. A more quantitative analysis is presented in subsect. 3·5 in the traditional case where the internal times T_{int} are much shorter than the external times T_{ext}. We evaluate the friction coefficient and give an order of magnitude of the equilibrium temperature. Finally, some indications are given in subsect. 3·6 on the less usual case where the external times become of the order of or shorter than the internal times. Such a case is actually important because it corresponds to the situation where the low-intensity Sisyphus cooling reaches its limits.

We will follow here the presentation of ref. [19] and [20]. More details may

be found in these references, and in ref. [21] which gives the results of a numerical integration of optical Bloch equations. A general review of the field is presented in ref. [22].

3·2. *Presentation of the model.*

3·2.1. Laser configuration. We consider two counterpropagating waves along $0z$, with orthogonal polarizations $\boldsymbol{\varepsilon}_x$ and $\boldsymbol{\varepsilon}_y$, and the same amplitude $\mathcal{E}_0$ (fig. 1*a*)). With an appropriate choice of the relative phases of the two waves, the laser electric field in z can be written

$$\boldsymbol{E}_{\mathrm{L}}(z, t) = \boldsymbol{E}_{\mathrm{L}}^{+}(z) \exp[-i\omega_{\mathrm{L}} t] + \text{c.c.} \tag{3.1}$$

with

$$\boldsymbol{E}_{\mathrm{L}}^{+}(z) = \frac{1}{2}(\boldsymbol{\varepsilon}_x \exp[ikz] - i\boldsymbol{\varepsilon}_y \exp[-ikz])\,\mathcal{E}_0 . \tag{3.2}$$

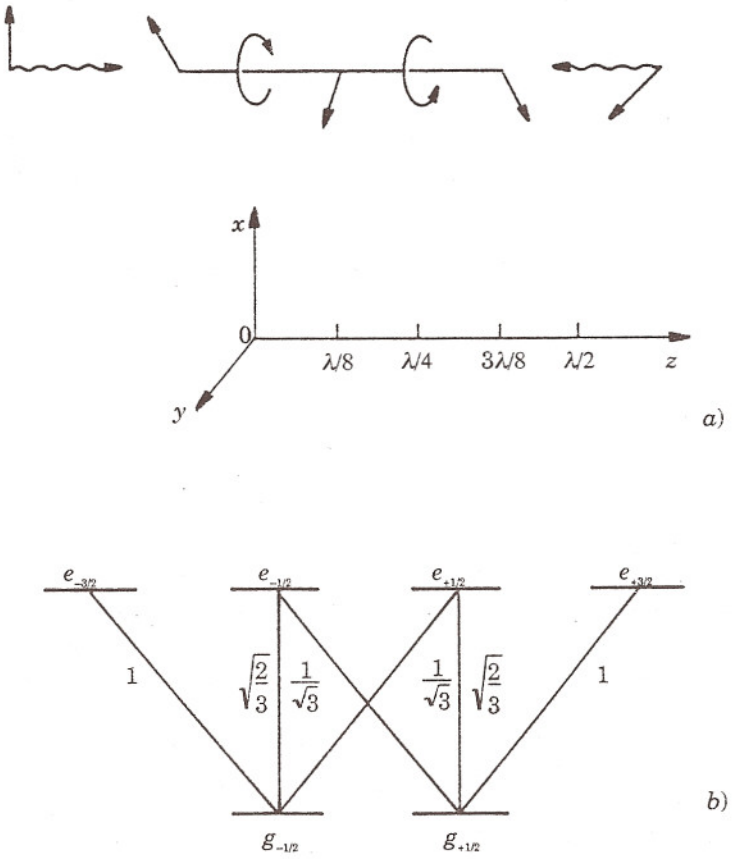

Fig. 1. – *a*) Lin ⊥ Lin laser configuration, exhibiting a strong polarization gradient along $0z$. *b*) Clebsch-Gordan coefficients for a $J_{\mathrm{g}} = 1/2 \leftrightarrow J_{\mathrm{e}} = 3/2$ transition.

As in (2.11), one can then write

$$\boldsymbol{E}_{\mathrm{L}}^{+}(z) = \frac{1}{2}\mathcal{E}_0\sqrt{2}\,\boldsymbol{\varepsilon}(z) = \frac{1}{2}\mathcal{E}_{\mathrm{L}}\,\boldsymbol{\varepsilon}(z)\,, \tag{3.3}$$

where $\mathcal{E}_{\mathrm{L}}$ is a real amplitude which is independent of z and equal to $\mathcal{E}_0\sqrt{2}$ and where the normalized polarization vector $\boldsymbol{\varepsilon}(z)$ is given by

$$\boldsymbol{\varepsilon}(z) = \cos kz\,\boldsymbol{\varepsilon}_{-} - i\sin kz\,\boldsymbol{\varepsilon}_{+}\,. \tag{3.4}$$

According to (3.4), the laser polarization is an elliptical one which is particularly simple in certain places: σ^- in $z = 0$, linear along $(\boldsymbol{\varepsilon}_x - \boldsymbol{\varepsilon}_y)/\sqrt{2}$ in $z = \lambda/8$, σ^+ in $z = \lambda/4$, linear along $(\boldsymbol{\varepsilon}_x + \boldsymbol{\varepsilon}_y)/\sqrt{2}$ in $z = 3\lambda/8$, σ^- in $z = \lambda/2$ and so on (see fig. 1*a*)).

The laser configuration of fig. 1*a*) exhibits, therefore, a strong gradient of ellipticity along $0z$, on a length scale equal to a fraction of wavelength. Since the internal atomic state depends on the polarization of the pumping light, such a configuration leads, as will be shown below, to large nonadiabatic effects, since a moving atom has to respond to the variations of the laser polarization due to its motion with an internal response time (the optical-pumping time) which becomes very long at low intensity. By contrast, if the two counterpropagating laser waves had the same polarization, one would have just a gradient of intensity, without any polarization gradient. In the low-intensity regime considered here, this would produce only a slight change of the total population in the ground state g (which remains close to 1), without any change of the anisotropy in g (characterized by the population differences between the ground-state sublevels and the Zeeman coherences between them).

3·2.2. Atomic transition. Simplifications for the mean force. As for usual laser-cooling experiments, we consider a transition $J_{\mathrm{g}} \to J_{\mathrm{e}} = J_{\mathrm{g}} + 1$. We take the simplest possible value of J_{g} leading to a degenerate ground state, *i.e.* $J_{\mathrm{g}} = 1/2$. Figure 1*b*) gives the various Clebsch-Gordan coefficients corresponding to a transition $J_{\mathrm{g}} = 1/2 \to J_{\mathrm{e}} = 3/2$.

Since there are only two Zeeman sublevels in the ground state, the matrix representing $G^- G^+$ in the ground-state manifold is diagonal (see end of subsect. 2·6.4). It follows that the effective Hamiltonian H_{eff} describing the light shifts of the ground-state sublevels is diagonal in the basis $\{|g_{\pm 1/2}\rangle\}$ of eigenstates of J_z, so that the eigenstates of H_{eff}, which coincide with $|g_{\pm 1/2}\rangle$, are independent of z. One can thus, in the expression (2.51) of $\mathscr{F}_{\mathrm{react}}$, neglect the second line which is associated with the gradients of the wave functions, and write

$$\mathscr{F}_{\mathrm{react}} = -\Pi_{+1/2}\nabla E_{+1/2} - \Pi_{-1/2}\nabla E_{-1/2}\,, \tag{3.5}$$

where $\Pi_{\pm 1/2}$ and $E_{\pm 1/2}$ are the populations and the energies of $|g_{\pm 1/2}\rangle$.

Since we consider here a one-dimensional molasses, we can use the expres-

sion (2.66) of $\mathscr{F}_{\text{dissip}}$, which involves the radiation pressures exerted separately by the two counterpropagating waves. Here also, the matrices representing the two operators $G_1^- G_1^+$ and $G_2^- G_2^+$ appearing in (2.66) are diagonal in the basis $\{|g_{\pm 1/2}\rangle\}$ of eigenstates of J_z (see end of subsect. 2·6.4). Since both counterpropagating waves have a linear polarization, one can then easily show that $\langle G_1^- G_1^+ \rangle$ and $\langle G_2^- G_2^+ \rangle$ are equal and proportional to $\Pi_{-1/2} + \Pi_{+1/2} = 1$, *i.e.* independent of the internal atomic state. It follows that

$$\mathscr{F}_{\text{dissip}} = 0 . \tag{3.6}$$

The choice of the simple atomic transition of fig. 1*b*) leads, therefore, to a mean force which is due only to the spatial variations of the light-shifted energies of the ground-state sublevels. This is why the new cooling mechanism analysed in this section can be considered as a pure Sisyphus effect.

3·3. *Dynamics of the internal degrees of freedom.*

3·3.1. Light shifts of the ground-state sublevels. The light shifts $E_{\pm 1/2}(z)$ of $|g_{\pm 1/2}\rangle$ can be written

$$E_{\pm 1/2}(z) = \hbar \delta' \Lambda_{\pm\pm}(z) , \tag{3.7}$$

where $\Lambda_{++}(z)$ and $\Lambda_{--}(z)$ are the diagonal elements of the operator $\Lambda(z)$ defined in (2.32), which are the only nonzero matrix elements of this operator, and where δ' is given by (2.33*b*). Note that, since the laser amplitude in z, $\mathscr{E}_L = \mathscr{E}_0 \sqrt{2}$, is independent of z (see eq. (3.3)), the Rabi frequency Ω_1, appearing in (2.33*b*), is also independent of z, so that the only z-dependence in (3.7) comes from the matrix elements of Λ, and not from δ'. Note that δ' can be written

$$\delta' = \delta \frac{s}{2} = \delta s_0 , \tag{3.8}$$

where s is the saturation parameter associated with $\mathscr{E}_L$ and $s_0 = s/2$ the saturation parameter associated with $\mathscr{E}_0$, *i.e.* with each of the two counterpropagating waves.

Inserting (3.4) into (2.32), and using for the matrix elements of $\boldsymbol{\varepsilon}_q \cdot \hat{\boldsymbol{d}}_{\pm}$ the Clebsch-Gordan coefficients of fig. 1*b*) (see eqs. (2.9) and (2.10)), we get

$$\Lambda_{++}(z) = \sin^2 kz + \frac{1}{3}\cos^2 kz = 1 - \frac{2}{3}\cos^2 kz , \tag{3.9a}$$

$$\Lambda_{--}(z) = \cos^2 kz + \frac{1}{3}\sin^2 kz = 1 - \frac{2}{3}\sin^2 kz . \tag{3.9b}$$

Figure 2 represents the spatial variations of $E_{\pm 1/2}(z)$. We have supposed $\delta < 0$, so that the light shifts are negative. At $z = 0$, $\lambda/2$..., where the polarization is σ^-, the sublevel $|g_{-1/2}\rangle$ is shifted downwards (with respect to the zero of en-

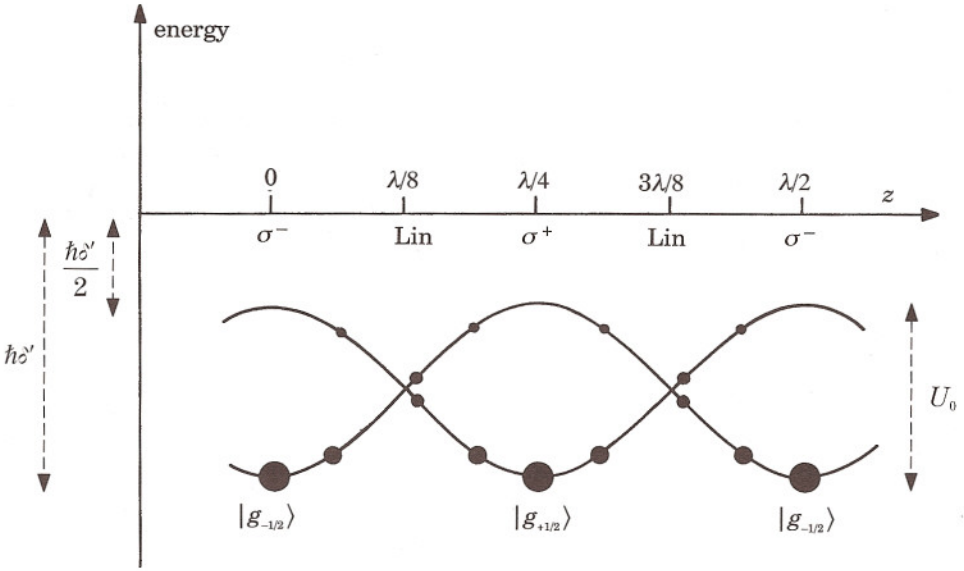

Fig. 2. – Light shifts $E_{\pm 1/2}(z)$ of $|g_{\pm 1/2}\rangle$ *vs.* z. The size of the solid circles is proportional to the steady-state populations of $|g_{\pm 1/2}\rangle$ for an atom at rest in z. We have supposed $\delta < 0$.

ergy, corresponding to the absence of laser) three times more than the sublevel $|g_{+1/2}\rangle$, because the σ^- transition starting from $|g_{-1/2}\rangle$ is three times more intense than the σ^- transition starting from $|g_{+1/2}\rangle$. The situation is opposite in $z = \lambda/4$, where the polarization is σ^+, and where the sublevel $|g_{+1/2}\rangle$ is shifted three times more than $|g_{-1/2}\rangle$. Finally, in $z = \lambda/8, 3\lambda/8 \ldots$, where the polarization is linear, both sublevels undergo the same light shift.

Using (3.9) and (3.7), we can also write

$$E_{+1/2}(z) = -\frac{3U_0}{2} + U_0 \cos^2 kz\,, \tag{3.10a}$$

$$E_{-1/2}(z) = -\frac{3U_0}{2} + U_0 \sin^2 kz\,, \tag{3.10b}$$

where

$$U_0 = -\frac{2}{3}\hbar\delta' = -\frac{2}{3}\hbar\delta s_0 \tag{3.11}$$

is the depth of the potential wells associated with the spatial oscillations of $E_{+1/2}(z)$ and $E_{-1/2}(z)$. Equations (3.10) also allow the expression (3.5) of the reactive force, which coincides with the total mean force because of (3.6), to be transformed into

$$\mathscr{F}_{\text{react}}(z) = \mathscr{F}(z) = \varepsilon_z k U_0 \mathscr{M}(z) \sin 2kz\,, \tag{3.12}$$

where

$$\mathscr{M}(z) = \Pi_{+1/2}(z) - \Pi_{-1/2}(z) \tag{3.13}$$

is the difference between the populations of the two sublevels.

3·3.2. Optical-pumping rates. First we consider the departure rates from $|g_{\pm 1/2}\rangle$, $\Gamma'_{\pm 1/2}(z)$, associated with the anticommutator of (2.35), and given by (see also (2.39) and (2.40))

$$\Gamma'_{+1/2}(z) = \Gamma' \Lambda_{++}(z) = \Gamma' \left(1 - \frac{2}{3}\cos^2 kz\right), \tag{3.14a}$$

$$\Gamma'_{-1/2}(z) = \Gamma' \Lambda_{--}(z) = \Gamma' \left(1 - \frac{2}{3}\sin^2 kz\right), \tag{3.14b}$$

where

$$\Gamma' = \Gamma \frac{s}{2} = \Gamma s_0 . \tag{3.15}$$

The last term of (2.35), which describes how atoms return to the ground state after having absorbed one photon, can be easily calculated, using the expression (3.4) of $\varepsilon(z)$ and the Clebsch-Gordan coefficients of fig. 1*b*). Such a term couples populations only to populations, because the value 1/2 of J_g excludes any off-diagonal element $\langle g_m | \sigma_{gg} | g_{m'} \rangle$ of σ_{gg} with $m - m' = \pm 2$.

Adding the contributions of the last two terms of (2.35), and using (3.14), we finally get, for the populations $\Pi_{\pm 1/2}$ of $|g_{\pm 1/2}\rangle$, the following rate equations describing the effect of optical pumping:

$$\frac{\mathrm{d}}{\mathrm{d}t}\Pi_{+1/2}(z) = -\Gamma_{+\to -}(z)\Pi_{+1/2}(z) + \Gamma_{-\to +}(z)\Pi_{-1/2}(z), \tag{3.16a}$$

$$\frac{\mathrm{d}}{\mathrm{d}t}\Pi_{-1/2}(z) = -\Gamma_{-\to +}(z)\Pi_{-1/2}(z) + \Gamma_{+\to -}(z)\Pi_{+1/2}(z), \tag{3.16b}$$

where

$$\Gamma_{+\to -}(z) = \frac{2}{9}\Gamma' \cos^2 kz, \tag{3.17a}$$

$$\Gamma_{-\to +}(z) = \frac{2}{9}\Gamma' \sin^2 kz \tag{3.17b}$$

are, respectively, the optical-pumping rates from $|g_{+1/2}\rangle$ to $|g_{-1/2}\rangle$ and from $|g_{-1/2}\rangle$ to $|g_{+1/2}\rangle$.

Subtracting (3.16*b*) from (3.16*a*) and using (3.13) and (3.17), we also get for $\mathscr{M}(z)$ the following equation:

$$\frac{\mathrm{d}}{\mathrm{d}t}\mathscr{M}(z) = -\frac{1}{\tau_P}[\mathscr{M}(z) + \cos 2kz], \tag{3.18}$$

where τ_P, given by

$$\tau_P = \frac{9}{2\Gamma'} = \frac{9}{2\Gamma s_0}, \tag{3.19}$$

is the optical-pumping time characterizing the time constant with which the population difference reaches its equilibrium value.

It is clear from (3.17) that, as the light shifts $E_{\pm 1/2}(z)$ given in (3.10), the optical-pumping rates from one sublevel to the other are spatially modulated. The same function of z, $\cos^2 kz$, appears in (3.10a) and (3.17a). There is, therefore, a perfect correlation between the spatial dependence of the light shift of $|g_{+1/2}\rangle$ and the spatial dependence of the optical-pumping rate from $|g_{+1/2}\rangle$ to $|g_{-1/2}\rangle$. More precisely, $E_{+1/2}(z)$ and $\Gamma_{+\to -}(z)$ reach their maximal values for the same values of z, those for which $\cos^2 kz = 1$. A similar results holds for $E_{-1/2}(z)$ and $\Gamma_{-\to +}(z)$. This means that the transition rate from $|g_{+1/2}\rangle$ (respectively, $|g_{-1/2}\rangle$) to $|g_{-1/2}\rangle$ (respectively, $|g_{+1/2}\rangle$) is maximum at the places where the energy of $|g_{+1/2}\rangle$ (respectively, $|g_{-1/2}\rangle$) is the highest. We will see in the next subsection that, for a moving atom, the most probable processes are those where the atom leaves one of the two oscillating potential curves of fig. 2 at the top of one hill and is transferred to the bottom of one valley of the other potential curve. This is the key point of the cooling mechanism discussed in this section.

3·3.3. Steady-state populations for an atom at rest. If we suppose that the atom is at rest in z, all coefficients of (3.18) are time independent. This equation has, therefore, a steady-state solution given by

$$\mathscr{M}^{st}(z) = \Pi^{st}_{+1/2}(z) - \Pi^{st}_{-1/2}(z) = -\cos 2kz\,. \tag{3.20}$$

Combining this equation with the normalization condition $\Pi^{st}_{+1/2}(z) + \Pi^{st}_{-1/2}(z) = 1$, we get

$$\Pi^{st}_{+1/2}(z) = \sin^2 kz\,, \tag{3.21a}$$

$$\Pi^{st}_{-1/2}(z) = \cos^2 kz\,. \tag{3.21b}$$

The size of the solid circles of fig. 2 is proportional to these steady-state populations. For a given value of z, the most populated sublevel is the lowest one. At the top of the hills, the population is equal to zero, whereas it is equal to 1 at the bottom of the valleys.

3·4. *Cooling mechanism for a moving atom.*

3·4.1. Sisyphus effect. Consider an atom moving with velocity v along $0z$ in the bipotential $E_{\pm 1/2}(z)$ of fig. 2. We suppose that initially v is large enough:

$$\frac{1}{2}Mv^2 \gg U_0, \tag{3.22a}$$

$$kv \gg \Gamma', \tag{3.22b}$$

so that, on the one hand, the atom is not trapped in one of the potential wells and, on the other hand, it travels over several wavelengths before being optically pumped from one sublevel to the other. Note, however, that v is small enough so that we can still neglect kv in comparison with Γ (negligible Doppler cooling)

$$kv \ll \Gamma. \tag{3.23}$$

Condition (3.23), which can be written $v\Gamma^{-1} \ll \lambda$, means also that the atom travels over a distance very small compared to λ during the duration Γ^{-1} of a fluorescence cycle. In other words, each optical-pumping cycle can be considered as occurring instantaneously in a given point of the $0z$ axis.

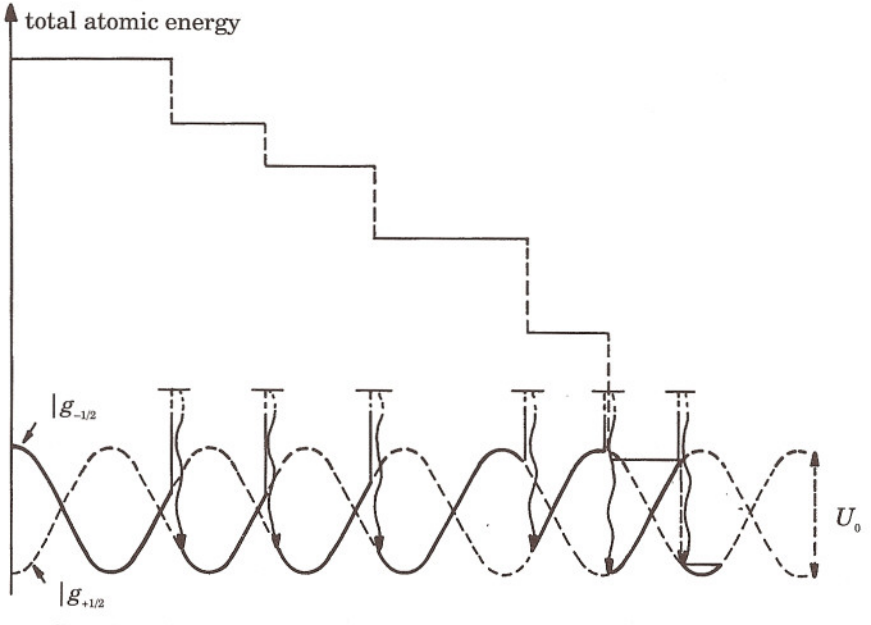

Fig. 3. – Sisyphus effect for a moving atom. Because of the strong correlation between the spatial dependences of light shifts and optical-pumping rates, the atom loses potential energy when it jumps from one sublevel to the other. The upper part of the figure gives the corresponding variations of the total energy. The random path sketched here has been obtained for $\delta = -5\Gamma$, $\Omega_1 = 2.3\Gamma$ and for the cesium recoil shift $\hbar k^2/M\Gamma = 7.8 \cdot 10^{-4}$.

Suppose that initially the atom is in the sublevel $|g_{-1/2}\rangle$ (fig. 3). As long as it remains in this sublevel, its total (kinetic + potential) energy, represented in the upper part of fig. 3, remains constant. We neglect for the moment the recoil due to the absorbed and re-emitted photons in the fluorescence cycles $g_{-1/2} \rightarrow$ $\rightarrow e_{+1/2}$ (or $e_{-3/2}$) $\rightarrow g_{-1/2}$ where the atom returns in $g_{-1/2}$. Because of the spatial dependence of the optical-pumping rates, discussed at the end of subsect. 3·3.2, the transfer by optical pumping from $g_{-1/2}$ to $g_{+1/2}$ will occur preferentially near the maxima of $E_{-1/2}(z)$, and the atom will jump suddenly from a point near the top of one hill of $E_{-1/2}(z)$ to a point near the bottom of one valley of $E_{+1/2}(z)$. The corresponding change δU of its potential energy will, therefore, be negative and on the order (in absolute value) of U_0. If we neglect here also the recoil of the absorbed and re-emitted photons, the total energy of the atom will decrease suddenly by an amount δU (first discontinuity in the curve represented in the upper part of fig. 3).

From there, the same sequence can be repeated. On the average, the atom is running up the hills more than down and its total energy decreases by a series of discontinuous steps until its kinetic energy becomes on the order of or smaller than U_0 (see, for example, the last jump of fig. 3). Such a qualitative analysis, which is confirmed by the results of more quantitative treatments, therefore shows that the kinetic energies which can be achieved by low-intensity Sisyphus cooling are on the order of the depth U_0 of the potential wells associated with the spatially modulated light shifts: $Mv^2/2 \sim U_0$. For large detunings ($|\delta| \gg \Gamma$), which is the interesting case where the light shifts of the ground-state sublevels are larger than their widths, U_0 is on the order of $\hbar\Omega_1^2/|\delta|$, so that

$$k_B T \sim \frac{\hbar\Omega_1^2}{|\delta|} . \tag{3.24}$$

3·4.2. Threshold intensity. Cooling limit. According to eq. (3.24), the temperature can be decreased by decreasing the laser intensity $I_L \sim \Omega_1^2$, or by increasing the detuning δ. Obviously, one cannot decrease I_L indefinitely. There must be, therefore, a threshold intensity below which eq. (3.24) is no longer valid.

Actually, in deriving (3.24), we have neglected the recoil due to the absorbed and re-emitted photons in each fluorescence cycle. We have thus implicitly assumed that the mean loss of potential energy at each optical-pumping cycle, on the order of U_0, is much larger than the mean increase of kinetic energy due to the recoil, on the order of $E_R = \hbar^2 k^2/2M$. If I_L is decreased, U_0 also decreases, and, when U_0 becomes on the order of a few E_R, the cooling due to the Sisyphus effect is no longer sufficient to overcome the heating due to the recoil.

There is, therefore, a threshold intensity given by

$$(U_0)_{\text{thr}} > \text{a few } E_R . \tag{3.25}$$

The previous analysis also shows that low-intensity Sisyphus cooling cannot lead to minimum energies lower than a few E_R. The characteristic energy is now the recoil energy E_R, and not $\hbar\Gamma$ as was the case for Doppler cooling.

3·4.3. Comparison of internal and external times. In the cooling scheme discussed in this section, internal variables evolve with a characteristic time T_{int} equal to the optical-pumping time τ_P:

$$T_{\text{int}} \simeq \tau_P = \frac{9}{2\Gamma s_0} . \tag{3.26}$$

To characterize the evolution of external variables, we suppose that the atom has been cooled during a time long enough that it is quasi-trapped in the potential wells of fig. 3, and we introduce the oscillation frequency Ω_{osc} in these wells. Near the bottom of one potential well, for example near $z = 0$, we have, according to (3.10*b*),

$$E_{-1/2}(z) \simeq -\frac{3U_0}{2} + k^2 U_0^2 z^2 \qquad \text{for } |z| \ll 1/k , \tag{3.27}$$

so that Ω_{osc} is given by

$$\Omega_{\text{osc}} = k\sqrt{\frac{2U_0}{M}} = \sqrt{\frac{4\hbar|\delta|\, s_0}{3M}} . \tag{3.28}$$

The external time T_{ext} is on the order of the oscillation period:

$$T_{\text{ext}} \simeq \frac{1}{\Omega_{\text{osc}}} . \tag{3.29}$$

An important parameter for characterizing atomic motion is, therefore,

$$\Omega_{\text{osc}}\tau_P = \sqrt{\frac{27\hbar k^2|\delta|}{Ms_0\Gamma^2}} \simeq \frac{T_{\text{int}}}{T_{\text{ext}}} . \tag{3.30}$$

If $\Omega_{\text{osc}}\tau_P \ll 1$, the atom makes several transitions between $|g_{-1/2}\rangle$ and $|g_{+1/2}\rangle$ in a single oscillation period. In such a «jumping regime», internal variables are much faster than external variables. This is the usual regime considered up to now in the semi-classical treatment of laser cooling. One can adiabatically eliminate the internal variables and describe atomic motion in terms of a velocity-dependent force and a momentum diffusion coefficient. Such a treatment, which is given in detail in ref. [19], will be sketched in subsect. 3·5.

If $\Omega_{\text{osc}}\tau_P \gg 1$, we are in the opposite situation where the atom makes several oscillations in a potential well before being optically pumped into the other sublevel. Such an «oscillating regime», where external variables are faster than in-

ternal variables, is quite unusual in laser cooling of free atoms. It is important here since, if one decreases Ω_1, at fixed δ, in order to decrease the temperature estimated in (3.24), one sees from (3.30) that one can go from the jumping regime to the oscillating regime. A few remarks on this regime will be given in subsect. 3·6. More details may be found in ref. [20] and [23].

Before ending this subsection, we would like to mention other cooling mechanisms, closely related to the one discussed in this section, but which do not use polarization gradients [24, 25]. Suppose, for example, that the laser configuration consists of two counterpropagating waves along $0z$, with the same circular polarization σ^+. We have in this case a pure σ^+ standing wave. If we still consider a $J_g = 1/2 \leftrightarrow J_e = 3/2$ transition, the light shifts $E_{\pm 1/2}(z)$ of $|g_{\pm 1/2}\rangle$ oscillate in space (with $E_{+1/2} = 3E_{-1/2}$), the splitting between the two sublevels being equal to zero at the nodes of the standing wave and maximum at the antinodes. Because of optical pumping, all atoms are pumped into $|g_{+1/2}\rangle$ and the steady-state population of this state for an atom at rest in z remains equal to 1 and independent of z, since, in the limit $s \ll 1$, the population of the excited state is negligible. Suppose now that one adds a small static magnetic field $\boldsymbol{B}_0$, perpendicular to $0z$. If B_0 is small enough, its effect will be important only near the nodes where it mixes the sublevels $|g_{\pm 1/2}\rangle$ which become degenerate in such places. Consider then a moving atom, initially pumped in the sublevel $|g_{+1/2}\rangle$. When such an atom passes through a node, Landau-Zener transitions can transfer it to the other sublevel $|g_{-1/2}\rangle$, which is less light shifted than $|g_{+1/2}\rangle$. The atom will remain in this sublevel for a time on the order of τ_P before being optically pumped back to $|g_{+1/2}\rangle$. One can then easily see that such a scheme provides a new example of situations where the atom is running up the hills of oscillating potential curves more than down.

3·5. *The jumping regime* ($\Omega_{osc}\,\tau_P \ll 1$). – We suppose in this subsection that $\Omega_{osc}\,\tau_P \ll 1$, so that

$$T_{int} \ll T_{ext}\,. \tag{3.31}$$

It follows that during the time required by the internal variables to reach a steady state, or more precisely a forced regime, the atomic velocity does not change appreciably. We can thus set

$$z = vt \tag{3.32}$$

in the equations of motion (3.16) of internal variables and consider v as a constant when solving these equations.

3·5.1. Internal state for an atom with velocity v. Inserting (3.32) into the equation of motion (3.18) of the population difference $\mathscr{M}$ leads to

$$\frac{\mathrm{d}}{\mathrm{d}t}\mathscr{M}(t) + \frac{1}{\tau_P}\mathscr{M}(t) = -\frac{1}{\tau_P}\cos 2kvt\,, \tag{3.33}$$

which is a linear differential equation with constant coefficients (since τ_P is, according to (3.19), independent of z and thus of t) and with a source term modulated at the angular frequency $2kv$. The forced-regime solution of (3.33) can be written

$$\mathscr{M}(t) = -\,\mathrm{Re}\,\frac{\tau_P^{-1}}{2ikv + \tau_P^{-1}}\exp[2ikvt], \tag{3.34}$$

that is also, coming back to the variable z with (3.32),

$$\mathscr{M}(z) = -\,\frac{1}{1+\left(\frac{v}{v_c}\right)^2}\cos 2kz - \frac{\frac{v}{v_c}}{1+\left(\frac{v}{v_c}\right)^2}\sin 2kz, \tag{3.35}$$

where v_c is a critical velocity defined by

$$v_c = \frac{1}{2k\tau_P} = \frac{\lambda}{4\pi\tau_P} = \frac{\Gamma'}{9k}. \tag{3.36}$$

In order to get some physical insight into (3.35), it will be useful to study the limit of this expression for $v \ll v_c$. To order 1 in v/v_c, (3.35) can be written using (3.36) and the definition (3.20) of the population difference for an atom at rest in z:

$$\mathscr{M}(z) = -\cos 2kz - 2kv\tau_P \sin 2kz = \tag{3.37}$$

$$= \mathscr{M}^{st}(z) - v\tau_P \frac{d}{dz}\mathscr{M}^{st}(z) \simeq \mathscr{M}^{st}(z - v\tau_P).$$

Such a result clearly shows that (after a transient regime) the internal state of an atom passing in z with a small velocity v lags behind the internal state of an atom which would be at rest in z. Because of the finite response time τ_P of internal variables, $\mathscr{M}(z)$ does not adjust instantaneously to the variations of the laser polarization «seen» by the moving atom. There is a nonlocality in the response of the atom which is characterized by the distance $v\tau_P$ travelled by the atom during the internal time τ_P.

3·5.2. Velocity-dependent mean force. Friction coefficient. Inserting (3.35) into the expression (3.12) of the mean force, and taking a spatial average, we get for the z-component of the spatially averaged force acting upon an atom moving with velocity v

$$\overline{\mathscr{F}_z(v)} = -\,\frac{kU_0}{2}\,\frac{\frac{v}{v_c}}{1+\left(\frac{v}{v_c}\right)^2} = -\,\frac{\alpha_S v}{1+\left(\frac{v}{v_c}\right)^2}, \tag{3.38}$$

where α_S is equal, according to (3.36), (3.11) and (3.19), to

$$\alpha_S = k^2 U_0 \tau_P = -3\hbar k^2 \frac{\delta}{\Gamma}. \tag{3.39}$$

For $v \ll v_c$, $\overline{\mathcal{F}_z(v)}$ can be written

$$\overline{\mathcal{F}_z(v)} = -\alpha_S v, \tag{3.40}$$

which shows that α_S is the friction coefficient associated with low-intensity Sisyphus cooling. It is interesting to compare α_S with the friction coefficient α_D given in (4.8) of ref. [1] for a two-level atom moving in a laser plane wave and due to the Doppler effect. A remarkable property of α_S, given in (3.39), is that it is independent of the laser intensity I_L, whereas eq. (4.8) of ref. [1] shows that α_D is proportional to s, and thus to I_L, if $s \ll 1$. At first sight, such a result seems quite surprising, since decreasing I_L decreases the depth U_0 of the potential wells of fig. 2, and consequently the corresponding gradient forces. But eq. (3.39) shows that α_S is proportional to the product of U_0 by τ_P, so that, when I_L decreases, the decrease of U_0, which varies as I_L, is compensated for by the increase of τ_P, which varies as $1/I_L$. In other words, at low intensity, the weakness of light shifts is compensated for by the length of optical-pumping times. Note also that, according to (3.39), the value of α_S is, for $|\delta| \gg \Gamma$, larger than the optimal value of α_D which, according to (4.9) in ref. [1], is on the order of $\hbar k^2/4$.

When v increases, $\overline{\mathcal{F}_z(v)}$ reaches a maximum when $v = v_c$ and then decreases as $1/v$ when $v \gg v_c$. The critical velocity v_c, which is a velocity such that the atom, moving with this velocity, travels over a distance on the order of λ during the optical-pumping time τ_P, can thus be considered as defining the velocity range, sometimes called «velocity capture range», over which low-intensity Sisyphus friction is most efficient. According to (3.36), v_c is proportional to $1/\tau_P$, *i.e.* to the laser intensity I_L. Such a result is to be contrasted with what happens for Doppler cooling, where the velocity capture range, given by the width of the curve of fig. 4 of sect. 4 in ref. [1], is, for the optimal value $\delta = -\Gamma/2$ of the detuning, such that $kv_c \simeq \Gamma$, and is, therefore, independent of I_L.

To summarize the results derived in this subsection, one can say that, for low-intensity Sisyphus cooling, the friction coefficient α_S remains constant, and very large, when I_L decreases, whereas the velocity capture range decreases. On the contrary, for Doppler cooling, the friction coefficient α_D decreases when I_L decreases, whereas the velocity capture range remains constant.

3·5.3. Equilibrium temperature. In order to evaluate the equilibrium temperature T_S associated with low-intensity Sisyphus cooling, we must find first an order of magnitude of the momentum diffusion coefficient D for an atom at rest in z.

As in the case of a two-level atom, we have a contribution D_{vac} to D coming from the fluctuations of the momentum carried away by the spontaneously emitted photons, and a contribution D_{abs} coming from the fluctuations in the difference between the number of photons absorbed in each of the two counter-propagating waves. Considerations similar to those developed in subsect. 5.2.3 of ref. [1] show that these two contributions are, for $s_0 \ll 1$, which is the case considered in this section, on the order of

$$D_{vac} \simeq D_{abs} \simeq \hbar^2 k^2 \Gamma' = \hbar^2 k^2 \Gamma s_0 . \tag{3.41a}$$

We also have a contribution D_{dip} to D coming from the fluctuations of the instantaneous dipole force oscillating back and forth between $-\nabla E_{+1/2}$ and $-\nabla E_{-1/2} = +\nabla E_{+1/2}$ when the atom undergoes, at random times, optical-pumping transitions between the two ground-state Zeeman sublevels at a rate $1/\tau_P$. A calculation, quite similar to the one presented in subsection 4*B* of ref. [18], gives for this contribution the following result:

$$D_{dip} = 2\hbar^2 k^2 \frac{\delta^2}{\Gamma} s_0 \sin^4(2kz) , \tag{3.41b}$$

whose spatial average is equal to

$$\overline{D_{dip}} = \frac{3}{4} \hbar^2 k^2 \frac{\delta^2}{\Gamma} s_0 . \tag{3.41c}$$

Note that, according to (3.41*b*), D_{dip} vanishes in certain places. But, since the departure rates from $|g_{\pm 1/2}\rangle$ never vanish (see eq. (3.14)), D_{vac} and D_{abs} never vanish.

If $|\delta| \gg \Gamma$, $\overline{D_{dip}}$ is larger than D_{vac} and D_{abs} by a factor on the order of $\delta^2/\Gamma^2 \gg 1$, so that

$$D \simeq \overline{D_{dip}} = \frac{3}{4} \hbar^2 k^2 \frac{\delta^2}{\Gamma} s_0 . \tag{3.42}$$

The equilibrium temperature T_S results from a competition between the cooling, described by the friction coefficient α_S, and the heating due to momentum diffusion. We then have, for $|\delta| \gg \Gamma$,

$$k_B T = \frac{D}{\alpha_S} \simeq -\frac{1}{4} \hbar \delta s_0 = \frac{3}{8} U_0 . \tag{3.43}$$

This confirms the result predicted above in a qualitative way (see (3.24)), according to which the equilibrium energy is on the order of the depth U_0 of the potential wells of fig. 2. Using the definition of s_0 as the saturation parameter

associated with each of the two counterpropagating waves, we have, for $|\delta| \gg \Gamma$,

$$k_B T \simeq \frac{\hbar \Omega_1^2}{8|\delta|}, \tag{3.44}$$

where Ω_1 is the Rabi frequency associated with each of the two counterpropagating waves. Experiments [26] done on cesium have given results showing that T depends linearly on $\Omega_1^2/|\delta|$ over a large range of values of the parameters. This agreement with (3.44) is somewhat unexpected since the theory presented here is valid only in one dimension and for a $J_g = 1/2 \leftrightarrow J_e = 3/2$ transition, whereas the experiments are done in three dimensions on a $J_g = 4 \leftrightarrow J_e = 5$ transition.

One can finally ask under what condition the whole velocity distribution falls in the linear part of $\overline{\mathscr{F}_z(v)}$. Such a condition can be written

$$v_{\text{r.m.s.}} \ll v_c \Rightarrow \Omega_1 \gg \sqrt{\frac{\hbar k^2}{M} \frac{|\delta|^3}{\Gamma^2}} \tag{3.45}$$

and turns out to be equivalent to $\Omega_{\text{osc}} \tau_P \ll 1$, which is the condition of validity of the jumping regime considered in this section.

3·6. *The limits of low-intensity Sisyphus cooling.* – The treatment presented in the previous subsect. 3·5 relies on a semi-classical approximation (atomic spatial coherence length ξ_A much smaller than the laser wavelength λ—see the discussion of subsect. 2.3.2 in ref. [1]) and on the assumption that $T_{\text{int}} \ll T_{\text{ext}}$. Its predictions for the equilibrium temperature (3.44) are certainly wrong when Ω_1 becomes too small. In order to determine the lowest temperatures which can be reached by low-intensity Sisyphus cooling, we need, therefore, a more precise theory.

3·6.1. Results of a full quantum treatment. Reference [20] presents a full quantum treatment of low-intensity Sisyphus cooling, where both internal and external degrees of freedom are quantized. We will not give here the details of such calculations. We just present a few important results.

Consider first the predictions concerning the variations with U_0 of the mean kinetic energy $\langle P^2/2M \rangle$, for a fixed value of the detuning δ. For $U_0 \gg E_R$, the quantum result agrees with the semi-classical one, and one gets a straight line. When U_0 is decreased, $\langle P^2/2M \rangle$ decreases, passes through a minimum and then diverges (see fig. 3*b* of ref. [20]). This confirms the qualitative predictions of subsect. 3·4.2 for the existence of a threshold for U_0. Two important results must be noted concerning the minimum $\langle P^2/2M \rangle_{\text{min}}$ of $\langle P^2/2M \rangle$. First, for the values of δ and U_0 corresponding to this minimum, the dispersion Δp of the possible values of p, characterized by $\Delta p \sim \langle P^2 \rangle^{1/2}$, remains always larger than $\hbar k$. Actually, the smallest possible value of $\langle P^2 \rangle^{1/2}$, which is achieved for $U_0 = 95 E_R$

and $|\delta| \gg \Gamma$, is equal to $5.5\hbar k$. This means that the semi-classical approximation is not too bad, since the coherence length $\xi_A \sim \hbar/\Delta p$ remains always smaller than $\lambda = 2\pi/k$. Second, for the values of U_0 corresponding to $\langle P^2/2M\rangle_{\min}$, $\Omega_{osc}\tau_P$ is no longer small compared to 1. Actually the smallest possible value of $\langle P^2/2M\rangle_{\min}$ is reached in the limit $\Omega_{osc}\tau_P \to \infty$. These results show that the optimum of Sisyphus cooling cannot be properly described by the treatment of subsect. 3·5, not because of the semi-classical approximation, which is not bad, but because of the assumption $T_{int} \ll T_{ext}$, which has to be reversed.

Reference [20] presents a few approximations which can be done on the quantum equations of motion and which are still semi-classical in the sense that, as in subsect. 5.3 of ref. [1], the atomic Wigner functions are expanded in powers of $\hbar k/\Delta p$, up to order 2. The difference with the treatment of subsect. 5.3 in ref. [1] is that internal variables are no longer adiabatically eliminated. Some other approximations are then introduced. We will focus here on the limit $\Omega_{osc}\tau_P \gg 1$, where the so-called «secular approximation» allows one to describe laser cooling of neutral atoms with physical pictures quite similar to the ones used to describe laser cooling of trapped ions [27].

3·6.2. The oscillating regime ($\Omega_{osc}\tau_P \gg 1$). In this regime, the atom oscillates several times in one of the potential wells of fig. 2, before being optically pumped into the other sublevel. One can, therefore, in a first step, neglect the dissipative part of the atom-field coupling which is responsible for the real absorption and emission of photons by the atom, and consider only the reactive part of this coupling which is at the origin of light shifts. This amounts to considering an atom moving in a bipotential $E_{\pm 1/2}(z)$, without any dissipative process. As shown in ref. [23], the diagonalization of the corresponding Hamiltonian gives a series of energy levels which are actually energy bands because of the periodicity of $E_{\pm 1/2}(z)$. The lowest bands are very narrow because of the smallness of the tunnel effect between two adjacent potential wells. For example, for $\delta = -20\Gamma$, $\Omega_1 = 1.5\Gamma$ and the cesium recoil shift, one finds $U_0 \simeq 100 E_R$, which gives 6 bound bands [23], the width of the lowest band being smaller than $10^{-6} E_R$ and the distance between two successive bands being on the order of $\hbar\Omega_{osc}$ with $\Omega_{osc}/2\pi \simeq 40$ kHz.

The second step of such an approach consists in introducing the effect of optical pumping which induces transitions between different energy bands or inside a given band. Condition $\Omega_{osc}\tau_P \gg 1$ then allows one to neglect any «nonsecular» coupling between the populations of the energy levels and the off-diagonal elements of the density matrix between different energy levels separated by an energy on the order of $\hbar\Omega_{osc}$. Reference [23] shows how such a «secular approximation» (supplemented by symmetry considerations) leads to a set of rate equations involving only the populations of the energy levels. Such equations have a clear physical meaning in terms of optical-pumping rates and they are much easier to solve numerically than the full quantum equations written in the basis $|g_{\pm 1/2}, p\rangle$,

where p is the atomic momentum along $0z$. For example, one finds that, for the values of the parameters given above, more than 50% of the atoms are trapped in the two lowest bound bands, and the value obtained in this way for $\langle P^2/2M \rangle$ is in a very good agreement with the result obtained in ref. [20].

Such an approach provides a description of laser cooling in terms of spontaneous anti-Stokes-Raman transitions between bound states, quite analogous to the one given for laser cooling of trapped ions [27]. It thus suggests new phenomena which could be observed on neutral atoms trapped in optical molasses. For example, one could hope to observe discrete sidebands in the fluorescence spectrum of the trapped atoms, with a frequency shift from ω_L on the order of $\pm\Omega_{osc}$. Such sidebands could be easily resolved since their distance from ω_L, Ω_{osc}, is much larger than their width, on the order of $1/\tau_P$. Their observation would represent a direct evidence for the quantization of atomic motion in optical molasses (*).

4. – The σ^+-σ^- laser configuration. Semi-classical theory.

4·1. *Introduction.* – The purpose of this section is to present another example of a new laser cooling mechanism allowing one to beat the Doppler limit. As in the previous section, this mechanism is based on the existence of several ground-state Zeeman sublevels, and on polarization gradients. The polarization gradient is, however, of a different nature and gives rise to physical processes which are quite different from the Sisyphus effect discussed in

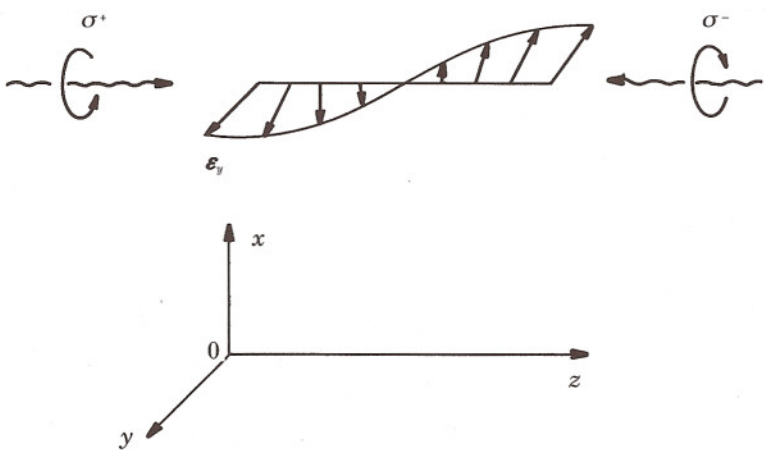

Fig. 4. – σ^+-σ^- laser configuration. The resulting laser electric field has a linear polarization which rotates in space, forming a helix with a pitch λ.

(*) *Note added in proofs.* – Such effects have been recently observed experimentally [28, 29].

sect. 3. Another important motivation for studying the σ^+-σ^- configuration is that it will allow us to introduce, in the specific case of a $J_g = 1 \leftrightarrow J_e = 1$ transition, the idea of «coherent population trapping». This phenomenon is at the basis of another cooling scheme, which will be analysed in sect. 5, and which can lead to temperatures below the single-photon recoil limit.

As in sect. 3, we consider two counterpropagating laser waves along $0z$, with the same amplitude $\mathcal{E}_0$ and the same frequency ω_L. But, instead of having orthogonal linear polarizations, the two waves have now orthogonal circular polarizations, σ^+ for the wave propagating along $0z$, σ^- for the counterpropagating wave (see fig. 4).

With an appropriate choice of the relative phases of the two waves, the laser electric field in z can be written

$$\boldsymbol{E}_L(z, t) = \boldsymbol{E}_L^+(z) \exp[-i\omega_L t] + \text{c.c.} \tag{4.1}$$

with

$$\boldsymbol{E}_L^+(z) = \frac{1}{2}(\boldsymbol{\varepsilon}_+ \exp[ikz] + \boldsymbol{\varepsilon}_- \exp[-ikz])\,\mathcal{E}_0. \tag{4.2}$$

Using $\boldsymbol{\varepsilon}_\pm = \mp(\boldsymbol{\varepsilon}_x \pm i\boldsymbol{\varepsilon}_y)/\sqrt{2}$, we get

$$\boldsymbol{E}_L^+(z) = -\frac{i}{\sqrt{2}}\mathcal{E}_0\,\boldsymbol{\varepsilon}(z) = -\frac{i}{2}\mathcal{E}_L\,\boldsymbol{\varepsilon}(z), \tag{4.3}$$

where $\mathcal{E}_L = \mathcal{E}_0\sqrt{2}$ is a real amplitude which is independent of z, and where the normalized linear polarization vector $\boldsymbol{\varepsilon}(z)$

$$\boldsymbol{\varepsilon}(z) = \frac{i}{\sqrt{2}}[\boldsymbol{\varepsilon}_+ \exp[ikz] + \boldsymbol{\varepsilon}_- \exp[-ikz]] = \boldsymbol{\varepsilon}_x \sin kz + \boldsymbol{\varepsilon}_y \cos kz \tag{4.4}$$

is deduced from $\boldsymbol{\varepsilon}_y$ by a rotation $\phi = -kz$ around $0z$. It follows that the resulting laser electric field has, for all values of z, the same amplitude $\mathcal{E}_L$ and a linear polarization $\boldsymbol{\varepsilon}(z)$ which rotates when z varies, forming a helix with a pitch λ (fig. 4).

Since the laser electric fields at two different points z_1 and z_2 are deduced from each other by a pure rotation, the light shifts of the ground-state sublevels have the same magnitude in z_1 and z_2, whereas the corresponding wave functions are deduced from each other by a rotation. It follows that, contrary to the situation studied in sect. 3, the light-shifted energies do not exhibit any spatial gradient, whereas the wave functions of the ground-state Zeeman sublevels having a well-defined light shift are position dependent. This shows that the light-shifted energies of the ground-state sublevels do not oscillate in space, which excludes any possibility of Sisyphus effect for the σ^+-σ^- configuration. In such a configuration, the reactive component of the mean force, given in (2.51), is entirely due to the spatial gradient of the wave functions. We thus have a situation which is, in some sense, complementary to the one analysed in sect. 3.

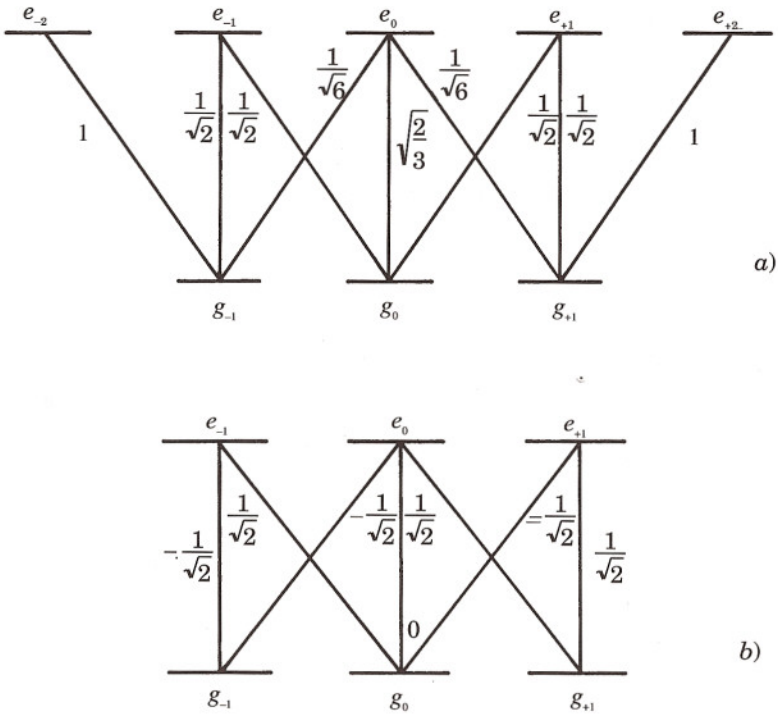

Fig. 5. – Clebsch-Gordan coefficients for the transitions $J_g = 1 \leftrightarrow J_e = 2$ (*a*)) and $J_g = 1 \leftrightarrow$ $\leftrightarrow J_e = 1$ (*b*)).

The fact that the polarization $\varepsilon(z)$ of the laser electric field is linear has an important consequence. The light shifts, which have the same symmetry as d.c. Stark shifts produced by a static electric field parallel to $\varepsilon(z)$, are the same for two Zeeman sublevels having opposite magnetic quantum numbers along $\varepsilon(z)$. It follows that, if we take $J_g = 1/2$, as in sect. 3, the Zeeman degeneracy of the ground state is not removed by light shifts, so that we have in this case neither energy gradients, nor gradients of wave functions. Since the radiation pressures of the two counterpropagating waves remain always equal for $J_g = 1/2$ (if we neglect Doppler cooling), we conclude that no new laser cooling mechanism can occur for $J_g = 1/2$. This is why we consider in this section two atomic transitions $J_g = 1 \leftrightarrow J_e = 2$ and $J_g = 1 \leftrightarrow J_e = 1$ having the simplest possible value of J_g leading to new cooling mechanisms in the σ^+-σ^- configuration (fig. 5). The first one is a standard transition $J_g \leftrightarrow J_e = J_g + 1$. The second one is considered here, in order to introduce in a simple way the idea of coherent population trapping.

We begin (subsect. 4·2) by giving the general expression of the mean force which is now the sum of a contribution due to the spatial gradients of the wave functions of the light-shifted Zeeman sublevels and of a contribution due to the

difference between the radiation pressures exerted by the two counterpropagating waves. We then study in subsect. 4·3 the light shifts and the steady-state populations of an atom at rest in z. For a moving atom, we show in subsect. 4·4 that it is possible to introduce a moving rotating frame in which the evolution of the atom can be analysed with a time-independent Hamiltonian. Such a transformation then allows us in subsect. 4·5 to interpret in a simple way the new cooling mechanism which appears for a $J_g = 1 \leftrightarrow J_e = 2$ transition. The important physical effect is essentially an ultrasensitive motion-induced population difference which appears among the ground-state sublevels and which gives rise to an imbalance between the radiation pressures exerted by the two counterpropagating waves. Finally, we analyse in subsect. 4·6 the case of a $J_g = 1 \leftrightarrow J_e = 1$ transition which gives rise to the phenomenon of coherent population trapping.

The σ^+-σ^- configuration has been considered from the beginning in the first explanations [30,31] proposed for the new laser cooling mechanisms. We will follow here the more quantitative presentation of ref. [19]. Some numerical results are also presented in ref. [21]. The combination of the σ^+-σ^- laser configuration with applied static magnetic fields has been also considered in ref. [32].

4·2. *General expression of the mean force.* – As in sect. 3, we introduce

$$\delta' = \delta s/2 = \delta s_0 , \tag{4.5a}$$

$$\Gamma' = \Gamma s/2 = \Gamma s_0 , \tag{4.5b}$$

where s_0 is the saturation parameter associated with the amplitude $\mathcal{E}_0$ of each of the two counterpropagating waves and $s = 2s_0$ the saturation parameter associated with $\mathcal{E}_L = \mathcal{E}_0\sqrt{2}$.

4·2.1. Effective Hamiltonian associated with light shifts. According to (2.36), such a Hamiltonian can be written

$$H_{\text{eff}} = \hbar\delta' \sum_{m,m'} |g_m\rangle\langle g'_m| \langle g_m|\Lambda(z)|g'_m\rangle , \tag{4.6}$$

where $\Lambda(z)$ is given in (2.32). Using the expansion (4.4) of $\varepsilon(z)$ in ε_+ and ε_- and the Clebsch-Gordan coefficients of fig. 5, one can easily calculate the matrix elements of $\Lambda(z)$. Inserting them into (4.6), one gets for a $J_g = 1 \leftrightarrow J_e = 2$ transition

$$H_{\text{eff}}(1 \leftrightarrow 2) = + \frac{\hbar\delta'}{2}|g_0\rangle\langle g_0| + \frac{7\hbar\delta'}{12}[|g_1\rangle\langle g_1| + |g_{-1}\rangle\langle g_{-1}|] + \tag{4.7a}$$

$$+ \frac{\hbar\delta'}{12}[|g_1\rangle\langle g_{-1}| \exp[2ikz] + |g_{-1}\rangle\langle g_1| \exp[-2ikz]]$$

and for a $J_g = 1 \leftrightarrow J_e = 1$ transition

$$(4.7b) \quad H_{\text{eff}}(1 \leftrightarrow 1) = + \frac{\hbar\delta'}{2} |g_0\rangle\langle g_0| + \frac{\hbar\delta'}{4}[|g_1\rangle\langle g_1| + |g_{-1}\rangle\langle g_{-1}|] - \\ - \frac{\hbar\delta'}{4}[|g_1\rangle\langle g_{-1}| \exp[2ikz] + |g_{-1}\rangle\langle g_1| \exp[-2ikz]].$$

It is clear in (4.7) that the only nonzero off-diagonal elements of H_{eff} in the basis $\{|g_m\rangle\}$ of eigenstates of J_z are those connecting $|g_1\rangle$ to $|g_{-1}\rangle$ or *vice versa*. This is a manifestation of the selection rule $\Delta m = \pm 2$ mentioned at the end of subsect. 2·6.4. Note also that the only terms of (4.7) which depend on z are those where both $|g_1\rangle$ and $|g_{-1}\rangle$ appear. This is due to the fact that these terms involve both counterpropagating waves (redistribution processes) which have a relative phase which varies as $\exp[\pm 2ikz]$ when z varies.

4·2.2. Reactive force. Using the expression (2.48) of this force, we get for a $J_g = 1 \leftrightarrow J_e = 2$ transition

$$(4.8a) \quad \mathscr{F}_{\text{react}}(1 \leftrightarrow 2) = -\langle \nabla H_{\text{eff}}(1 \leftrightarrow 2) \rangle = \\ = -\frac{i}{6}\hbar k\delta' \varepsilon_z [\sigma_{g_{-1}g_1} \exp[2ikz] - \sigma_{g_1 g_{-1}} \exp[-2ikz]]$$

and for a $J_g = 1 \leftrightarrow J_e = 1$ transition

$$(4.8b) \quad \mathscr{F}_{\text{react}}(1 \leftrightarrow 1) = -\langle \nabla H_{\text{eff}}(1 \leftrightarrow 1) \rangle = \\ = +\frac{i}{2}\hbar k\delta' \varepsilon_z [\sigma_{g_{-1}g_1} \exp[2ikz] - \sigma_{g_1 g_{-1}} \exp[-2ikz]].$$

It will be useful, for subsequent calculations, to introduce a new notation

$$(4.9) \quad \tilde{\sigma}_{g_1 g_{-1}} = \sigma_{g_1 g_{-1}} \exp[-2ikz] = \tilde{\sigma}^*_{g_{-1}g_1}$$

for the off-diagonal elements of the density matrix. The physical interpretation of the transformation relating $\sigma_{g_1 g_{-1}}$ to $\tilde{\sigma}_{g_1 g_{-1}}$ will be given in subsect. 4·4. Let C_r and C_i be the real and imaginary parts of $\tilde{\sigma}_{g_1 g_{-1}}$:

$$(4.10) \quad \tilde{\sigma}_{g_1 g_{-1}} = C_r + iC_i.$$

Using (4.9) and (4.10), one can rewrite (4.8) as

$$(4.11a) \quad \mathscr{F}_{\text{react}}(1 \leftrightarrow 2) = -\frac{\hbar k}{3}\delta' C_i \varepsilon_z,$$

$$(4.11b) \quad \mathscr{F}_{\text{react}}(1 \leftrightarrow 1) = +\hbar k\delta' C_i \varepsilon_z.$$

It is clear from (4.11) that the reactive component of the mean force is proportional to the imaginary part of the Zeeman coherence between g_1 and g_{-1}. This reflects the fact that the reactive force is a redistribution force (see subsect.

2·6.2) and that the two counterpropagating waves have orthogonal circular polarizations σ^+ and σ^-.

4·2.3. *Dissipative force.* – Such a force, which is given by (2.66), is the difference between the radiation pressures exerted by the two waves. Using the definition (2.46) of $G_\mu^\pm$ and the saturation parameter s_0 associated with each wave, one easily finds that the radiation pressure exerted by the wave 1 (with wave vector $k\varepsilon_z$ and polarization σ^+) is equal to the product of $\hbar k\Gamma s_0/2$ and the sum of the populations Π_m of the various Zeeman sublevels g_m weighted by the square of the Clebsch-Gordan coefficient of the σ^+ transition starting from g_m. A similar result holds for the radiation pressure exerted by wave 2, provided that one replaces ε_z by $-\varepsilon_z$ and σ^+ by σ^-. This yields for a $J_g = 1 \leftrightarrow J_e = 2$ transition

$$(4.12a) \qquad \mathscr{F}_{\text{dissip}}(1 \leftrightarrow 2) = +\hbar k \frac{\Gamma'}{2} \varepsilon_z \left[\Pi_1 + \frac{\Pi_0}{2} + \frac{\Pi_{-1}}{6} - \frac{\Pi_1}{6} - \frac{\Pi_0}{2} - \Pi_{-1} \right] = + \frac{5}{12} \hbar k \Gamma' \varepsilon_z [\Pi_1 - \Pi_{-1}]$$

and for a $J_g = 1 \leftrightarrow J_e = 1$ transition

$$(4.12b) \qquad \mathscr{F}_{\text{dissip}}(1 \leftrightarrow 1) = +\hbar k \frac{\Gamma'}{2} \varepsilon_z \left[\frac{\Pi_0}{2} + \frac{\Pi_{-1}}{2} - \frac{\Pi_0}{2} - \frac{\Pi_1}{2} \right] = - \frac{1}{4} \hbar k \Gamma' \varepsilon_z [\Pi_1 - \Pi_{-1}].$$

It clearly appears in (4.12) that the dissipative component of the mean force is proportional to the population difference $\Pi_1 - \Pi_{-1}$ between the two Zeeman sublevels. Note also the change of sign between (4.12*a*) and (4.12*b*). It is due to the fact that the most intense σ^+ transition starts from g_1 for a $J_g = 1 \leftrightarrow J_e = 2$ transition, whereas it starts from g_{-1} for a $J_g = 1 \leftrightarrow J_e = 1$ transition (see fig. 5).

4·3. *Internal state of an atom at rest.*

4·3.1. Light shifts. The effective Hamiltonians given in (4.7) are easy to diagonalize. First, the state $|g_0\rangle$ which is not coupled to any other state is obviously an eigenstate of H_{eff}. Then, the 2×2 matrix representing H_{eff} in the manifold $\{|g_{\pm 1}\rangle\}$ has equal diagonal elements. It follows that the symmetric and antisymmetric linear combinations of $|g_1\rangle \exp[ikz]$ and $|g_{-1}\rangle \exp[-ikz]$ are also eigenstates of H_{eff}. If we put

$$(4.13a) \qquad |\psi_S(z)\rangle = \frac{1}{\sqrt{2}} [|g_1\rangle \exp[ikz] + |g_{-1}\rangle \exp[-ikz]],$$

$$(4.13b) \qquad |\psi_A(z)\rangle = \frac{1}{\sqrt{2}} [|g_1\rangle \exp[ikz] - |g_{-1}\rangle \exp[-ikz]],$$

we get for a $J_g = 1 \leftrightarrow J_e = 2$ transition

$$(4.14a) \qquad \begin{cases} H_{\text{eff}}(1 \leftrightarrow 2)|g_0\rangle = (\hbar\delta'/2)|g_0\rangle, \\ H_{\text{eff}}(1 \leftrightarrow 2)|\psi_S(z)\rangle = (2\hbar\delta'/3)|\psi_S(z)\rangle, \\ H_{\text{eff}}(1 \leftrightarrow 2)|\psi_A(z)\rangle = (\hbar\delta'/2)|\psi_A(z)\rangle, \end{cases}$$

and for a $J_g = 1 \leftrightarrow J_e = 1$ transition

$$(4.14b) \qquad \begin{cases} H_{\text{eff}}(1 \leftrightarrow 1)|g_0\rangle = (\hbar\delta'/2)|g_0\rangle, \\ H_{\text{eff}}(1 \leftrightarrow 1)|\psi_S(z)\rangle = 0|\psi_S(z)\rangle, \\ H_{\text{eff}}(1 \leftrightarrow 1)|\psi_A(z)\rangle = (\hbar\delta'/2)|\psi_A(z)\rangle. \end{cases}$$

As predicted above (see subsect. 4·1), we find that the light shifts are independent of z, whereas the eigenstates of H_{eff} depend on z. Figure 6 represents for both transitions the light shifts of the ground-state Zeeman sublevels. As in sect. 3, we have supposed $\delta < 0$, so that light shifts are negative. Note that $|g_0\rangle$ and $|\psi_A(z)\rangle$ have the same light shift, so that they remain degenerate.

The results obtained in (4.14) and represented in fig. 6 could have been found more quickly by noting that the laser polarization in z is linear and parallel to the unit vector $\varepsilon(z)$ given in (4.4). It is then clear that the eigenstates of

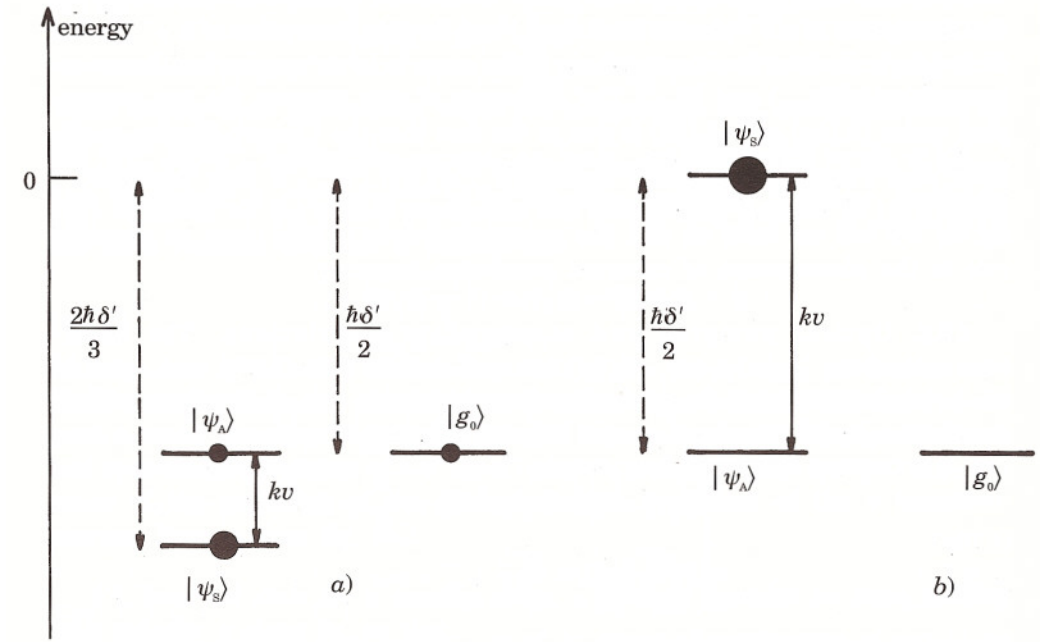

Fig. 6. – Light shifts of the ground-state Zeeman sublevels for a $J_g = 1 \leftrightarrow J_e = 2$ transition (a)) and for a $J_g = 1 \leftrightarrow J_e = 1$ transition (b)). The size of the solid circles is proportional to the steady-state population of the corresponding sublevels for an atom at rest in z. We have supposed $\delta < 0$. The vertical arrows represent the motional coupling between $|\psi_S\rangle$ and $|\psi_A\rangle$, characterized by an angular frequency kv.

the component $\varepsilon(z)\cdot\boldsymbol{J}$ of the angular momentum $\boldsymbol{J}$ have a well-defined light shift, which is equal to the product of $\hbar\mathscr{E}'$ by the square of the Clebsch-Gordan coefficients of the π transitions of fig. 5. This gives immediately the eigenvalues written in (4.14) and their degeneracy. One can also check that $|\psi_S(z)\rangle$, given in (4.13*a*), coincides with the eigenstate of $\varepsilon(z)\cdot\boldsymbol{J}$ with eigenvalue 0, whereas $|g_0\rangle$ and $|\psi_A(z)\rangle$ given in (4.13*b*) are two orthogonal linear combinations of the two eigenstates of $\varepsilon(z)\cdot\boldsymbol{J}$ with eigenvalues $+\hbar$ and $-\hbar$. It turns out, however, that the two states $|\psi_S(z)\rangle$ and $|\psi_A(z)\rangle$, which we have introduced for diagonalizing H_{eff}, will play an important role in the following sections and that they are more convenient to use than the eigenstates of $\varepsilon(z)\cdot\boldsymbol{J}$. First, we will see in the next subsect. 4·4 that atomic motion couples only $|\psi_S\rangle$ to $|\psi_A\rangle$ and *vice versa*. Second, the states $|\psi_A(z)\rangle$ for a $J_g = 1 \leftrightarrow J_e = 2$ transition, $|\psi_S(z)\rangle$ for a $J_g = 1 \leftrightarrow J_e = 1$ transition are linear combinations of $|g_{-1}\rangle$ and $|g_1\rangle$, which are not coupled to the excited state $|e_0\rangle$ by the laser-atom interaction Hamiltonian V_{AL} (for an atom at rest in z). One can easily check that

$$\langle e_0 | V_{AL}(1 \leftrightarrow 2) | \psi_A(z)\rangle = 0, \tag{4.15a}$$

$$\langle e_0 | V_{AL}(1 \leftrightarrow 1) | \psi_S(z)\rangle = 0. \tag{4.15b}$$

The physical interpretation of this result is that the absorption amplitudes for the absorption of a σ^+ photon from $|g_{-1}\rangle$ and for the absorption of a σ^- photon from $|g_{+1}\rangle$ can interfere destructively if the atom is in an appropriate linear superposition of $|g_{-1}\rangle$ and $|g_{+1}\rangle$. The difference of sign between the two noncoupled states (4.15*a*) and (4.15*b*) is due to the fact that the Clebsch-Gordan coefficients of the σ^+ and σ^- transitions arriving in e_0 are equal for a $J_g = 1 \leftrightarrow J_e = 2$ transition, whereas they are opposite for a $J_g = 1 \leftrightarrow J_e = 1$ transition (see fig. 5). We will see later on that the noncoupled state (4.15*b*) plays an essential role in the phenomenon of coherent population trapping.

4·3.2. Optical pumping and steady-state populations. The departure rates from $|g_0\rangle$, $|\psi_S(z)\rangle$, $|\psi_A(z)\rangle$ are well defined (see (2.39)), and equal to the product of Γ' by the eigenvalues of Λ, which are the coefficients of $\hbar\mathscr{E}'$ in (4.14). We get in this way

$$\begin{cases} \Gamma'_0(1 \leftrightarrow 2) = \Gamma'_A(1 \leftrightarrow 2) = \dfrac{\Gamma'}{2}, \\ \Gamma'_S(1 \leftrightarrow 2) = \dfrac{2\Gamma'}{3} \end{cases} \tag{4.16a}$$

for a $J_g = 1 \leftrightarrow J_e = 2$ transition and

$$\begin{cases} \Gamma'_0(1 \leftrightarrow 1) = \Gamma'_A(1 \leftrightarrow 1) = \dfrac{\Gamma'}{2}, \\ \Gamma'_S(1 \leftrightarrow 1) = 0 \end{cases} \tag{4.16b}$$

for a $J_g = 1 \leftrightarrow J_e = 1$ transition. The vanishing of $\Gamma'_S(1 \leftrightarrow 1)$ reflects the fact that $|\psi_S(z)\rangle$ is a noncoupled state for a $J_g = 1 \leftrightarrow J_e = 1$ transition. For a $J_g = 1 \leftrightarrow J_e = 2$ transition, the state $|\psi_A(z)\rangle$ is not coupled to e_0, but it remains coupled to $|e_{+2}\rangle$ and $|e_{-2}\rangle$, which explains why $\Gamma'_A(1 \leftrightarrow 2)$ does not vanish as $\Gamma'_S(1 \leftrightarrow 1)$.

In order to find the steady-state density matrix for an atom at rest in z, which results from the competition between the departure rates and the return rates, respectively, associated with the second and third terms of the right-hand side of (2.35), we use the basis of eigenstates of $\boldsymbol{\varepsilon}(z)\cdot\boldsymbol{J}$, where the laser polarization can be considered as a π polarization and where the steady-state density matrix is diagonal. Consider first a $J_g = 1 \leftrightarrow J_e = 2$ transition. A simple detailed-balance argument, expressing that the number of transitions from g_0 to g_{-1} by absorption of a π photon and spontaneous emission of a σ^+ photon must balance the number of transitions from g_{-1} to g_0 by absorption of a π photon and spontaneous emission of a σ^- photon, then shows that the populations of the eigenstates of $\boldsymbol{\varepsilon}(z)\cdot\boldsymbol{J}$ with eigenvalues $-\hbar$, 0, $+\hbar$ are, respectively, equal to $4/17$, $9/17$, $4/17$. It follows that, in the basis $\{|g_0\rangle, |\psi_S\rangle, |\psi_A\rangle\}$, the density matrix is also diagonal, the corresponding populations being equal to

$$\text{(4.17}a\text{)} \qquad \begin{cases} \Pi_0(1 \leftrightarrow 2) = \Pi_A(1 \leftrightarrow 2) = \dfrac{4}{17}, \\ \Pi_S(1 \leftrightarrow 2) = \dfrac{9}{17}. \end{cases}$$

These steady-state populations, which are independent of z, are represented by the solid circles of fig. 6*a*).

Consider now a $J_g = 1 \leftrightarrow J_e = 1$ transition. Since the departure rate from $|\psi_S\rangle$ vanishes, all the atomic population will be optically pumped in $|\psi_S\rangle$ where the atom remains trapped. It follows that

$$\text{(4.17}b\text{)} \qquad \begin{cases} \Pi_0(1 \leftrightarrow 1) = \Pi_A(1 \leftrightarrow 1) = 0, \\ \Pi_S(1 \leftrightarrow 1) = 1. \end{cases}$$

Such a result can be also obtained by using the basis of eigenstates of $\boldsymbol{\varepsilon}(z)\cdot\boldsymbol{J}$. In such a basis, the atom is optically pumped into g_0 by absorption of a π photon and spontaneous emission of a σ^+ or σ^- photon, and it remains trapped in g_0 because of the vanishing of the Clebsch-Gordan coefficient of the π transition starting from g_0 (see fig. 5*b*)).

4·4. *Internal state for a moving atom.* – We now consider an atom moving with velocity v along $0z$, so that

$$z = vt, \tag{4.18}$$

and we also suppose that

$$T_{\text{int}} \ll T_{\text{ext}}, \tag{4.19}$$

so that we can neglect the variation of v during the time T_{int} required by internal variables to reach a steady state.

4·4.1. Transformation to the moving rotating frame. Replacing z by vt in the expression (4.4) of $\varepsilon(z)$ shows that, in its rest frame, moving with velocity v along $0z$, the atom «sees» a laser field with a polarization rotating around $0z$ with an angular frequency $-kv$. This suggests the introduction, in the atomic rest frame, of a rotating frame such that, in this moving rotating frame, the laser field keeps a fixed direction.

Such a transformation is achieved by applying a unitary transformation

$$T(t) = \exp[-ikvtJ_z/\hbar]. \tag{4.20}$$

One can easily check (see appendix A of ref. [19]) that, in the new representation, the laser-atom interaction Hamiltonian describes the coupling of the atomic dipole moment with a laser electric field keeping a fixed linear polarization, parallel to ε_y.

In the new representation, the atomic density matrix is equal to

$$\tilde{\sigma} = \exp[-ikvtJ_z/\hbar]\,\sigma\,\exp[+ikvtJ_z/\hbar], \tag{4.21}$$

which shows that the change of variables introduced above in (4.9) corresponds to a trasformation to the rotating frame. Note that the populations $\Pi_{-1}, \Pi_0, \Pi_{+1}$ of the three Zeeman sublevels $|g_{-1}\rangle$, $|g_0\rangle$, $|g_{+1}\rangle$ are not modified by the transformation (4.20).

4·4.2. New Hamiltonian. New equations of motion. Since $T(t)$ depends on t, the dynamics in the new representation is governed by the Hamiltonian

$$\tilde{H} = T(t)\,HT^+(t) + i\hbar\left[\frac{\mathrm{d}T(t)}{\mathrm{d}t}\right]T^+(t), \tag{4.22}$$

where H is the Hamiltonian of the old representation. We have already mentioned that $T(t)\,HT^+(t)$ describes the dynamics of the atom coupled to a laser field with a fixed linear polarization parallel to ε_y. This dynamics is, therefore, described by eq. (2.35) where $\varepsilon(\boldsymbol{r})$ is replaced by ε_y, and σ by $\tilde{\sigma}$.

Using (4.20), one can show that the last term of (4.22) is equal to

$$i\hbar\left[\frac{\mathrm{d}T(t)}{\mathrm{d}t}\right]T^+(t) = V_{\text{rot}} = kvJ_z. \tag{4.23}$$

Such a term, which is time independent, has the same form as an interaction Hamiltonian with a static (fictitious) magnetic field $\boldsymbol{B}_f$, parallel to $0z$, and having an amplitude such that the corresponding Larmor frequency is equal to kv. Actually, such a fictitious field is nothing but an inertial field appearing in the new frame because of its rotation (Larmor's theorem).

Finally, the dynamics of a moving atom is the same as the dynamics of an atom at rest in $z = 0$ submitted in addition to the effect of a static magnetic field $\boldsymbol{B}_f$ parallel to $0z$. From (2.35) and (4.23), one deduces that the equation of motion of $\tilde{\sigma}_{gg}$ in the new representation can be written

$$\dot{\tilde{\sigma}}_{gg} = -i\delta'[\Lambda(z=0), \tilde{\sigma}_{gg}] - \frac{\Gamma'}{2}\{\Lambda(z=0), \tilde{\sigma}_{gg}\}_+ + \tag{4.24}$$

$$+ \Gamma' \sum_{q=-1,0,+1} (\boldsymbol{\varepsilon}_q^* \cdot \hat{\boldsymbol{d}}^-)(\boldsymbol{\varepsilon}_y \cdot \hat{\boldsymbol{d}}^+)\tilde{\sigma}_{gg}(\boldsymbol{\varepsilon}_y^* \cdot \hat{\boldsymbol{d}}^-)(\boldsymbol{\varepsilon}_q \cdot \hat{\boldsymbol{d}}^+) - ikv\left[\frac{J_z}{\hbar}, \tilde{\sigma}_{gg}\right].$$

In (4.24), $\Lambda(z)$ is the coefficient of $\hbar\delta'$ in (4.7). Using (4.7), (4.10) and the Clebsch-Gordan coefficients of fig. 5, one can deduce from (4.24) a closed set of 5 equations for Π_{-1}, Π_0, Π_1, C_r, C_i which can be written

$$\begin{cases} \dot{\Pi}_1 = -\frac{5\Gamma'}{72}\Pi_1 + \frac{9\Gamma'}{72}\Pi_0 + \frac{\Gamma'}{72}\Pi_{-1} - \frac{\Gamma'}{18}C_r - \frac{\delta'}{6}C_i, \\ \dot{\Pi}_{-1} = +\frac{\Gamma'}{72}\Pi_1 + \frac{9\Gamma'}{72}\Pi_0 - \frac{5\Gamma'}{72}\Pi_{-1} - \frac{\Gamma'}{18}C_r + \frac{\delta'}{6}C_i, \\ \dot{\Pi}_0 = -(\dot{\Pi}_1 + \dot{\Pi}_{-1}), \\ \dot{C}_r = +\frac{\Gamma'}{24}\Pi_1 + \frac{\Gamma'}{8}\Pi_0 + \frac{\Gamma'}{24}\Pi_{-1} - \frac{5\Gamma'}{12}C_r + 2kvC_i, \\ \dot{C}_i = +\frac{\delta'}{12}(\Pi_1 - \Pi_{-1}) - 2kvC_r - \frac{5\Gamma'}{12}C_i \end{cases} \tag{4.25a}$$

for a $J_g = 1 \leftrightarrow J_e = 2$ transition, and

$$\begin{cases} \dot{\Pi}_1 = -\frac{\Gamma'}{8}\Pi_1 + \frac{\Gamma'}{8}\Pi_0 + \frac{\Gamma'}{8}\Pi_{-1} + \frac{\delta'}{2}C_i, \\ \dot{\Pi}_{-1} = +\frac{\Gamma'}{8}\Pi_1 + \frac{\Gamma'}{8}\Pi_0 - \frac{\Gamma'}{8}\Pi_{-1} - \frac{\delta'}{2}C_i, \\ \dot{\Pi}_0 = -(\dot{\Pi}_1 + \dot{\Pi}_{-1}) = -\frac{\Gamma'}{4}\Pi_0, \\ \dot{C}_r = \frac{\Gamma'}{8} - \frac{\Gamma'}{4}C_r + 2kvC_i, \\ \dot{C}_i = -\frac{\delta'}{4}(\Pi_1 - \Pi_{-1}) - 2kvC_r - \frac{\Gamma'}{4}C_i \end{cases} \tag{4.25b}$$

for a $J_g = 1 \leftrightarrow J_e = 1$ transition. The Zeeman coherences $\Delta m = \pm 1$ are not coupled to Π_0, $\Pi_{\pm 1}$, C_r, C_i because of the selection rule $\Delta m = 0, \pm 2$ followed by Λ and because the $|g_m\rangle$ are eigenstates of J_z. Since all coefficients of eqs. (4.25) are time independent, these equations have a steady-state solution.

The third equation in (4.25*b*) shows that, for a $J_g = 1 \leftrightarrow J_e = 1$ transition, Π_0 is damped with a rate $\Gamma'/4$. This is due to the fact that an atom initially in g_0 is optically pumped into $g_{\pm 1}$. From $g_{\pm 1}$, it can be re-excited

to e_0 but it can then never fall back in g_0 because of the vanishing of the Clebsch-Gordan coefficient of the transition $e_0 \leftrightarrow g_0$ (see fig. 5*b*)).

4·4.3. New expression of the mean force. Suppose that the atom has reached a steady state so that all left-hand sides of eqs. (4.25) can be put equal to zero.

Consider first a $J_g = 1 \leftrightarrow J_e = 2$ transition. If one subtracts the second equation (4.25*a*) from the first one, one gets,

$$\text{for} \quad J_g = 1 \leftrightarrow J_e = 2, \qquad \Pi_1 - \Pi_{-1} = -\frac{4\delta'}{\Gamma'} C_i . \tag{4.26}$$

Equation (4.26), combined with (4.11*a*) and (4.12*a*), implies that

$$\mathscr{F}_{\text{dissip}}(1 \leftrightarrow 2) = 5\mathscr{F}_{\text{react}}(1 \leftrightarrow 2) . \tag{4.27}$$

The dissipative force is proportional to the reactive force, and 5 times more important, so that the total mean force is equal to

$$\mathscr{F}(1 \leftrightarrow 2) = \frac{6}{5}\mathscr{F}_{\text{dissip}}(1 \leftrightarrow 2) = \frac{1}{2}\hbar k \Gamma' \varepsilon_z (\Pi_1 - \Pi_{-1}) . \tag{4.28}$$

For a $J_g = 1 \leftrightarrow J_e = 2$ transition, the main effect is, therefore, the imbalance between the radiation pressures exerted by the two counterpropagating waves. It may appear surprising that the reactive force is smaller than the dissipative force, even if $|\delta| \gg \Gamma$ (which implies $|\delta'| \gg \Gamma'$). This is due to the fact that the redistribution processes, which are at the origin of the reactive force, are limited to a finite number of steps in the case of a σ^+-σ^- configuration. Starting from g_{-1}, the atom can absorb a σ^+ photon in the $k\varepsilon_z$ wave, jump into e_0, then make a stimulated emission of a σ^- photon in the $-k\varepsilon_z$ wave, which brings it into g_{+1}, then absorb again a σ^+ photon in the $k\varepsilon_z$ wave and jump into e_2. But, from e_2, it can no longer make a stimulated emission of a σ^- photon and the redistribution stops. This would not be the case if, as in sect. 3, the polarizations of the two counterpropagating waves both contain an admixture of σ^+ and σ^-.

Consider now a $J_g = 1 \leftrightarrow J_e = 1$ transition. Since Π_0 vanishes in steady state, the first two equations (4.25*b*) are identical in steady state and lead to,

$$\text{for} \quad J_g = 1 \leftrightarrow J_e = 1, \qquad \Pi_1 - \Pi_{-1} = +\frac{4\delta'}{\Gamma'} C_i , \tag{4.29}$$

which, combined with (4.11*b*) and (4.12*b*), gives

$$\mathscr{F}_{\text{dissip}}(1 \leftrightarrow 1) = -\mathscr{F}_{\text{react}}(1 \leftrightarrow 1) . \tag{4.30}$$

This shows that the reactive and dissipative forces are equal and opposite. For a $J_g = 1 \leftrightarrow J_e = 1$ transition, the mean total radiative force always vanishes, even for a moving atom

$$\mathscr{F}(1 \leftrightarrow 1) = \mathscr{F}_{\text{react}}(1 \leftrightarrow 1) + \mathscr{F}_{\text{dissip}}(1 \leftrightarrow 1) = \mathbf{0} . \tag{4.31}$$

There is, therefore, in this case no friction force. We will show, however, in the next section that a new cooling mechanism, not based on friction, but on momentum diffusion and velocity-selective coherent population trapping, can appear for such a transition.

4·5. *Friction force for a* $J_g = 1 \leftrightarrow J_e = 2$ *transition.*

4·5.1. Friction coefficient. In order to calculate the total mean force (4.28) experienced by the atom, we must solve eqs. (4.25*a*) and find the steady-state value of $\Pi_1 - \Pi_{-1}$.

Consider first the limit of very small velocities. For an atom with $v = 0$ at $z = 0$, we know the steady-state density matrix which is given in (4.17*a*) and from which we can deduce the steady-state values of Π_1, Π_0, Π_{-1}, C_r, C_i

for $v = 0$,

$$\begin{cases} \Pi_1 = \Pi_{-1} = 13/34, \\ \Pi_0 = 4/17, \\ C_r = 5/34, \\ C_i = 0. \end{cases} \tag{4.32}$$

We can then use eqs. (4.25*a*) with $v \neq 0$ to find the linear term in v of $\Pi_1 - \Pi_{-1}$ for an atom which is still at $z = 0$ in its moving rotating rest frame. Using (4.26), we can transform the last equation (4.25*a*) and express in steady state $\Pi_1 - \Pi_{-1}$ as a function of C_r. Since C_r is already multiplied by kv in this equation, we can replace C_r by the its zeroth-order value given in (4.32). We get in this way

$$\Pi_1 - \Pi_{-1} = \frac{240}{17} \frac{kv\delta'}{4\delta'^2 + 5\Gamma'^2} \tag{4.33}$$

and consequently, when (4.33) is inserted into (4.28),

$$\frac{kv}{|\delta'|} \ll 1 \rightarrow \mathscr{F}_z(1 \leftrightarrow 2) = -\alpha v, \tag{4.34}$$

where the friction coefficient α is given by

$$\alpha = -\frac{120}{17} \hbar k^2 \frac{\Gamma' \delta'}{4\delta'^2 + 5\Gamma'^2} = -\frac{120}{17} \hbar k^2 \frac{\Gamma\delta}{4\delta^2 + 5\Gamma^2}. \tag{4.35}$$

We have used (4.5).

It is possible to give a more physical derivation of (4.35) in the limit $|\delta| \gg \Gamma$, where $\Pi_1 - \Pi_{-1}$ and α are, according to (4.33) and (4.35), given by

$$|\delta| \gg \Gamma \rightarrow \Pi_1 - \Pi_{-1} \simeq +\frac{60}{17} \frac{kv}{\delta'}, \tag{4.36a}$$

(4.36b) $$\alpha \simeq -\frac{30}{17}\hbar k^2 \frac{\Gamma}{\delta}.$$

We come back to fig. 6a) giving the light shifts and steady-state populations of $|g_0\rangle$, $|\psi_S\rangle$ and $|\psi_A\rangle$ for an atom at rest and we try to understand the perturbation due to atomic motion, which is described by the Hamiltonian V_{rot} given in (4.23). Since $J_z|g_0\rangle = 0$, V_{rot} cannot couple $|g_0\rangle$ to any other state. Furthermore, one can easily check, using (4.13a) (without the exponentials $\exp[\pm ikz]$ since the atom is at $z = 0$ in its moving rotating rest frame), that V_{rot} has no diagonal elements in $|\psi_S\rangle$ and $|\psi_A\rangle$. The only nonzero matrix element of V_{rot} is between $|\psi_S\rangle$ and $|\psi_A\rangle$ and is equal to

(4.37) $$\langle\psi_S|V_{rot}|\psi_A\rangle = \hbar kv.$$

It is represented by the vertical arrow of fig. 6a). In the limit $kv \ll |\delta'|$, which is the condition of validity of (4.36), leading to $|\Pi_1 - \Pi_{-1}| \ll 1$, the motional coupling $\hbar kv$ between ψ_S and ψ_A is small compared to the splitting $E_S - E_A$ which, according to (4.14a), is equal to

(4.38) $$E_S - E_A = \frac{2}{3}\hbar\delta' - \frac{1}{2}\hbar\delta' = \frac{\hbar\delta'}{6}.$$

The effect of V_{rot} can thus be treated by perturbation theory. To lowest order in kv/δ', *i.e.* to order 1, the main effect of V_{rot} is to change the wave functions. The wave function of ψ_A is contaminated by ψ_S and *vice versa*. If $\overline{|\psi_S\rangle}$ and $\overline{|\psi_A\rangle}$ are the perturbed states associated with $|\psi_S\rangle$ and $|\psi_A\rangle$, we have, to first order in kv/δ',

(4.39a) $$\overline{|\psi_S\rangle} = |\psi_S\rangle + \frac{\hbar kv}{E_S - E_A}|\psi_A\rangle = |\psi_S\rangle + \frac{6kv}{\delta'}|\psi_A\rangle =$$

$$= \frac{1}{\sqrt{2}}\left[\left(1 + \frac{6kv}{\delta'}\right)|g_{+1}\rangle + \left(1 - \frac{6kv}{\delta'}\right)|g_{-1}\rangle\right],$$

(4.39b) $$\overline{|\psi_A\rangle} = |\psi_A\rangle + \frac{\hbar kv}{E_A - E_S}|\psi_S\rangle = |\psi_A\rangle - \frac{6kv}{\delta'}|\psi_S\rangle =$$

$$= \frac{1}{\sqrt{2}}\left[\left(1 - \frac{6kv}{\delta'}\right)|g_{+1}\rangle - \left(1 + \frac{6kv}{\delta'}\right)|g_{-1}\rangle\right].$$

Whereas $|\psi_S\rangle$ and $|\psi_A\rangle$ contain both the same proportion of $|g_1\rangle$ and $|g_{-1}\rangle$, this is no longer true for $\overline{|\psi_S\rangle}$ and $\overline{|\psi_A\rangle}$. For example, since $\delta' < 0$, the weight of $|g_{-1}\rangle$ in $\overline{|\psi_S\rangle}$ is larger than the weight of $|g_1\rangle$. The conclusions are reversed for $\overline{|\psi_A\rangle}$. Since levels $\overline{|\psi_S\rangle}$ and $\overline{|\psi_A\rangle}$ have unequal populations, one understands how the motional coupling $\hbar kv$ between $|\psi_S\rangle$ and $|\psi_A\rangle$ can give rise to a motion-induced difference between Π_1 and Π_{-1}. As in ref. [19], such an argument can be

formulated in quantitative terms (*) and leads exactly to (4.36). We want to emphasize here that the motion-induced population difference $\Pi_1 - \Pi_{-1}$ varies as kv/δ', and not as kv/Γ, as is the case for Doppler cooling. Since $|\delta'| \ll \Gamma$ at low intensity, the new cooling mechanism discussed here is, therefore, much more sensitive to the velocity than Doppler cooling.

It is clear in (4.35) that, as in sect. 3, the friction coefficient is independent of the laser intensity I_L. This results from a compensation in (4.28) between the I_L-dependence of the absorption rate Γ', which decreases as I_L when I_L decreases, and the I_L-dependence of $\Pi_1 - \Pi_{-1}$, which increases as $1/I_L$ (see (4.33) and (4.36*a*)). In particular, one sees in fig. 6*a*) that, when I_L decreases, the distance between ψ_S and ψ_A decreases, which explains why the contamination of wave functions induced by the motional coupling $\hbar kv$ between ψ_S and ψ_A increases when I_L decreases. Note also that, according to (4.36*b*), α is on the order of $-(30/17)\hbar k^2\Gamma/\delta$ for $|\delta| \gg \Gamma$. Such a value is smaller than the corresponding value (3.39) of α_S found in sect. 3 by a factor of the order of Γ^2/δ^2 which is small for $|\delta| \gg \Gamma$. We will see, however, in subsect. 4·5.3, that the momentum diffusion coefficient is also reduced by the same factor Γ^2/δ^2, so that the equilibrium temperatures are on the same order for both σ^+-σ^- and Lin $\perp$ Lin configurations.

4·5.2. Velocity capture range. From now on, we will suppose that $|\delta| \gg \Gamma$. When kv is no longer small compared to $|\delta'|$, all perturbative calculations of the previous subsection, based on the smallness of kv/δ', are no longer valid. One must then come back to eqs. (4.25*a*) and determine their exact steady-state solution, either numerically or analytically. One then finds that the variations with v of the mean force (4.28) are those of a dispersion curve, the maximum of the modulus of the force being reached for a critical velocity v_c, or velocity capture range, such that

$$kv_c \sim |\delta'| . \tag{4.40}$$

Figure 8 of ref. [19], which also includes the effect of Doppler cooling, gives an example of such a calculation.

As the velocity capture range (3.36) found for low-intensity Sisyphus cooling, the value (4.40) of v_c is proportional to the laser intensity I_L. There is, however, an important difference between (3.36) and (4.40). For the Lin $\perp$ Lin configuration, kv_c is proportional to the absorption rate Γ', whereas, for the σ^+-σ^- configuration, kv_c is proportional to the light shift δ'.

The discussion of this subsection can be presented in more physical terms by

(*) In ref. [19], the calculation is done in the basis of eigenstates of $\varepsilon_y \cdot J$. The motional coupling V_{rot} has then two nonzero off-diagonal elements. Using the basis $\{|g_0\rangle, |\psi_S\rangle, |\psi_A\rangle\}$, as we do here, simplifies the calculations because only $|\psi_S\rangle$ and $|\psi_A\rangle$ are coupled by V_{rot}.

considering that the atom is submitted in the ground state to two perturbations with different symmetries. We have first the effect of the laser-atom interaction which, in the moving rotating frame, has the symmetry of a static electric field parallel to ε_y and which is characterized by a Hamiltonian part, proportional to δ', and a relaxation part, proportional to Γ'. We also have the effect of atomic motion which has the symmetry of a magnetic field parallel to ε_z and which is proportional to kv. Depending on the relative values of kv and $|\delta'|$, one perturbation is predominant over the other. Both are of the same order for $v = v_c$. In this sense, there is a certain analogy between the narrow structures appearing in the variations with v of the mean force (4.28) and the narrow Hanle resonances which can be observed in atomic ground states (see subsect. 2·5.3).

4·5.3. Order of magnitude of the equilibrium temperature. First we try to evaluate the momentum diffusion coefficient D for an atom at rest in z. Using the same notation and the same arguments as in subsect. 3·5.3, we get for D_{vac} and D_{abs} the same result as in (3.41a). This amounts to assuming that D_{vac} and D_{abs} have the same order of magnitude as for a two-level atom (see subsect. 5.2.3 of ref. [1]). We will see in the next subsection that this is not a good approximation for D_{abs}.

Since there is no spatial gradient of light shifts in the σ^+-σ^- configuration, there is no dipole force and no contribution D_{dip} to D as in (3.41b). It follows that

$$D \sim D_{\text{vac}} \sim D_{\text{abs}} \sim \hbar^2 k^2 \Gamma' . \tag{4.41}$$

Comparing (4.41) to (3.42), we see that D is smaller in the σ^+-σ^- configuration by a factor on the order of Γ^2/δ^2. This reduction of D compensates for the reduction of α found above, so that the equilibrium temperature

$$k_B T \sim \frac{D}{\alpha} \sim \hbar\delta' \sim \frac{\hbar\Omega_1^2}{|\delta|} \tag{4.42}$$

is on the same order for both σ^+-σ^- and Lin $\perp$ Lin configurations.

4·5.4. Anomalous momentum diffusion. A quantum calculation of the momentum diffusion coefficient is done in ref. [33]. Such a calculation shows that D_{vac} has the order of magnitude given in (4.41), but that D_{abs} can be much larger than D_{vac} for certain values of δ and kv. We now discuss the physical meaning of such an anomalous momentum diffusion. More details may be found in ref. [33]. See also ref. [19, 21, 34].

The enhancement of D_{abs} is due to correlations between the directions of two successively absorbed photons. Because of optical pumping, just after the absorption of a σ^+ photon, the atom has a high probability to be in g_1 from where it has a higher probability to absorb a σ^+ photon than a σ^- one, since the σ^+ transi-

tion starting from g_1 is 6 times more intense than the σ^- one (see fig. 5*a*)). It follows that the atom absorbs in sequence several σ^+ photons until it absorbs a σ^- photon which optically pumps it into g_{-1} from where it absorbs in sequence several σ^- photons and so on .... As a consequence, the steps of the random walk in momentum space (due to absorption) can be several $\hbar k$ instead of $\hbar k$ and this explains the increase of D_{abs}. Such an effect becomes more and more important for larger values of J_g.

Such an enhancement of D_{abs} occurs only if the eigenstates of J_z can be considered as stationary between two successive fluorescence cycles, separated by a time on the order of $\tau_P = 1/\Gamma'$. This is achieved, either for a moving atom with $kv \gg |\delta'|$, or for a slow atom if the detuning is small ($kv \ll |\delta'|$, $|\delta'| \ll \Gamma'$). In the first case ($kv \gg |\delta'|$) the perturbation $V_{\text{rot}} = kvJ_z$ predominates over the effect of light shifts described by H_{eff}, so that the eigenstates of J_z are quasi-stationary. In the second case, V_{rot} is negligible in comparison with H_{eff} (since $kv \ll |\delta'|$), but the precession induced by H_{eff} between the eigenstates of J_z occurs at a frequency $|\delta'|$, which is too small compared to the absorption rate Γ' to produce any observable effect between two fluorescence cycles.

The previous discussion explains why D_{abs} varies rapidly with kv for a given large value of δ. It is possible to understand in this way the profiles of the momentum distributions derived from a numerical integration of the full quantum equations of motion [34]. The broad pedestal which appears in these distributions, and which becomes more pronounced for larger values of J_g, reflects the increase of D_{abs} when v increases. Note, however, that the width of the narrow peak around $p = 0$ appearing in these distributions remains large compared to $\hbar k$, so that the semi-classical approximation is not bad. But, for large values of J_g, the atom can make in sequence so many σ^+ transitions starting from the sublevel with the highest magnetic quantum number $m = J_g$ that it remains trapped in this sublevel for a time T_{int} which can become on the order of or even longer than T_{ext}. As in the case of low-intensity Sisyphus cooling (see subsect. 3·6.1), we find here a new example of a situation where usual treatments of laser cooling become questionable, not because of the semi-classical approximation, but because the usual assumption $T_{\text{int}} \ll T_{\text{ext}}$ is no longer valid.

4·6. *Coherent population trapping for a* $J_g = 1 \leftrightarrow J_e = 1$ *transition.* – The fact that the mean total force vanishes for a $J_g = 1 \leftrightarrow J_e = 1$ transition (see (4.31)), even if the atom is moving, does not mean that no interesting effect can occur for such a transition. We show in this subsection how atomic motion can induce spectacular changes in the internal dynamics.

4·6.1. Qualitative discussion. We have already mentioned at the end of subsect. 4·4.2 that atoms initially in g_0 are optically pumped into $g_{\pm 1}$, from where they can never come back to g_0. Since there is no motional coupling between g_0 and $g_{\pm 1}$, we can thus completely ignore g_0, and consider that the

ground state has only two relevant sublevels, g_1 and g_{-1}, or their linear combinations ψ_S and ψ_A given in (4.13), with $z = 0$.

For $v = 0$, all the atomic population is optically pumped into $|\psi_S\rangle$ (see fig. 6*b*)). When the atom is moving, a motional coupling $\hbar kv$ appears between the two states $|\psi_S\rangle$ and $|\psi_A\rangle$ (vertical arrow of fig. 6*b*)), which are separated by a distance

$$E_S - E_A = -\frac{\hbar\delta'}{2}. \tag{4.43}$$

In the same way as for a $J_g = 1 \leftrightarrow J_e = 2$ transition, the wave functions of $|\psi_S\rangle$ and $|\psi_A\rangle$ are perturbed and this gives rise to a nonzero value of $\Pi_1 - \Pi_{-1}$. But we now have an additional spectacular effect which comes from the fact that, when $v = 0$, the absorption rate from $|\psi_S\rangle$ vanishes (see (4.16*b*)). The contamination of $|\psi_S\rangle$ by $|\psi_A\rangle$, induced by atomic motion, transfers to $|\psi_S\rangle$ a small part of the instability of $|\psi_A\rangle$, and the absorption rate from the perturbed state $\overline{|\psi_S\rangle}$ corresponding to $|\psi_S\rangle$ no longer vanishes. In other words, the total fluorescence rate R_F, which vanishes when $v = 0$ because all atoms are in the nonabsorbing state $|\psi_S\rangle$, reappears when the atom is moving because a slight absorption can take place from $\overline{|\psi_S\rangle}$. Such an effect is characterized by the perturbation parameter $kv/(E_S - E_A) \sim kv/\delta'$, so that the variations of R_F with v occur in a very small velocity range around $v = 0$, on the order of v_c given by (4.40).

For the transition $J_g = 1 \leftrightarrow J_e = 2$, the motional coupling $\hbar kv$ between $|\psi_S\rangle$ and $|\psi_A\rangle$ also changes the absorption rates from these sublevels. In this case, it is the sublevel $|\psi_A\rangle$ which is not coupled to $|e_0\rangle$ (see (4.15*a*)) and which becomes partially coupled when contaminated by $|\psi_S\rangle$. The effect is, however, less spectacular because, even if $v = 0$, the state $|\psi_A\rangle$ can absorb light (see (4.16*a*)), since it is always coupled to e_2 and e_{-2}. One, therefore, expects variations of the total fluorescence rate when v is slightly varied around $v = 0$, but the fluorescence never stops completely, as is the case for a $J_g = 1 \leftrightarrow J_e = 1$ transition.

Note also that, when the atom is moving with velocity v, it «sees» in its rest frame the two counterpropagating laser waves with opposite Doppler shifts $\pm kv$, so that these two waves have different apparent frequencies $\omega_L \pm kv$, differing by a frequency shift $\Delta = 2kv$ which vanishes for $v = 0$. As long as one is interested only in the internal atomic dynamics, one would get the same equations and the same results by considering another problem where an atom, always at rest, interacts with two laser waves (not necessarily counterpropagating) having different frequencies, $\omega_L \pm \Delta/2$. When $\Delta = 0$, the atom gets trapped into $|\psi_S\rangle$ and the fluorescence stops. When Δ is slightly varied from zero, the fluorescence reappears. One can finally show that similar equations also apply to the situation where $g_1 = g$ and $g_{-1} = g'$ have different energies E and E', and where the two laser waves have different frequencies, ω_L for the wave exciting the transition $g \leftrightarrow e_0$, ω'_L for the wave exciting the transition $g' \leftrightarrow e_0$. The fluorescence stops when $E + \hbar\omega_L = E' + \hbar\omega'_L$, *i.e.* when the two detunings of the

two laser excitations are equal, and reappears when ω_L' is slightly varied, ω_L, E and E' being fixed, or when $E - E'$ is slightly varied, ω_L and ω_L' being fixed. Such a phenomenon, called «coherent population trapping», was observed for the first time on sodium atoms irradiated by a bimodal laser and put in a gradient of magnetic field [35]. Because of the corresponding spatial variation of the Zeeman effect, the fluorescence of the sodium cell was disappearing at certain places along the laser beam, where two Zeeman sublevels belonging to the two different hyperfine levels were separated by a frequency splitting equal to the mode spacing.

4·6.2. Velocity dependence of the total fluorescence rate. We now give a more quantitative description of coherent population trapping. Since the only excited Zeeman sublevel which can be reached from g_1 and g_{-1} is e_0 (see fig. 5*b*)), the total fluorescence rate R_F is given by

$$R_F = \Gamma \sigma_{e_0 e_0}. \tag{4.44}$$

According to (2.28), the population $\sigma_{e_0 e_0}$ of e_0 can be expressed in terms of the ground-state density matrix. Using (2.28), (4.4), (4.5) and the Clebsch-Gordan coefficients of fig. 5*b*), we get

$$R_F = \frac{\Gamma'}{4}[\Pi_1 + \Pi_{-1} - 2C_r] = \frac{\Gamma'}{4}(1 - 2C_r). \tag{4.45}$$

To evaluate C_r, we come back to eqs. (4.25*b*). We already know that, in steady state, $\Pi_1 - \Pi_{-1}$ and C_i are proportional (see (4.29)). The last two equations thus couple only C_r and C_i and they allow one to calculate the steady-state value of C_r

$$C_r = \frac{1}{2}\,\frac{4\delta'^2 + \Gamma'^2}{4\delta'^2 + \Gamma'^2 + 64k^2v^2}, \tag{4.46}$$

which, inserted into (4.45), yields

$$R_F(v) = \Gamma'\,\frac{16k^2v^2}{4\delta'^2 + \Gamma'^2 + 64k^2v^2}. \tag{4.47}$$

It is clear from (4.47) that R_F vanishes for $v = 0$, and then increases when v increases, as an inverted Lorentz curve of amplitude $\Gamma'/4$ and of half-width at half maximum

$$\Delta v = \frac{\sqrt{4\delta'^2 + \Gamma'^2}}{8k}, \tag{4.48}$$

which decreases as I_L when I_L decreases. For $v \ll \Delta v$, R_F varies as

$$v \ll \Delta v \rightarrow R_F(v) \simeq 16k^2v^2\,\frac{\Gamma'}{4\delta'^2 + \Gamma'^2} = \frac{8k^2v^2\Gamma}{\Omega_1^2}, \tag{4.49}$$

which no longer depends on the detuning δ (we have used (4.5) and the definition of s_0 in terms of the Rabi frequency Ω_1, associated with each wave).

Calculations similar to the previous one and based on optical Bloch equations have been made [36] shortly after the discovery of coherent population trapping. Dressed-atom interpretations, using coupled and uncoupled states analogous to the states $|\psi_A\rangle$ and $|\psi_S\rangle$ introduced here, have been also given (see, for example, ref. [37] and [38]).

4·6.3. Consequences for atomic motion. We come back to the external dynamics of the atom. Although the mean friction force vanishes, the fact that the fluorescence rate R_F varies very rapidly with v around $v = 0$ has interesting consequences for atomic motion.

First, one expects that the momentum diffusion coefficient varies also very rapidly with v around $v = 0$ and tends to zero when $v \to 0$, since such a phenomenon is due to the random exchanges of momentum associated with fluorescence cycles.

In all previous discussions, we have considered an atom with a fixed velocity v and we have ignored any change of v. This is usual in semi-classical treatments of laser cooling where one calculates the friction and diffusion coefficients for a fixed value of v. In fact, because of the random changes of momentum following a fluorescence cycle, the atomic velocity makes a random walk in velocity space. The important new feature which appears here, and which is not included in usual treatments, is that such a random walk can be profoundly perturbed by the strong velocity dependence of the fluorescence rate. After a fluorescence cycle, depending whether v gets closer or farther from $v = 0$, the next fluorescence cycle will occur after a longer or shorter delay. We will see in the next section how such a velocity-dependent random walk can provide a new scheme for obtaining very narrow velocity distributions, *i.e.* very cold atoms.

5. – Laser cooling below the single-photon recoil limit.

5·1. *Introduction.*

5·1.1. The single-photon recoil limit. All cooling mechanisms described in the previous sections are based on a friction force which damps the atomic velocity. Spontaneous-emission processes also play a basic role for dissipating the energy removed from the external degrees of freedom of the atom. For example, in the Sisyphus cooling mechanism, either at high (sect. 7 of ref. [1] and ref. [18]) or low (sect. 3) intensity, spontaneous Raman anti-Stokes processes dissipate the potential energy gained by the atom (at the expense of its kinetic energy) when it climbs a potential hill. For Doppler cooling and for polarization gradient cooling in a σ^+-σ^- configuration, it is a blue Doppler shift of the spontaneously emitted photons

which explains the dissipation of energy (see discussion of subsect. 3.B.6 in ref. [19]).

Since, in all these cooling mechanisms, fluorescence cycles never stop, it seems impossible to avoid the random recoil due to spontaneously emitted photons and the corresponding single-photon recoil energy

$$E_R = \frac{\hbar^2 k^2}{2M} = k_B T_R . \tag{5.1}$$

The temperature T_R defined by (5.1) is called the single-photon recoil limit and appears as a fundamental limit for any cooling process using spontaneous emission. The corresponding velocity

$$v_R = \frac{\hbar k}{M} \tag{5.2}$$

is called the recoil velocity. For sodium cooled on the resonance line, $T_R \simeq$ $\simeq 2.4\ \mu K$ and $v_R \simeq 3$ cm/s. For cesium, we have $T_R \simeq 0.13\ \mu K$ and $v_R \simeq 3$ mm/s, and for helium cooled on the $2^3S_1 \leftrightarrow 2^3P_1$ transition at $\lambda = 1.08\ \mu m$, $T_R \simeq 4\ \mu K$ and $v_R \simeq 9$ cm/s.

5·1.2. Velocity-selective coherent population trapping. The previous discussion clearly shows that, in order to get temperatures lower than T_R, spontaneous-emission processes must stop for the atoms we want to cool down to very small temperatures. Such a remark suggests the use of the phenomenon discussed in subsect. 3·6 for a $J_g = 1 \leftrightarrow J_e = 1$ transition and a σ^+-σ^- laser configuration. We have seen in this case that the fluorescence rate R_F vanishes for atoms with zero velocity (see (4.47) and (4.49)), because atoms are optically pumped in a linear superposition of the ground-state sublevels which appears as a trapping nonabsorbing state. This trap is perfect for $v = 0$ and less and less perfect when v increases. This is why such a phenomenon can be called velocity-selective coherent population trapping. It selects very cold atoms, having very small velocities, and protects them from the «bad» effects of spontaneous emission.

Actually, if we want to achieve a cooling, we must also compress the velocity distribution around $v = 0$. It is not sufficient to find a velocity selection mechanism which consists here of quenching the fluorescence rate for atoms contained in a small velocity range δv around $v = 0$. One must also increase the density of atoms in this velocity range.

5·1.3. Optical pumping in velocity space. Because of the momentum transferred to the atom by the absorbed photon and because of the momentum carried away by the fluorescence photon, there is a random change of atomic momentum after each fluorescence cycle. It may happen that an atom with $v > \delta v$ undergoes such a cycle and ends up with $v < \delta v$. Momentum diffusion can

thus be considered as an optical-pumping process in velocity space which transfers atoms from the absorbing velocity classes into the nonabsorbing velocity range δv around $v = 0$ where they remain trapped during the interaction time θ and where they pile up, forming a narrow peak in the velocity distribution.

The new cooling mechanism we have just described, and which has been first proposed and demonstrated in ref. [39] and [40], differs radically from the other ones since it is not based on friction but on a combination of momentum diffusion and velocity-selective coherent population trapping (*). We show in the subsequent subsection that it is limited only by the interaction time θ. Another important feature is that it does not depend on the sign of the detuning.

5·1.4. Failure of semi-classical treatments. The semi-classical treatment presented in sect. 4 considers atoms which are very well localized in the laser wave. For example, the state $|\psi_S(z)\rangle$, which we have introduced in (4.13*a*) for an atom «at rest in z» and which is a nonabsorbing state for a $J_g = 1 \leftrightarrow J_e = 1$ transition (see (4.15*b*)), refers to the internal state of an atom whose centre of mass is described as a wave packet so well localized around z that it is not necessary to describe the evolution of such a wave packet in fully quantum terms. In (4.13*a*), z is considered as a fixed parameter. If the atom is moving with velocity v, z is replaced by the c-number vt (see (4.18)).

If a cooling mechanism reduces the momentum spread δp of the atom below $\hbar k$, which is the case for laser cooling below the single-photon recoil limit, the spatial coherence length $\xi_A \sim \hbar/\delta p$ becomes larger than the laser wavelength and it is no longer possible to consider the atom as well localized in the laser wave. A fully quantum treatment of all degrees of freedom is then required. Such a treatment is presented in the next subsection. We will see that the nonabsorbing state is still given by (4.13*a*), but that $\psi_S(z)$ is no longer the internal state of a wave packet localized in z, but a two-component wave function of z.

5·2. *One-dimensional quantum treatment.* – We consider here a σ^+-σ^- laser configuration and a $J_g = 1 \leftrightarrow J_e = 1$ transition.

5·2.1. Quantum atomic states uncoupled to the laser light. The atomic states are now labelled by two quantum numbers, one for the internal state, one for the external state. We have already seen in sect. 4 (see end of subsect. 4·4.2) that, for a $J_g = 1 \leftrightarrow J_e = 1$ transition, the only relevant internal states are g_1 and g_{-1} in the ground state, e_0 in the excited state. For describing

(*) It has been also suggested that optical pumping in translation space might be used to cool the translational degrees of freedom below the recoil limit by velocity-selective recycling in a trap [41].

the external state, we will use the momentum p along $0z$, so that a state such as $|g_1, p\rangle$ represents the atom in g_1 with a momentum p along $0z$.

When the external degrees of freedom are quantized, the coordinate z of the centre of mass, which appears in the expression (4.1) of the laser electric field $\boldsymbol{E}_L(z, t)$, becomes an operator Z. The laser-atom interaction Hamiltonian (2.4) can then be written, using (4.2), the Rabi frequency Ω_1 associated with $\mathcal{E}_0$ and the Clebsch-Gordan coefficients of fig. 5*b*),

$$(5.3) \quad V_{AL} =$$

$$= \frac{\hbar\Omega_1}{2}\left[-\frac{1}{\sqrt{2}}\exp[ikZ]\,|e_0\rangle\langle g_{-1}| + \frac{1}{\sqrt{2}}\exp[-ikZ]\,|e_0\rangle\langle g_1|\right]\exp[-i\omega_L t] + \text{h.c.}$$

The operators $\exp[\pm ikZ]$ appearing in (5.3) are translation operators in momentum space, so that

$$(5.4a) \qquad V_{AL}\,|g_{-1}, p\rangle = -\frac{\hbar\Omega_1}{2\sqrt{2}}\exp[-i\omega_L t]\,|e_0, p + \hbar k\rangle,$$

$$(5.4b) \qquad V_{AL}\,|g_{+1}, p\rangle = +\frac{\hbar\Omega_1}{2\sqrt{2}}\exp[-i\omega_L t]\,|e_0, p - \hbar k\rangle.$$

The interpretation of (5.4*a*) is very clear. Starting from g_{-1}, the atom can only go to e_0 by absorption of a photon which must be σ^+ (conservation of angular momentum). This σ^+ photon propagates along the positive direction of $0z$ (see fig. 4) and thus carries a momentum $+\hbar k$ which is transferred to the atom during the absorption process, so that the atomic momentum changes from p to $p + \hbar k$. Similar considerations apply to (5.4*b*).

Equations (5.4) now suggest to introduce the states

$$(5.5) \qquad |\psi_{NC}(p)\rangle = \frac{1}{\sqrt{2}}[|g_{-1}, p - \hbar k\rangle + |g_{+1}, p + \hbar k\rangle]$$

which are not coupled to the laser light since

$$(5.6) \qquad V_{AL}\,|\psi_{NC}(p)\rangle = \frac{\hbar\Omega_1}{4}\exp[-i\omega_L t][-|e_0, p\rangle + |e_0, p\rangle] = 0.$$

The two absorption amplitudes, starting from $|g_{-1}, p - \hbar k\rangle$ and from $|g_1, p + \hbar k\rangle$ and ending both in the same final state $|e_0, p\rangle$, interfere destructively. Equations (5.5) and (5.6) generalize eqs. (4.13*b*) and (4.15*b*) of the previous section where the external degrees of freedom were not quantized. Note that different atomic momenta $p - \hbar k$ and $p + \hbar k$ appear in the two states which are linearly superposed in (5.5). This is due to the fact that the photons which can be absorbed by an atom in g_{-1} or g_1 have opposite momenta $+\hbar k$ and $-\hbar k$. Since the final state must be the same for the two paths, the two initial states corresponding to g_{-1} and g_1 must have momenta which differ by $2\hbar k$.

It is, of course, possible to introduce also the states

$$|\psi_C(p)\rangle = \frac{1}{\sqrt{2}}[-|g_{-1}, p - \hbar k\rangle + |g_{+1}, p + \hbar k\rangle], \tag{5.7}$$

i.e. the linear combinations of $|g_{-1}, p - \hbar k\rangle]$ and $|g_1, p + \hbar k\rangle]$ which are orthogonal to the noncoupled states (5.5). For such states, the two absorption amplitudes, starting from $|g_{-1}, p - \hbar k\rangle$ and $|g_1, p + \hbar k\rangle$ and ending in $|e_0, p\rangle$, interfere constructively rather than destructively, so that these states are coupled to the laser

$$V_{AL}|\psi_C(p)\rangle = \frac{\hbar\Omega_1}{2}\exp[-i\omega_L t]\,|e_0, p\rangle. \tag{5.8}$$

It is easy to check that V_{AL} couples $|e_0, p\rangle$ only to $|\psi_C(p)\rangle$:

$$V_{AL}|e_0, p\rangle = \frac{\hbar\Omega_1}{2}\exp[-i\omega_L t]\,|\psi_C(p)\rangle, \tag{5.9}$$

so that the only nonzero matrix elements of V_{AL} are

$$\langle e_0, p|V_{AL}|\psi_C(p)\rangle = \frac{\hbar\Omega_1}{2}\exp[-i\omega_L t] = \langle\psi_C(p)|V_{AL}|e_0, p\rangle^*. \tag{5.10}$$

5·2.2. Couplings induced by atomic motion. When the external degrees of freedom are quantized, the atomic Hamiltonian H_A contains a contribution H_A^{ext} which describes the kinetic energy of the centre-of-mass motion. The equation which generalizes the Hamiltonian of eq. (2.2) in ref. [1] for a multilevel atom is

$$H_A = H_A^{ext} + H_A^{int} = \frac{P^2}{2M} + \hbar\omega_A P_e, \tag{5.11}$$

where P_e is the projector onto the manifold of excited Zeeman sublevels, since we suppose here that the ground-state Zeeman sublevels have all the same internal energy, taken equal to 0. In (5.11), P is the atomic-momentum operator along $0z$, since we restrict ourselves in this section to a one-dimensional treatment.

The states $|g_{\pm1}, p \pm \hbar k\rangle$ are eigenstates of H_A:

$$H_A|g_{\pm1}, p \pm \hbar k\rangle = \frac{(p \pm \hbar k)^2}{2M}|g_{\pm1}, p \pm \hbar k\rangle, \tag{5.12}$$

the corresponding eigenvalues being the kinetic energies associated with the

values $p \pm \hbar k$ of the atomic momentum. From (5.12), one deduces

(5.13a) $$H_A |\psi_{NC}(p)\rangle = \frac{1}{\sqrt{2}}\left[\frac{(p-\hbar k)^2}{2M}|g_{-1}, p-\hbar k\rangle + \frac{(p+\hbar k)^2}{2M}|g_1, p+\hbar k\rangle\right] = \left(\frac{p^2}{2M} + E_R\right)|\psi_{NC}(p)\rangle + \frac{\hbar k p}{M}|\psi_C(p)\rangle,$$

(5.13b) $$H_A |\psi_C(p)\rangle = \left(\frac{p^2}{2M} + E_R\right)|\psi_C(p)\rangle + \frac{\hbar k p}{M}|\psi_{NC}(p)\rangle.$$

Such a result shows that H_A shifts the two states $|\psi_{NC}(p)\rangle$ and $|\psi_C(p)\rangle$ by the same amount $p^2/2M + E_R$, where E_R is the recoil energy given in (5.1), and introduces a «motional coupling» between these two states

(5.14) $$\langle\psi_C(p)|H_A|\psi_{NC}(p)\rangle = \frac{\hbar k p}{M}$$

characterized by an angular frequency equal to the Doppler shift kp/M associated with the velocity p/M.

5·2.3. Decay rates due to spontaneous emission. As long as spontaneous emission is ignored, the three states $|e_0, p\rangle$, $|g_1, p+\hbar k\rangle$, $|g_{-1}, p-\hbar k\rangle$ form a three-dimensional subspace, or family, which we denote $\mathcal{F}(p)$, and which remains stable under the effect of the atom-laser coupling V_{AL} and the

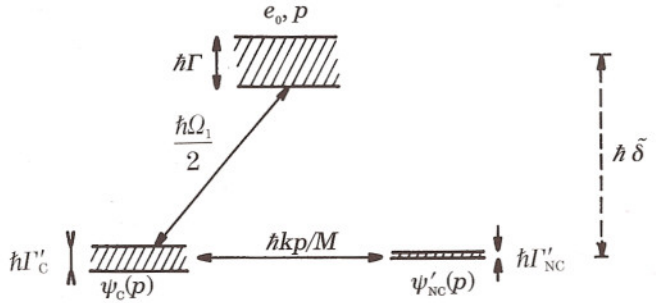

Fig. 7. – Various couplings between the three states $|e_0, p\rangle$, $|\psi_C(p)\rangle$ and $|\psi_{NC}(p)\rangle$ of the family $\mathcal{F}(p)$. The energy separation between $|e_0, p\rangle$ and $|\psi_C(p)\rangle$ (or $|\psi_{NC}(p)\rangle$) is $-(\hbar\delta + E_R) = -\hbar\tilde{\delta}$ (after elimination of the time dependence of V_{AL}). The two states $|e_0, p\rangle$ and $|\psi_C(p)\rangle$ are coupled by V_{AL} (matrix element $\hbar\Omega_1/2$), whereas the two states $|\psi_C(p)\rangle$ and $|\psi_{NC}(p)\rangle$ are coupled by H_A (matrix element $\hbar kp/M$). In the absence of V_{AL} and H_A, the only radiatively unstable state of the family is $|e_0, p\rangle$ (natural width or departure rate Γ). Because of the contamination of $|\psi_C(p)\rangle$ and $|\psi_{NC}(p)\rangle$ by $|e_0, p\rangle$ due to V_{AL} and H_A, the two states $|\psi_C(p)\rangle$ and $|\psi_{NC}(p)\rangle$ also acquire finite widths, or departure rates, which are denoted Γ'_C and Γ'_{NC}.

atomic Hamiltonian H_A. Without spontaneous emission, an atomic state, which initially belongs to $\mathscr{F}(p)$, cannot leave $\mathscr{F}(p)$. Since $|\psi_C(p)\rangle$ and $|\psi_{NC}(p)\rangle$ are linear combinations of $|g_{\pm 1}, p \pm k\rangle$, $\mathscr{F}(p)$ can also be considered as subtended by the three orthogonal states $|e_0, p\rangle$, $|\psi_C(p)\rangle$, $|\psi_{NC}(p)\rangle$:

$$\mathscr{F}(p) = \{|e_0, p\rangle, |g_{+1}, p + \hbar k\rangle, |g_{-1}, p - \hbar k\rangle\} = \tag{5.15}$$

$$= \{|e_0, p\rangle, |\psi_C(p)\rangle, |\psi_{NC}(p)\rangle\}.$$

Figure 7 represents these three states and the various couplings which exist between them and which are due to V_{AL} (matrix element $\hbar\Omega_1/2$ between $|e_0, p\rangle$ and $|\psi_C(p)\rangle$) and to H_A (matrix element $\hbar kp/M$ between $|\psi_C(p)\rangle$ and $|\psi_{NC}(p)\rangle$). We have eliminated the exponentials $\exp[\pm i\omega_L t]$ appearing in expression (5.3) by using the transformation (2.19) (or by quantizing the laser mode), which amounts to replacing ω_A by $\omega_A - \omega_L = -\delta$. If one includes the diagonal elements of H_A in the unperturbed energies of the three states of $\mathscr{F}(p)$, the energy separation between $|e_0, p\rangle$ and $|\psi_C(p)\rangle$ (or $|\psi_{NC}(p)\rangle$) is $-\hbar\tilde{\delta}$, where

$$\hbar\tilde{\delta} = \hbar\delta + E_R. \tag{5.16}$$

In this subsection, we investigate the departure rates from $\mathscr{F}(p)$ due to spontaneous emission. If we ignore V_{AL} and H_A, the only radiatively unstable state of $\mathscr{F}(p)$ is $|e_0, p\rangle$ since no real (*) spontaneous-emission process can occur from any one of the two ground-state sublevels $|g_1\rangle$ and $|g_{-1}\rangle$. The departure rate from $|e_0, p\rangle$ is equal to the natural width Γ of $|e_0, p\rangle$. As long as one is interested only in the decay amplitude of an initial state belonging to $\mathscr{F}(p)$, and not in the final states resulting from this spontaneous decay, one can show (**) that the quantum evolution within $\mathscr{F}(p)$ is correctly described if one just adds an imaginary part $-i\hbar\Gamma/2$ to the energy of $|e_0, p\rangle$. The quantum evolution within $\mathscr{F}(p)$ is thus governed by the following 3×3 non-Hermitian effective Hamiltonian:

$$H_{eff} = \hbar \begin{bmatrix} -\tilde{\delta} - i\Gamma/2 & \Omega_1/2 & 0 \\ \Omega_1/2 & 0 & kp/M \\ 0 & kp/M & 0 \end{bmatrix}, \tag{5.17}$$

(*) Photons can be virtually emitted an reabsorbed from g_1 and g_{-1}, when the rotating-wave approximation is not made in the atom-vacuum field interaction Hamiltonian V_{AV} appearing in (2.1) of ref. [1]. One can show that these «virtual» processes give rise to energy shifts of g_1 and g_{-1} which are the same for these two sublevels as a consequence of the rotational invariance of V_{AV}. These Lamb shifts of g_{-1} and g_1, as well as the Lamb shift of e_0, are supposed here to be reincluded in the atomic frequency ω_A.

(**) One possible method for demonstrating such a result is to study the restriction of the resolvent operator within the subspace subtended by the three states of $\mathscr{F}(p)$ (see, for example, ref. [42], Chapt. III).

which has in general three complex eigenvalues having different imaginary parts. This means that there are in general three different spontaneous-decay modes from $\mathcal{F}(p)$. We want here to discuss the physical meaning of these modes in the perturbative limit where the couplings $\hbar\Omega_1/2$ and $\hbar kp/M$ due to V_{AL} and H_A are sufficiently small.

Consider first the particular case where $p = 0$. It is clear from fig. 7 that the state $|\psi_{NC}(p = 0)\rangle$, given by

$$|\psi_{NC}(p = 0)\rangle = \frac{1}{\sqrt{2}}[|g_{-1}, -\hbar k\rangle + |g_{+1}, +\hbar k\rangle], \tag{5.18}$$

is completely isolated from the other two states of $\mathcal{F}(p = 0)$ since the coupling $\hbar kp/M$ between $|\psi_{NC}(p)\rangle$ and $|\psi_C(p)\rangle$ vanishes for $p = 0$. This means that an atom which is put at $t = 0$ in $|\psi_{NC}(p = 0)\rangle$ will remain there indefinitely. The state $|\psi_{NC}(p = 0)\rangle$, given in (5.18), is, therefore, a perfect trap. The departure rate $\Gamma'_{NC}(p = 0)$ from $|\psi_{NC}(p = 0)\rangle$ is strictly zero:

$$\Gamma'_{NC}(p = 0) = 0. \tag{5.19}$$

The other two departure rates from $\mathcal{F}(p = 0)$ may be found by using (5.17), which splits up into two submatrices when $p = 0$, one 1×1 submatrix corresponding to $|\psi_{NC}(p = 0)\rangle$ and one 2×2 submatrix

$$\hbar\begin{pmatrix} -\tilde{\delta} - i\Gamma/2 & \Omega_1/2 \\ \Omega_1/2 & 0 \end{pmatrix} \tag{5.20}$$

in the subspace $\{|e_0, p = 0\rangle, |\psi_C(p = 0)\rangle\}$. If

$$\Omega_1 \ll \sqrt{\tilde{\delta}^2 + \Gamma^2/4}, \tag{5.21}$$

i.e. if $\Omega_1 \ll \Gamma$ or $\Omega_1 \ll |\tilde{\delta}|$, the eigenvalues of (5.20) can be found perturbatively. The eigenvalue which tends to zero when $\Omega_1 \to 0$ is given by the well-known second-order perturbative expression

$$\frac{\left(\frac{\hbar\Omega_1}{2}\right)^2}{\hbar\left(\tilde{\delta} + i\frac{\Gamma}{2}\right)} = \hbar\left(\delta'_C - i\frac{\Gamma'_C}{2}\right), \tag{5.22}$$

where

$$\Gamma'_C = \Gamma\frac{\left(\frac{\Omega_1}{2}\right)^2}{\tilde{\delta}^2 + \frac{\Gamma^2}{4}}, \tag{5.23a}$$

$$\delta'_C = \tilde{\delta}\frac{\left(\frac{\Omega_1}{2}\right)^2}{\tilde{\delta}^2 + \frac{\Gamma^2}{4}}. \tag{5.23b}$$

Such a result means that, under the effect of V_{AL}, the state $|\psi_C(p=0)\rangle$ is light shifted by $\hbar\delta'_C$ and gets a finite width Γ'_C, which can be also considered as the photon scattering rate from $|\psi_C(p=0)\rangle$. This departure rate from $|\psi_C(p=0)\rangle$ is obviously due to the «contamination», induced by V_{AL}, of $|\psi_C(p=0)\rangle$ by $|e_0, p=0\rangle$. The other eigenvalue of (5.20) is very close to $-\hbar\tilde{\delta} - i\hbar\Gamma/2$.

Suppose now that p is different from zero, but very small. More precisely, the coupling $\hbar kp/M$ between $|\psi_{NC}(p)\rangle$ and $|\psi_C(p)\rangle$ is assumed to be very small compared with the light shift or the width of $|\psi_C(p)\rangle$ calculated above for $p=0$:

$$\frac{k|p|}{M} \ll |\delta'_C| \quad \text{or} \quad \Gamma'_C. \tag{5.24}$$

Two of the three eigenvalues of (5.17) are then still very close to the two eigenvalues of (5.20), *i.e.* to $-\hbar\tilde{\delta} - i\hbar(\Gamma/2)$ and $\hbar\delta'_C - i\hbar\Gamma'_C/2$. As for the third one, one can get it by applying second-order perturbation theory to the coupling $\hbar kp/M$ induced by H_A between $|\psi_{NC}(p)\rangle$ and the perturbed state $\overline{|\psi_C(p)\rangle}$ resulting from the coupling $\hbar\Omega_1/2$ induced by V_{AL} between $|\psi_C(p)\rangle$ and $|e_0, p\rangle$. One gets in this way, using (5.23),

$$\frac{(\hbar kp/M)^2}{\hbar\left(-\delta'_C + i\dfrac{\Gamma'_C}{2}\right)} = \hbar\left(\delta'_{NC} - i\frac{\Gamma'_{NC}}{2}\right), \tag{5.25}$$

where

$$\delta'_{NC}(p) = \frac{\left(\dfrac{kp}{M}\right)^2}{\delta'^2_C + \dfrac{\Gamma'^2_C}{4}}\delta'_C = \frac{4k^2p^2}{M^2\Omega_1^2}\tilde{\delta}, \tag{5.26a}$$

$$\Gamma'_{NC}(p) = \frac{\left(\dfrac{kp}{M}\right)^2}{\delta'^2_C + \dfrac{\Gamma'^2_C}{4}}\Gamma'_C = \frac{4k^2p^2}{M^2\Omega_1^2}\Gamma. \tag{5.26b}$$

In (5.25), $\hbar\delta'_{NC}(p)$ is the light shift of $|\psi_{NC}(p)\rangle$, whereas $\Gamma'_{NC}(p)$ is the departure rate from $|\psi_{NC}(p)\rangle$, more precisely from the eigenstate $\overline{|\psi_{NC}(p)\rangle}$ of (5.17) which tends to $|\psi_{NC}(p)\rangle$ when $p \to 0$ ($\overline{|\psi_{NC}(p)\rangle}$ is a linear superposition of the three states (5.15) where $|\psi_{NC}(p)\rangle$ has the largest weight). Here also, the departure rate from $\overline{|\psi_{NC}(p)\rangle}$ is due to the contamination of $|\psi_{NC}(p)\rangle$ by $|e_0, p\rangle$. But this contamination results now from two contaminations: the contamination induced by V_{AL} between $|\psi_C(p)\rangle$ and $|e_0, p\rangle$ which gives rise to a perturbed state $\overline{|\psi_C(p)\rangle}$ containing a small admixture of $|e_0, p\rangle$, then the contamination induced by H_A between $|\psi_{NC}(p)\rangle$ and $\overline{|\psi_C(p)\rangle}$.

It is clear from (5.26*b*) that the departure rate $\Gamma'_{NC}(p)$ is very small when p is small, and vanishes for $p = 0$ (*). This means that an atom, which is put in $|\overline{\psi_{NC}(p)}\rangle$ at time $t = 0$, can remain there for a very long time if p is small enough, on the order of $(\Gamma'_{NC}(p))^{-1}$. Conversely, for a given interaction time Θ, we can find a range δp of values of p around $p = 0$ such that, if $|p| < \delta p$, an atom in $|\overline{\psi_{NC}(p)}\rangle$ has a high probability to remain trapped in $|\overline{\psi_{NC}(p)}\rangle$ during the whole interaction time Θ. The corresponding value of δp is given by the condition

$$\Gamma'_{NC}(\delta p)\,\Theta < 1\,, \tag{5.27}$$

which, using (5.26*b*), leads to

$$\delta p < \frac{M}{2k\sqrt{\Gamma}}\,\frac{\Omega_1}{\sqrt{\Theta}}\,. \tag{5.28}$$

The previous analysis thus demonstrates the existence of a velocity selection mechanism. The set of states $|\overline{\psi_{NC}(p)}\rangle$ with $|p| < \delta p$ can be considered as protected from the «bad» effects of spontaneous emission, since a spontaneous-decay process from such states, during a time interval Θ, is very unlikely. We have thus been able to give a correct full quantum description of the phenomenon of velocity-selective coherent population trapping, introduced semi-classically in subsect. 4·6. We now see that the correct trapping states are linear superposition of states which differ not only by the internal state g_1 or g_{-1}, but also by the linear momentum which is $p + \hbar k$ for g_1 and $p - \hbar k$ for g_{-1}. We also see that δp can be as small as we want, and in particular smaller than $\hbar k$, provided that Θ is long enough, since, according to (5.28), δp varies as $1/\sqrt{\Theta}$.

5·2.4. Spontaneous transfers between different families. In the previous subsection, we have studied how an atom leaves a family $\mathcal{F}(p)$ by spontaneous emission. We now show that, after a spontaneous-emission process, the atom can move into a new family. This diffusion in momentum space is essential for transferring atoms into the trapping states $|\overline{\psi_{NC}(p)}\rangle$ with $|p| \ll \delta p$.

Suppose that, at time t, an atom whose state is described by a ket $|\psi(t)\rangle$ of $\mathcal{F}(p)$ spontaneously emits a photon with a momentum $\hbar\boldsymbol{k}$ having a component $\hbar k_z = u$ along $0z$. Such an emission is possible only if $|\psi(t)\rangle$ contains a certain admixture of the unstable state $|e_0, \boldsymbol{p}\rangle$. We momentarily use a vector $\boldsymbol{p}$ for the atomic momentum and not only the component p of $\boldsymbol{p}$ along $0z$. Just after the

(*) The spontaneous-decay rate $\Gamma'_{NC}(p)$ is equal to half the semi-classical fluorescence rate R_F ($v = p/M$) found in (4.49). The factor 1/2 is due to the fact that, in steady state, the state $|\overline{\psi_C(p)}\rangle$ is also populated and contributes equally to the fluorescence rate.

spontaneous-emission process, the atom is in a linear superposition of $|g_1, \boldsymbol{p} - \hbar\boldsymbol{k}\rangle$ and $|g_{-1}, \boldsymbol{p} - \hbar\boldsymbol{k}\rangle$ which is determined by the direction of $\boldsymbol{k}$ and the polarization of the spontaneously emitted photon. If one is not interested in the x and y components of the atomic momentum, *i.e.* if one traces the final density matrix over these momentum quantum numbers, keeping $\hbar k_z = u$ fixed, and if one averages over the polarization of the emitted photon and on the azimuthal direction of $\boldsymbol{k}$, one finds that the final atomic density matrix is a statistical mixture, with equal weights, of $|g_1, p - u\rangle$ and $|g_{-1}, p - u\rangle$. Such a result is a clear manifestation of the conservation of the total linear momentum along $0z$.

Figure 8 represents the three states $|g_1, p + \hbar k\rangle$, $|g_{-1}, p - \hbar k\rangle$ and $|e_0, p\rangle$ of $\mathscr{F}(p)$ and the two possible final states $|g_1, p - u\rangle$ (a)) and $|g_{-1}, p - u\rangle$ (b)) of the statistical mixture obtained after the spontaneous emission of a photon with momentum u along $0z$. According to (5.5), $|g_1, p - u\rangle$ belongs to $\mathscr{F}(p - \hbar k - u)$, whereas $|g_{-1}, p - u\rangle$ belongs to $\mathscr{F}(p + \hbar k - u)$. Since u can take any value between $-\hbar k$ and $+\hbar k$, this shows that spontaneous transfers can occur from $\mathscr{F}(p)$ to $\mathscr{F}(p')$ with $p - 2\hbar k \leqslant p' \leqslant p + 2\hbar k$.

Combining the results of this subsection and the previous one, it would be possible to make a Monte Carlo simulation of the time evolution of an atom. Just after a spontaneous-emission process, one knows the state of the atom, which is, for example, the state $|g_1, p - u\rangle$ or $|g_{-1}, p - u\rangle$. Knowing this initial state and the effective Hamiltonian (5.17) corresponding to the family of this initial state, one can then calculate the probability that the *next* spontaneous photon will be emitted after a time t. When such a process occurs, one knows the new

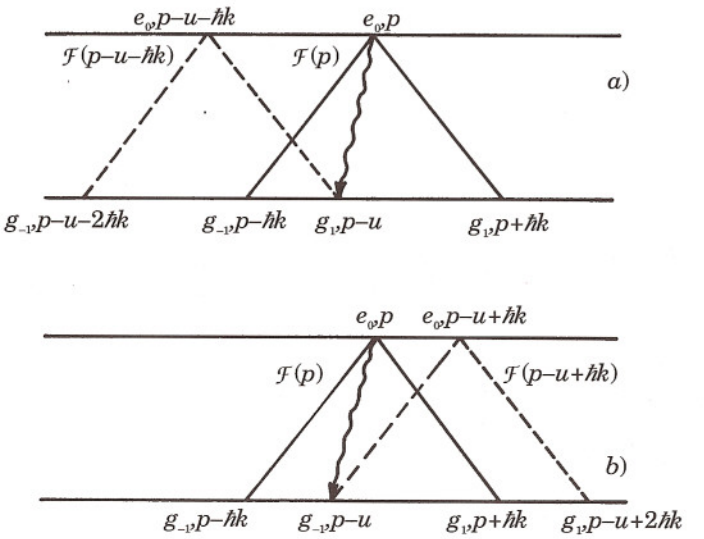

Fig. 8. – Transfers between families due to spontaneous emission. Starting from $|e_0, p\rangle$ which belongs to $\mathscr{F}(p)$, the atom can, by spontaneous emission of a photon with momentum u along $0z$, go either into $|g_1, p - u\rangle$ which belongs to $\mathscr{F}(p - u - \hbar k)$ (a)), or into $|g_{-1}, p - u\rangle$ which belongs to $\mathscr{F}(p - u + \hbar k)$ (b)).

initial state of the atom and the new family, and so on. There is a certain analogy between the calculation sketched here and the calculation of the delay function used for interpreting the phenomenon of intermittent fluorescence and quantum jumps (see ref. [43] and ref. [42], Chapt. VI, subsect. E.3.*c*). In the two situations, one calculates the distribution of the time delays between two *successive* emissions of photons by the same atom, and the existence of very slow decay rates explains why the fluorescence can stop for a very long time. Such an analysis also explains the mechanism for entering into the trapping state $\overline{|\psi_{NC}\rangle}$. Just after a spontaneous-emission process, the atom is, for example, in $|g_1, p - u\rangle$ which is a linear superposition of the three eigenstates of the effective Hamiltonian corresponding to the family $\mathscr{F}(p - u - \hbar k)$ to which $|g_1, p - u\rangle$ belongs. But these three states decay with quite different rates so that, if no spontaneous-emission process has occurred after a long enough time, the initial state is filtered and reduces to $\overline{|\psi_{NC}(p - \hbar k - u)\rangle}$. Finally note an important difference between the situation analysed here and the one analysed in ref. [43]. We take into account here the momentum change following spontaneous emission. Since the slow decay rates are very sensitive to p (see (5.26*b*)), the length of the dark periods, during which the fluorescence stops, can change appreciably during the time evolution (*).

5·2.5. Expected final momentum distribution. Consider an atom in the state $|\psi_{NC}(p)\rangle$. Such a state is not an eigenstate of the component P_z of the atomic-momentum operator $\boldsymbol{P}$. According to (5.5), a measurement of P_z for an atom in $|\psi_{NC}(p)\rangle$ gives two possible results, $p - \hbar k$ and $p + \hbar k$, with equal probabilities. After an interaction time Θ, a notable fraction of the atoms will be trapped in the states $\overline{|\psi_{NC}(p)\rangle}$ (which are very close to $|\psi_{NC}(p)\rangle$) with $|p| \ll \delta p$, δp being related to Θ by (5.28). One, therefore, expects to see in the final atomic-momentum distribution (*i.e.* after an interaction time Θ) two peaks centred around $+\hbar k$ and $-\hbar k$, each of these two peaks having a width δp. If Θ is large enough so that δp is smaller than $\hbar k$, one expects these two peaks to be well resolved. Increasing Θ should decrease their width, and hopefully increase their weight since atoms will have a longer time to diffuse in momentum space towards $p = 0$.

All these predictions are quantitatively confirmed (**) by a numerical integration of the quantum equations of motion [40]. The interested reader may find in ref. [40] a detailed description of such calculations and of their conclusions. In particular, the predictions (5.28) that the width δp of the two peaks at $\pm \hbar k$

(*) *Note added in proofs.* – Such a Monte Carlo simulation has been recently performed [44].

(**) Note, however, that the problem of the evolution of the weight of the peaks in the long-time limit is still open.

should vary as $\Omega_1/\sqrt{\theta}$ is very well confirmed. We just mention here that the quantum equations of motion cannot be transformed, as in subsect. 5.3.3 of ref. [1], into coupled Fokker-Planck equations. Since the atomic-momentum distribution contains sharp peaks, with a width δp which can become smaller than $\hbar k$, it is no longer possible to make an expansion of the density matrix elements in powers of $\hbar k/\delta p$.

Finally note that a one-dimensional laser cooling of the type described in this section was recently demonstrated on a beam of metastable ^{4}He atoms [39]. Two counterpropagating σ^+ and σ^- laser beams were exciting perpendicularly the atomic beam on the $2^3S_1 \leftrightarrow 2^3P_1$ transition of ^{4}He at $\lambda = 1.08$ nm. Double-peak structures with a width δp smaller than $\hbar k$ were observed on the final momentum distribution, corresponding to a one-dimensional temperature of 2 μK, smaller than the recoil limit of 4 μK corresponding to this transition of ^{4}He.

5·3. *Generalization to higher dimensions.* – In this last subsection, we present possible extensions to higher dimensions of the one-dimensional cooling scheme analysed in the previous subsection. A few proposals have been published, extending the idea of velocity-selective coherent population trapping to two dimensions [40, 45] or three dimensions [45, 46]. We will follow here the presentation of ref. [46], restricting ourselves to the particular case of a $J_g = 1 \leftrightarrow J_e = 1$ transition. Other transitions have been also considered in the literature [47].

5·3.1. Equivalent expression for the absorption amplitude. At two or three dimensions, it is no longer possible to ignore the ground-state sublevel g_0 and the two excited Zeeman sublevels e_{-1} and e_1. In the position representation, the most general wave function representing the quantum state of the atom (both internal and external) in the lower state g can be written

$$\Psi_g(\boldsymbol{r}) = \psi_{-1}(\boldsymbol{r})|g_{-1}\rangle + \psi_0(\boldsymbol{r})|g_0\rangle + \psi_{+1}(\boldsymbol{r})|g_{+1}\rangle . \tag{5.29}$$

It is in fact a three-component wave function, one wave function $\psi_m(\boldsymbol{r})$ being associated with each of the three Zeeman sublevels $|g_m\rangle$ of g. Changing from the spherical basis $\{|g_m\rangle\}$ to the Cartesian basis

$$\begin{cases} |g_x\rangle = -\dfrac{1}{\sqrt{2}}(|g_{+1}\rangle - |g_{-1}\rangle), \\ |g_y\rangle = +\dfrac{1}{\sqrt{2}}(|g_{+1}\rangle + |g_{-1}\rangle), \\ |g_z\rangle = +|g_0\rangle \end{cases} \tag{5.30}$$

transforms (5.29) into

$$\Psi_g(\boldsymbol{r}) = \psi_x(\boldsymbol{r})|g_x\rangle + \psi_y(\boldsymbol{r})|g_y\rangle + \psi_z(\boldsymbol{r})|g_z\rangle , \tag{5.31}$$

where $\psi_x(\boldsymbol{r})$, $\psi_y(\boldsymbol{r})$, $\psi_z(\boldsymbol{r})$ are three wave functions which are transformed by rotation as the three components of a vector field $\boldsymbol{\psi}_g(\boldsymbol{r})$:

$$\boldsymbol{\psi}_g(\boldsymbol{r}) = \{\psi_x(\boldsymbol{r}), \psi_y(\boldsymbol{r}), \psi_z(\boldsymbol{r})\}. \tag{5.32}$$

A similar argument shows that the most general quantum state in the upper state e is described by a vector field $\boldsymbol{\phi}_e(\boldsymbol{r})$:

$$\boldsymbol{\phi}_e(\boldsymbol{r}) = \{\phi_x(\boldsymbol{r}), \phi_y(\boldsymbol{r}), \phi_z(\boldsymbol{r})\}. \tag{5.33}$$

We now consider the probability amplitude $\mathcal{A}$ for the atom to be excited from the state $\boldsymbol{\psi}_g(\boldsymbol{r})$ to the state $\boldsymbol{\phi}_e(\boldsymbol{r})$ by absorption of one laser photon. Such an amplitude depends not only on the initial and final states $\boldsymbol{\psi}_g(\boldsymbol{r})$ and $\boldsymbol{\phi}_e(\boldsymbol{r})$, but also on the laser electric field $\boldsymbol{E}_L^+(\boldsymbol{r})$, which is, as $\boldsymbol{\psi}_g(\boldsymbol{r})$ and $\boldsymbol{\phi}_e(\boldsymbol{r})$, a vector field. From the Clebsch-Gordan coefficients of a $J_g = 1 \leftrightarrow J_e = 1$ transition, one can show that

$$\mathcal{A} = \langle \Phi_e \,|\, V_{AL} \,|\, \Psi_g \rangle = C \int d^3r\, \boldsymbol{\phi}_e(\boldsymbol{r}) \cdot [\boldsymbol{E}_L^+(\boldsymbol{r}) \times \boldsymbol{\psi}_g(\boldsymbol{r})], \tag{5.34}$$

where C is a constant. In fact, the structure of (5.34) can be easily understood if one notes that the only vector field which can be constructed from the two vector fields $\boldsymbol{\psi}_g(\boldsymbol{r})$ and $\boldsymbol{E}_L^+(\boldsymbol{r})$ is $\boldsymbol{E}_L^+(\boldsymbol{r}) \times \boldsymbol{\psi}_g(\boldsymbol{r})$.

5·3.2. Conditions for having a trapping state. Going back to the approach followed in the previous subsection, we can now identify two general conditions which must be fulfilled by an atomic state $\boldsymbol{\psi}_g^T(\boldsymbol{r})$ in g if one wants this state to be a perfectly trapping state, *i.e.* such that, if an atom is put in $\boldsymbol{\psi}_g^T(\boldsymbol{r})$ at time $t = 0$, it remains there indefinitely.

Firstly, this state must be insensitive to the laser light. More precisely, one must have

$$V_{AL} \,|\, \Psi_g^T \rangle = 0, \tag{5.35}$$

which generalizes (5.6), or equivalently, according to (5.34),

$$\int d^3r\, \boldsymbol{\phi}_e(\boldsymbol{r}) \cdot [\boldsymbol{E}_L^+(\boldsymbol{r}) \times \boldsymbol{\psi}_g^T(\boldsymbol{r})] = 0, \qquad \forall \boldsymbol{\phi}_e(\boldsymbol{r}). \tag{5.36}$$

Secondly, the atomic Hamiltonian H_A must not couple Ψ_g^T to any other state which could be coupled to the laser light. Such a condition implies that Ψ_g^T must be an eigenfunction of H_A, or equivalently that Ψ_g^T is a stationary state with respect to H_A. In the absence of magnetic field, the three Zeeman sublevels of g have the same internal energy, so that the requirement for Ψ_g^T to be an eigen-

function of H_A can be replaced by

$$H_A^{ext} |\Psi_g^T\rangle = \frac{\boldsymbol{P}^2}{2M} |\Psi_g^T\rangle = \frac{\boldsymbol{p}^2}{2M} |\Psi_g^T\rangle, \tag{5.37}$$

where $\boldsymbol{P}$ is the atomic-momentum operator and where the eigenvalue $\boldsymbol{p}^2/2M$ is a c-number.

5·3.3. Finding a trapping state. We now show that a very simple way to satisfy both conditions (5.36) and (5.37) is to take

$$\psi_g^T(\boldsymbol{r}) = \mu \boldsymbol{E}_L^+(\boldsymbol{r}), \tag{5.38}$$

where μ is a constant. Equation (5.38) defines an atomic state in g whose wave function is described by the same vector field as the laser electric field. Firstly, it is clear that (5.36) is fulfilled since

$$\boldsymbol{E}_L^+(\boldsymbol{r}) \times \psi_g^T(\boldsymbol{r}) = \mu \boldsymbol{E}_L^+(\boldsymbol{r}) \times \boldsymbol{E}_L^+(\boldsymbol{r}) = \boldsymbol{0}. \tag{5.39}$$

Secondly, we note that, the laser field being monochromatic with frequency ω_L, $\boldsymbol{E}_L^+(\boldsymbol{r})$ is necessarily a superposition of plane waves with wave vectors having all the same modulus $k_L = \omega_L/c$, so that

$$\nabla^2 \boldsymbol{E}_L^+ = -k_L^2 \boldsymbol{E}_L^+. \tag{5.40}$$

Since $\boldsymbol{P} = -i\hbar\nabla$, we then deduce from (5.38) and (5.40) that

$$\frac{\boldsymbol{P}^2}{2M} \psi_g^T = -\frac{\mu\hbar^2}{2M} \nabla^2 \boldsymbol{E}_L^+ = \frac{\hbar^2 k_L^2}{2M} \psi_g^T, \tag{5.41}$$

which shows that ψ_g^T also satisfies (5.37) since it is an eigenfunction of $\boldsymbol{P}^2/2M$ with the eigenvalue $E_R = \hbar^2 k_L^2/2M$.

It should be noted, however, that conditions (5.36) and (5.37), which must necessarily be fulfilled by a three-dimensional trapping state, are not sufficient for defining such a state. Consider, for example, a laser configuration which is formed by three coplanar plane waves whose wave vectors $\boldsymbol{k}_1, \boldsymbol{k}_2, \boldsymbol{k}_3$ are all in the $x0y$ plane, with

$$|\boldsymbol{k}_1| = |\boldsymbol{k}_2| = |\boldsymbol{k}_3| = k_L = \frac{\omega_L}{c}. \tag{5.42}$$

Suppose now that, instead of taking a constant μ in (5.38), we replace μ by $\exp[i\kappa z]$, so that we take for ψ_g^T

$$\psi_g^T(\boldsymbol{r}) = \exp[i\kappa z] \boldsymbol{E}_L^+(\boldsymbol{r}). \tag{5.43}$$

It is clear that (5.43) still fulfills (5.36) since $\psi_g^T \times \boldsymbol{E}_L^+$ is still equal to zero. On the other hand, the multiplication by $\exp[i\kappa z]$ in (5.43) amounts to adding to the wave vectors $\boldsymbol{k}_i$ $(i = 1,2,3)$ of the three plane waves forming $\boldsymbol{E}_L^+$ the vector $\boldsymbol{\kappa} = \kappa \boldsymbol{\varepsilon}_z$. It follows that the vector wave function (5.43) is now the sum of three

de Broglie plane waves with wave vectors $\boldsymbol{k}_i + \boldsymbol{\kappa}$ ($i = 1,2,3$). Since $\boldsymbol{\kappa}$, which is parallel to $0z$, is perpendicular to $\boldsymbol{k}_1, \boldsymbol{k}_2, \boldsymbol{k}_3$, which are all in the $x0y$ plane, the three wave vectors $\boldsymbol{k}_i + \boldsymbol{\kappa}$ have the same modulus $(k_L^2 + \kappa^2)^{1/2}$, so that (5.43) is still an eigenstate of $\boldsymbol{P}^2/2M$ with eigenvalue $\hbar^2(k_L^2 + \kappa^2)/2M$:

$$\frac{\boldsymbol{P}^2}{2M} \exp[i\kappa z] \boldsymbol{E}_L^+(\boldsymbol{r}) = \frac{\hbar^2(k_L^2 + \kappa^2)}{2M} \exp[i\kappa z] \boldsymbol{E}_L^+(\boldsymbol{r}). \tag{5.44}$$

We have thus demonstrated that (5.43) still satisfies (5.36) and (5.37). But, since κ can take any value, eqs. (5.43) now define a whole set of trapping states which differ from each other by the value of the momentum along $0z$. In other words, with a laser configuration formed by three coplanar plane waves, taking $\boldsymbol{\psi}_g^T$ proportional to $\boldsymbol{E}_L^+$ does not lead to a three-dimensional trapping state, since there are an infinite number of trapping states which differ by the momentum perpendicular to the plane of the three waves. We have only a two-dimensional trapping.

The previous discussion suggests that, in order to get a unique 3-D trapping state, one must take a laser configuration consisting of at least four plane waves $\boldsymbol{k}_i$ ($i = 1,2,3,4$), the directions of the four wave vectors $\boldsymbol{k}_i$ being such that there exists a single sphere (of radius $k_L = \omega_L/c$) centred on 0 and containing the extremities of the $\boldsymbol{k}_i$'s. Any translation $\boldsymbol{\kappa}$ then destroys the equality between the modulus of the four vectors $\boldsymbol{k}_i + \boldsymbol{\kappa}$. A 3-D atomic trapping state (for a $J_g = 1 \leftrightarrow$ $\leftrightarrow J_e = 1$ transition) must, therefore, be a superposition of at least four states $|g_i, \boldsymbol{k}_i\rangle$ (with $|\boldsymbol{k}_i| = k_L$), differing not only by the direction $\boldsymbol{k}_i/k_i$ of the momentum, but also by the internal state g_i. Since, according to (5.38), each state $|g_i, \boldsymbol{k}_i\rangle$ is the replica of a laser plane wave, and since such light waves are transverse, the internal atomic state g_i must be also transverse with respect to $\boldsymbol{k}_i$.

It would be very interesting to try to demonstrate the existence of such 3-D trapping states which exhibit nonseparable quantum correlations between internal and external degrees of freedom. A certain number of problems remain to be investigated. For example, one must get rid of gravity. Also, the filling efficiency of the trapping state, which depends on momentum diffusion, could be much smaller in three dimensions than in one dimension and it would be probably helpful to supplement the method by other schemes increasing the momentum diffusion towards the low values of p.

* * *

I warmly thank all my colleagues of the Ecole Normale Supérieure, in particular J. DALIBARD, for many helpful discussions and comments about this lecture. I am also very grateful to P. LETT for a careful reading of the manuscript and to M. SANCHEZ and I. GAZAN for their help in the preparation of these lecture notes.

REFERENCES

[1] C. COHEN-TANNOUDJI: in *Les Houches, Session LIII, 1990 - Fundamental Systems in Quantum Optics*, edited by J. DALIBARD, J. M. RAIMOND and J. ZINN-JUSTIN (Elsevier Science Publishers B.V., Amsterdam, 1992), p. 1.

[2] A. MESSIAH: *Quantum Mechanics* (North-Holland, Amsterdam, 1962).

[3] C. COHEN-TANNOUDJI: in *Les Houches, Session XXVII, 1975 - Frontiers in Laser Spectroscopy*, edited by R. BALIAN, S. HAROCHE and S. LIBERMAN (North-Holland, Amsterdam, 1977).

[4] J. P. BARRAT and C. COHEN-TANNOUDJI: *J. Phys. Rad.*, **22**, 329, 443 (1961).

[5] C. COHEN-TANNOUDJI: Thesis, Paris (1962); *Ann. Phys. (Paris)*, **7**, 423, 469 (1962).

[6] C. COHEN-TANNOUDJI: *C. R. Acad. Sci.*, **252**, 394 (1961).

[7] M. ARDITI and T. R. CARVER: *Phys. Rev.*, **124**, 800 (1961).

[8] W. HAPPER and S. MATHUR: *Phys. Rev.*, **163**, 12 (1967).

[9] C. COHEN-TANNOUDJI and J. DUPONT-ROC: *Phys. Rev. A*, **5**, 968 (1972).

[10] A. KASTLER: *J. Phys. Rad.*, **11**, 255 (1950).

[11] W. HANLE: *Z. Phys.*, **30**, 93 (1924); **35**, 346 (1926).

[12] J. DUPONT-ROC, S. HAROCHE and C. COHEN-TANNOUDJI: *Phys. Lett. A*, **28**, 638 (1969).

[13] C. COHEN-TANNOUDJI, J. DUPONT-ROC, S. HAROCHE and F. LALOË: *Phys. Rev. Lett.*, **22**, 758 (1969).

[14] R. KAISER, N. VANSTEENKISTE, A. ASPECT, E. ARIMONDO and C. COHEN-TANNOUDJI: *Z. Phys. D*, **18**, 17 (1991).

[15] G. NIENHUIS: in *Proceedings of Light Induced Kinetic Effects*, edited by L. MOI, S. GOZZINI, C. GABBANINI, E. ARIMONDO and F. STRUMIA (ETS Editrice, Pisa, 1991), p. 139.

[16] H. WALLIS: Thesis, Bonn (1990).

[17] P. LETT., R. WATTS, C. WESTBROOK, W. D. PHILLIPS, P. GOULD and H. METCALF: *Phys. Rev. Lett.*, **61**, 169 (1988).

[18] J. DALIBARD and C. COHEN-TANNOUDJI: *J. Opt. Soc. Am. B*, **2**, 1707 (1985). An extension of the method described here to multilevel atoms may be found in E. BONDERUP and K. MØLMER: *J. Opt. Soc. Am. B*, **6**, 2125 (1989).

[19] J. DALIBARD and C. COHEN-TANNOUDJI: *J. Opt. Soc. Am. B*, **6**, 2023 (1989).

[20] Y. CASTIN, J. DALIBARD and C. COHEN-TANNOUDJI: in *Proceedings of Light Induced Kinetic Effects*, edited by L. MOI, S. GOZZINI, C. GABBANINI, E. ARIMONDO and F. STRUMIA (ETS Editrice, Pisa, 1991), p. 5.

[21] P. J. UNGAR, D. S. WEISS, E. RIIS and S. CHU: *J. Opt. Soc. Am. B*, **6**, 2058 (1989).

[22] C. COHEN-TANNOUDJI and W. D. PHILLIPS: *Phys. Today* (October 1990), p. 33.

[23] Y. CASTIN and J. DALIBARD: *Europhys. Lett.*, **14**, 761 (1991).

[24] D. S. WEISS, E. RIIS, Y. SHEVY, P. J. UNGAR and S. CHU: *J. Opt. Soc. Am. B*, **6**, 2072 (1989).

[25] B. SHEEHY, S. Q. SHANG, P. VAN DER STRATEN, S. HATAMIAN and H. METCALF: *Phys. Rev. Lett.*, **64**, 858 (1990).

[26] C. SALOMON, J. DALIBARD, W. D. PHILLIPS, A. CLAIRON and S. GUELLATI: *Europhys. Lett.*, **12**, 683 (1990). See also C. MONROE, W. SWANN, H. ROBINSON and C. WIEMAN: *Phys. Rev. Lett.*, **65**, 1571 (1990).

[27] D. WINELAND and W. ITANO: *Phys. Rev. A*, **20**, 1521 (1979).

[28] P. VERKERK, B. LOUNIS, C. SALOMON, C. COHEN-TANNOUDJI, J.-Y. COURTOIS and G. GRYNBERG: *Phys. Rev. Lett.*, **68**, 3861 (1992).
[29] P. S. JESSEN, C. GERZ, P. D. LETT, W. D. PHILLIPS, S. L. ROLSTON, R. J. C. SPREEUW and C. I. WESTBROOK: *Phys. Rev Lett.*, **69**, 49 (1992).
[30] J. DALIBARD, C. SALOMON, A. ASPECT, E. ARIMONDO, R. KAISER, N. VANSTEENKISTE and C. COHEN-TANNOUDJI: in *Atomic Physics 11*, edited by S. HAROCHE, J. C. GAY and G. GRYNBERG (World Scientific, Singapore, 1989), p. 199.
[31] S. CHU, D. S. WEISS, Y. SHEVY and P. J. UNGAR: in *Atomic Physics 11*, edited by S. HAROCHE, J. C. GAY and G. GRYNBERG (World Scientific, Singapore, 1989), p. 636.
[32] H. J. METCALF: in *Proceedings of Light Induced Kinetic Effects*, edited by L. MOI, S. GOZZINI, C. GABBANINI, E. ARIMONDO and F. STRUMIA (ETS Editrice, Pisa, 1991), p. 79.
[33] Y. CASTIN and K. MØLMER: *J. Phys. B*, **23**, 4101 (1990).
[34] Y. CASTIN, K. MØLMER, J. DALIBARD and C. COHEN-TANNOUDJI: in *Laser Spectroscopy IX*, edited by M. FELD, J. THOMAS and A. MOORADIAN (Academic Press, San Diego, Cal., 1989).
[35] G. ALZETTA, A. GOZZINI, L. MOI and G. ORRIOLS: *Nuovo Cimento B*, **36**, 5 (1976).
[36] E. ARIMONDO and G. ORRIOLS: *Lett. Nuovo Cimento*, **17**, 333 (1976).
[37] P. M. RADMORE and P. L. KNIGHT: *J. Phys. B*, **15**, 561 (1982).
[38] J. DALIBARD, S. REYNAUD and C. COHEN-TANNOUDJI: in *Interaction of Radiation with Matter, a Volume in Honor of A. Gozzini* (Scuola Normale Superiore, Pisa, 1987).
[39] A. ASPECT, E. ARIMONDO, R. KAISER, N. VANSTEENKISTE and C. COHEN-TANNOUDJI: *Phys. Rev. Lett.*, **61**, 826 (1988).
[40] A. ASPECT, E. ARIMONDO, R. KAISER, N. VANSTEENKISTE and C. COHEN-TANNOUDJI: *J. Opt. Soc. Am. B*, **6**, 2112 (1989).
[41] D. E. PRITCHARD, K. HELMERSON, V. S. BAGNATO, G. P. LAFYATIS and A. G. MARTIN: in *Laser Spectroscopy VIII*, edited by S. SVANBERG and W. PERSSON (Springer-Verlag, Heidelberg, 1987), p. 68.
[42] C. COHEN-TANNOUDJI, J. DUPONT-ROC and G. GRYNBERG: *Processus d'interaction entre photons et atomes* (InterEditions et Editions du CNRS, Paris, 1988). English translation: *Atom-Photon Interactions. Basic Processes and Applications* (Wiley, New York, N.Y., 1992).
[43] C. COHEN-TANNOUDJI and J. DALIBARD: *Europhys. Lett.*, **1**, 441 (1986).
[44] C. COHEN-TANNOUDJI, F. BARDOU and A. ASPECT: in *Laser Spectroscopy X*, edited by M. DUCLOY, E. GIACOBINO and G. CAMY (World Scientific, Singapore, 1992), p. 3.
[45] F. MAURI, F. PAPOFF and E. ARIMONDO: in *Proceedings of Light Induced Kinetic Effects*, edited by L. MOI, S. GOZZINI, C. GABBANINI, E. ARIMONDO and F. STRUMIA (ETS Editrice, Pisa, 1991), p. 89.
[46] M. A. OL'SHANII and V. G. MINOGIN: in *Proceedings of Light Induced Kinetic Effects*, edited by L. MOI, S. GOZZINI, C. GABBANINI, E. ARIMONDO and F. STRUMIA (ETS Editrice, Pisa, 1991), p. 99.
[47] F. PAPOFF, F. MAURI and E. ARIMONDO: *J. Opt. Soc. Am. B*, **9**, 321 (1992).